INDIAN ASSOCIATION OF SEDIMENTOLOGISTS MAGAZINE ISSN NO 2582 – 2020
Vol. 3, Issue I, 2024, pp. 1 – 87
DOI: https://doi.org/10.51710/jias.v3i1.378

Reminiscing over six decades of global scientific journey (1962-2024): Sedimentary processes, environments, deposits, deformation, fossil fuels, Climate change and groupthink

G. Shanmugam
Department of Earth and Environmental Sciences
The University of Texas at Arlington, Arlington, Texas 76019, USA
Email: shanshanmugam@aol.com

Abstract: This review is based on my Address delivered as the Chief Guest at the 39th Convention of the Indian Association of Sedimentologists at Annamalai University in Tamil Nadu, India on December 6 2023, Wednesday Morning, just after the Inauguration of the above Convention (Shanmugam, 2023f). My scientific journey from Annamalai University to America and beyond is composed of the following attributes:

1. Covering a span of 62 years (1962─2024).
2. It began unexpectedly, but owes it to the great motivation of Prof. T. N. Muthuswami Iyer.
3. It began with no specific long-term agenda.
4. While, at Mobil Oil Company, fortunately, many research projects were assigned to me.
5. Thus inducing, enabling and culminating in over 150 projects - as a student, researcher, teacher, and consultant.
6. Duration of projects varied from just 3 months in some to about10 years in a few cases.
7. These Projects taught me to transform many obstacles to opportunities.
8. By investing 100% of my energy, focus, and efforts, irrespective of the Project being small or very large.
9. All the projects pursued are based on empirical data derived from drill cores, outcrops, and experiments. The underpinning of all my research work has always been to unravel the truth, without the distraction of Groupthink.
10. Thus, the unstinted devotion to work and research enabled the publication of almost every research topic during the past 62 years resulting in over 380 published works, including five Elsevier books.

The Convention Address was thus a glimpse of the scientific journey undertaken, in terms of
(1) People: Scientists and others,
(2) Projects: >150 (Global),
(3) Publications: >380,
(4) Recognition: Several,
(5) Nature Photography: Norway, China, Ecuador, Spain, India, China, Saudi Arabia, and,
(6) A Perspective.

Keywords: Annamalai University, IIT Bombay, Ohio University, University of Tennessee, Mobil Oil Company, Scientific Journey, Depositional Environments, Density Plumes, Sediment Deformation, Fossil Fuels, Climate Change, Groupthink

Introduction

The objective of this illustrated tome is to summarize the Address delivered as a Chief Guest at the 39th Convention of the Indian Association of Sedimentologists at Annamalai University in Tamil Nadu, India on December 6th 2023 (Shanmugam, 2023f) (Fig. 1). For discussion of the global scientific journey undertaken, the focus was on the 36 topics selected (Fig. 2). During this journey, multiple scientific methods were employed viz,

1. Theoretical analysis,
2. Laboratory experimental procedures,
3. Observational scientific methods during examination of subsurface drill cores, and Surface Outcrops
4. Petrographic microscopy,
5. Scanning electron microscopy,
6. Coal petrography,
7. Porosity and permeability measurements,
8. Pyrolysis,
9. Gas chromatography,
10. X-ray diffraction analysis,
11. Aerial photographs,
12. Underwater photographs,
13. Underwater current velocity measurements,

14. Satellite imagery,
15. Radar images,
16. Wireline logs,
17. Dip meter logs,
18. GLORIA (**G**eological **Lo**ng **R**ange **I**nclined **A**sdic) images,
19. EM300 Bathymetric Images,
20. Seismic reflection profiles,
21. RMS (root mean square) seismic amplitude maps,
22. Deliberate efforts in avoiding groupthink,
23. Routine application of common sense, and
24. Application of Artificial Intelligence (AI).

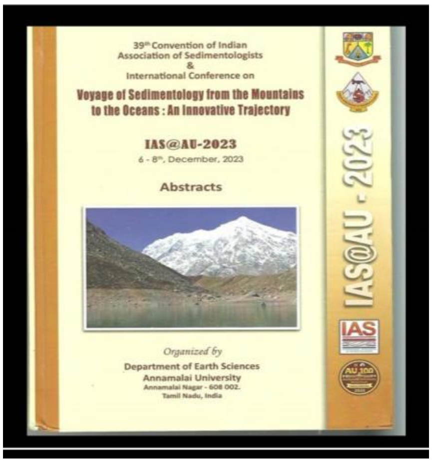

Fig. 1 39th IAS Abstract Volume. Annamalai University, Tamil Nadu, India

The studies have been published in both English and in Chinese (see Section 35). Since all the topics in this review have already been discussed in various publications, the text has been kept to a minimum, and instead includes a considerable number of descriptive / corroborative figures for easy transfer of beneficial knowledge to the students. In many respects, this is intended as an illustrated guide with 266 figures for interpreting sedimentary processes and facies.

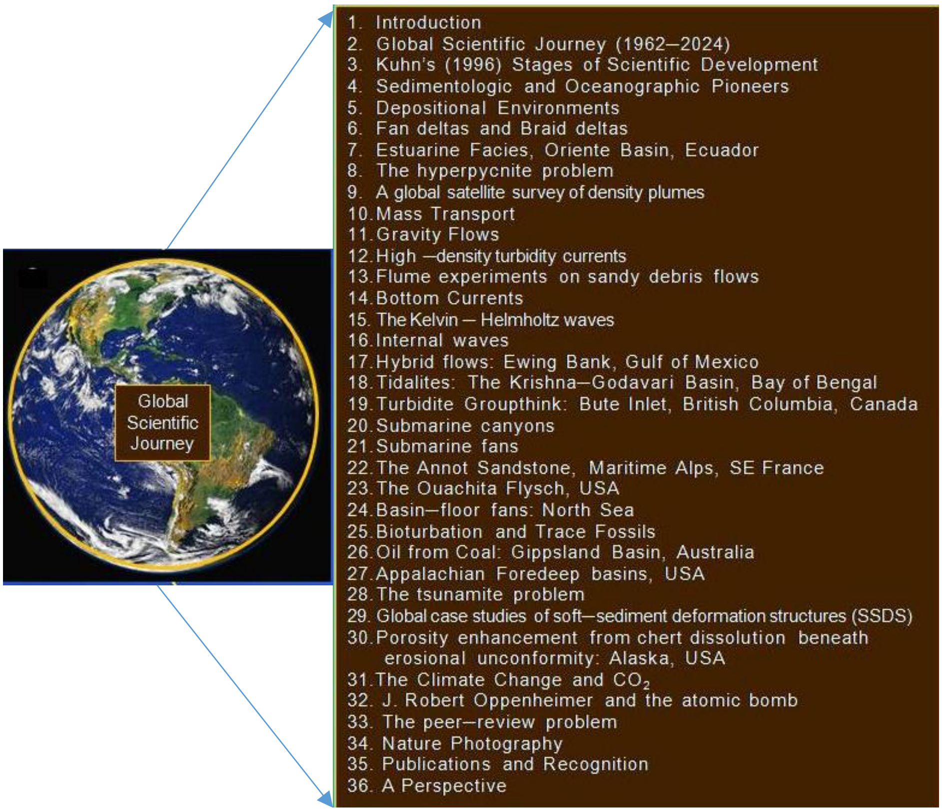

Fig. 2 Topics covered in the review. Globe: NASA

2. Global Scientific Journey (1962–2024)

The journey can be divided into 15 broad categories.

1. Motivation by Prof. T. N. Muthuswami Iyer (Fig. 3 and 4) (Shanmugam, 2022i).
2. B.Sc. and M.Sc. degrees in India.
3. Journey: Annamalai University to IIT Bombay to America (Fig. 5).
4. M.S., (Ohio University) and Ph.D.,(University of Tennessee) Degrees in the U. S.
5. Research Worldwide: Mobil Oil Company: Dallas, Texas (Fig. 6)
6. Teaching: University of Texas at Arlington. Consulting with Reliance (Figs.7 and 8), ONGC, PetroChina (Fig. 9), and China University of Petroleum at Qingdao (Fig.10).
7. Scientists' Influence: R. E. Bagnold, J. E. Sanders, G. D. Klein, F. P. Shepard, and C. D. Hollister, among many others.
8. Scientific Projects: Fan and Braid deltas, Estuarine sedimentation, Hyperpycnal flows, Submarine fans, MTD, Internal waves, Flume experiments on Sandy debris flows, Oil from Coal, Appalachian Tectonics, Soft-sediment deformation structures (SSDS), Erosional

unconformities, Chert dissolution, Fossil Fuels, Climate Change, and J. Robert Oppenheimer.

9. Nature Photography: Norway, China, Ecuador, Spain, India.
10. Editorial Boards: JIAS, JoP, and PED.
11. Invited Membership by CO_2Coalition.
12. 90 Invited International Lectures during the period 1980─2023 (2 per year).
13. 380 Publications with 5 Elsevier books during the period 1968─2024 (7 per year).
14. Awards and Recognition.
15. Research Gate Stats on March 1, 2024.

Research Items: 244
Reads: 195, 401
Citations: 8,730
Recommendations: 475.

Fig. 3 Shanmugam was born in Sirkazhi (Madras Presidency, British India) in 1944

Fig. 4 Motivation from TNM to Shanmugam to pursue M.Sc. in Applied Geology at IIT Bombay. This was the Life─Changing Event.

Fig. 5 Departure for USA

Fig. 6 Shanmugan's employment with Mobil in Dallas, Texas. Research locations are listed on the right. SAFL = St. Anthony Falls Laboratory (SAFL), University of Minnesota. Minneapolis, Minnesota. Project Period: 1996─1998. Director: Gary Parker.

Fig. 7 Deep-Water Sandstone Workshop organized for Reliance by G. Shanmugam.

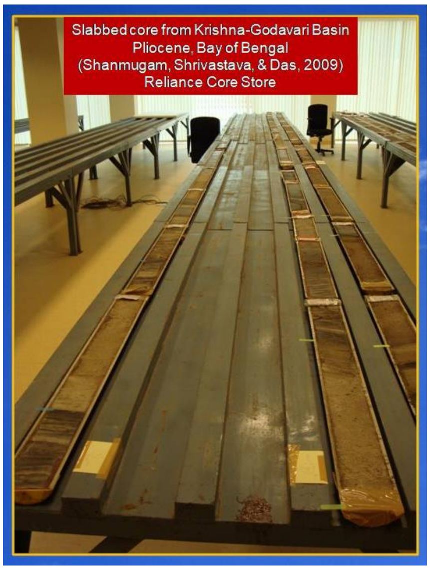

Fig. 8 Core used in Reliance Workshop

Fig. 9 Petro China Workshop participants in front of their Research Center in Beijing, China.

Fig. 10 "Deep-Water Sandstone Workshop" Organized by G. Shanmugam for the China University of Petroleum, Qingdao.

3. Kuhn's (1996) Stages of Scientific Development

Kuhn (1996) argued that science is not a steady, cumulative acquisition of knowledge as portrayed in the textbooks. Instead, it is a series of peaceful interludes punctuated by intellectually violent revolutions. In these revolutions, one conceptual worldview is replaced by another more complex view.

Kuhn's stages of scientific development may be grouped into five steps (Fig. 11):

(1) early random observations;
(2) first paradigm;
(3) crisis;
(4) revolution; and
(5) normal science or new paradigm (Fig.).

Once the final step or normal science is achieved (i.e., the new paradigm); however, scientists enjoy a sense of confidence as well as comfort. This comfort often leads to complacency. The normal science is influential in: (1) forcing scientists to force-fit nature into preconceived models of the paradigm; (2) encouraging scientists to ignore data or observations that do not fit the basic principles of the paradigm; (3) discouraging scientists from inventing new theories; and (4) making scientists intolerant of new theories invented by others (Kuhn, 1996, p. 24). There are ample examples of such influences on deep-water research. *For example*, Turbidite facies models may be considered to represent the normal science stage of Kuhn. However, the turbidite models are infested with unresolved problems. Therefore, I argued that we are still in a crisis mode in the turbidite paradigm (Shanmugam, 2000).

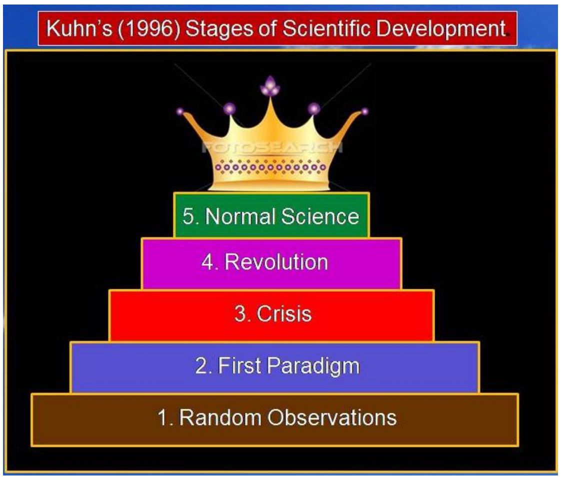

Fig. 11 Kuhn's (1996) Stages of Scientific Development.

4. Sedimentologic and Oceanographic Pioneers

Among 50 Scientists (Table 1) selected in this review, there are five pioneering process sedimentologists/oceanographers who influenced my research on deep-water sedimentation.These pioneers are (Fig. 12):

1) **R. A. Bagnold**: Recognition of the importance of sediment concentration in typical turbidity currents (Fluid mechanics).
2) **J. E. Sanders**: Recognition of the importance of stratified gravity flows with a basal laminar and upper turbulent layers (Fluid mechanics).
3) **G. D. Klein**: Recognition of critical sedimentary features in identifying deposits of deep─marine contour currents and tidal currents in the ancient rock record (Outcrop and core).
4) **F. P. Shepard**: Velocity measurements of tidal currents in submarine canyons (Modern).
5) **C. D. Hollister**: Introduction of the contourite concept for deposits formed by the thermohaline─driven geotropic contour currents (Modern).

Table 1 50 Selected sedimentologists and oceanographers and their contributions on deep-water research during the past 152 years.(1872-2024). This list is not definitive and may vary with the researcher who compiles it. Modified after Shanmugam (2022 f)

Serial Number	Contributor (Author)	Contribution	Reference
1	Allen, J.R.L.	Discussed fluid mechanics of turbidity currents	Allen (1985)
2	Apel, J.R	Compiled an Atlas of Oceanic Internal Solitary-Like Waves and Their Properties	Apel (2002)
3	Bagnold, R.A. (Pioneer) (Fig. 12)	Documented low sediment concentration, commonly below 9% sediment concentration by volume, in turbidity currents	Bagnold (1962)
4	Bouma, A.H.	Introduced the first turbidite facies model (The Bouma Sequence) with five divisions. See also Bouma *et al*. (1985)	Bouma (1962)
5	Briggs, G.	Conducted an outcrop study of the Ouachita flysch, USA	Briggs and Cline (1967)
6	Curray, J. R.	Discussed tectonics and sedimentation in the Bengal Fan	Curray and Moore (1974)
7	Damuth, J.E.	Documented sinuous channels on the modern Amazon Fan	Damuth *et al.* (1988)
8	Dill, R.F.	In situ submersible observations of sediment transport and erosive features in Rio Balsas Submarine Canyon, Mexico	Dill *et al.* (1975)
9	Dott, Jr., D. H.	Discussed dynamics of subaqueous gravity-driven depositional processes	Dott (1963)
10	Dzulynski, S.	Introduced the concept of fluxoturbidites (See comments by Strzeboński, 2022)	Dzulynski *et al*. (1959)
11	Embley, R.W.	Documented tongue-like distribution of mass-transport deposits (MTD) on the U.S. Atlantic Margin	Embley (1980)
12	Ewing, M.	Documented sediment transport and distribution in the Argentine Basin	Ewing *et al*. (1971)
13	Forel, F. A.	First reported the phenomenon of density plumes in the Lake Geneva (Loc Lèman), Switzerland	Forel (1885)
14	Gill, A. E.	Discussed density stratification in the ocean that is critical to explaining internal waves along pycnoclines (see Shanmugam, 2013)	Gill (1982)
15	Gordon, A. L.	Explained the origin of Antarctic Bottom Water (AABW) in the Weddell Sea	Gordon (2013)
16	Hampton, M. A.	Demonstrated the role of subaqueous debris flows in generating turbidity currents in experiments	Hampton (1972)
17	Haughton, P.	Classified hybrid sediment gravity flow deposits	Haughton *et al.* (2009)
18	He, Y. B.	Discussed evidence of internal-wave and internal-tide deposits in China (See comments by Shanmugam (2012c)	He *et al*. (2011)
19	Heezen, B. C.	Provided evidence for shaping of the continental rise by deep geotropic contour currents	Heezen *et al*. (1966)
20	Hernández-Molina, F.J.	Presented results from the IODP Expedition 339 in the Gulf of Cadiz, See a detailed study on bottom-current reworked sands in the Gulf of Cadiz (de Castro *et al*., 2020).	Hernández-Molina *et al*. (2013)
21	Hollister, C. D. (Pioneer) (Fig. 12)	Introduced the concept of contourites	Hollister (1967)

22	Hsü, K. J.	A critique of the Bouma Sequence	Hsü (1989)
23	Klein, G. D. (Pioneer) (Fig. 12)	Tidalites in Leg 30 DSDP cores	Klein (1975)
24	Kuenen, Ph. H.	Introduction of the term “turbidite”	Kuenen (1957)
25	Lonsdale, P.	Ripples by internal waves, Horizon Guyot, Mid-Pacific Mountains	Lonsdale *et al.* (1972)
26	Lowe, D. R.	Water escape structures Liquefied and fluidized sediment flows Grain flow and grain flow deposits Sediment gravity flows Slurry-flow deposits	Lowe (1975) Lowe (1976a) Lowe (1976b) Lowe (1982) Lowe & Guy (2000)
27	Marr, J. G.	Experiments on sandy debris flows	Marr *et al.* (2001)
28	Middleton, G. V.	Experiments on turbidity currents Walther’s Law of the correlation Sediment gravity flows	Middleton (1966) Middleton (1973) Middleton and Hampton (1973)
29	Moiola, R. J.	Reinterpretation of depositional processes in a classic flysch sequence (Pennsylvanian Jackfork Group), Ouachita Mountains, Arkansas and Oklahoma, USA	Shanmugam and Moiola (1995)
30	Mulder, T.	Marine hyperpycnal flows	Mulder *et al.* (2003)
31	Murray, J.	Report on deep-sea deposits based on specimens collected during the voyage of H.M.S. Challenger in the years 1872-1876	Murray and Renard (1891)
32	Mutti, E.	Turbidite sandstones	Mutti (1992)
33	Natland, M.L.	New classification of water-laid clastic sediments.	Natland (1967)
34	Nelson, C. H.	Outer-fan lobes of the Mississippi fan	Nelson *et al.* (1992)
35	Nilsen, T.H.	Upper Cretaceous Deep-Sea Fan Deposits, San Diego	Nilsen *et al.* (1979)
36	Normark, W.R.	Sedimentary facies and associated depositional elements of the Amazon Fan	Normark, Damuth *et al.* (1997)
37	Pequegnat, W.E.	A deep bottom-current on the Mississippi Cone	Pequegnat (1972)
38	Pickering, K.T.	Deep Marine Systems: Processes, Deposits, Environments, Tectonics and Sedimentation. See also Pickering *et al.* (1984, 1995)	Pickering and Hiscott (2015)
39	Piper, D.J.W.	Turbidite muds and silts in deep-sea fans Contourites in Antarctica The 1929 ‘Grand Banks’ earthquake, slump Mass-transport deposits of the Amazon Fan	Piper (1978) Piper and Brisco (1975) Piper *et al.* (1988) Piper *et al.* (1997)
40	Postma, G.	Conducted experiments on “High-density turbidity currents” (see a critique by Shanmugam (1996)	Postma *et al.* (1988)
41	Rebesco, M.	Edited a thematic volume on “Contourites”. See also Viana and Rebesco (2007).	Rebesco and Camerlenghi (2008)
42	Sanders, J. E. (Pioneer) (Fig. 12)	Primary sedimentary structures formed by turbidity currents	Sanders (1965)
43	Shanmugam, G.	Fine-grained carbonate debris flow Tectonic significance of distal turbidites in the Middle Ordovician	Shanmugam and Benedict (1978) Shanmugam and Walker (1978)

		Analogous tectonic evolution of the Ordovician foredeeps, southern and central Appalachians. Manganese distribution in the carbonate fraction of shallow and deep marine lithofacies Ophiolite source rocks for Taconic-age flysch Origin, recognition and importance of erosional unconformities in sedimentary basins Is the turbidite facies association scheme valid? Sedimentation in the Chile Trench Duplex-like structures in submarine fan channels High-density turbidity currents: are they sandy debris flows? The Bouma Sequence and the turbidite mind set Ten turbidite myths Deep-marine tidal bottom currents Deep-Water Processes and Facies Models The tsunamite problem The obsolescence of deep-water sequence stratigraphy in petroleum geology Deep-water bottom currents and their deposits The constructive functions of tropical cyclones and tsunamis New Perspectives on Deep-Water Sandstones Distinguishing paleo-tsunami deposits Modern internal waves and internal tides The Landslide problem Submarine fans The contourite problem The seismite problem Global case studies of soft-sediment deformation structures (SSDS) A global satellite survey of density plumes at river mouths The hyperpycnite problem Bioturbation and trace fossils in deep-water Global significance of wind forcing on deflecting sediment plumes Gravity flows: types, definitions, origins, identificationmarkers, and problems Mass Transport, Gravity Flows, and Bottom Currents Deep-water processes and deposits The turbidite-contourite-tidalite-baroclinite-hybridite problem Comment on “Ichnological analysis” Comment on “mixed systems” The Peer-Review Problem: a sedimentological perspective 200 Years of Fossil Fuels and Climate Change (1900-2100). The Life and Travails of J. Robert Oppenheimer, the Nuclear Scientist Fossil fuels, climate change, and the vital role of CO_2 to people and plants on planet Earth	Shanmugam and Lash (1982) Shanmugam and Benedict (1983) Shanmugam (1985b) Shanmugam (1988) Shanmugam *et al.* (1985) Shanmugam and McPherson (1987) Shanmugam *et al.* (1988) Shanmugam (1996) Shanmugam (1997) Shanmugam (2002a) Shanmugam (2003) Shanmugam (2006a) Shanmugam (2006b) Shanmugam (2007) Shanmugam (2008b) Shanmugam (2008a) Shanmugam (2012a) Shanmugam (2012b) Shanmugam (2013) Shanmugam (2015) Shanmugam (2016a) Shanmugam (2016b) Shanmugam (2016c) Shanmugam (2017a) Shanmugam (2018c) Shanmugam (2018a) Shanmugam (2018b) Shanmugam (2019) Shanmugam (2020) Shanmugam (2021a) Shanmugam (2021c) Shanmugam (2021b) Shanmugam (2022b) Shanmugam (2022c) Shanmugam (2022g)

			Shanmugam (2023b) Shanmugam (2023d) Shanmugam (2024)
44	Shepard, F. P. (Pioneer) (Fig. 12)	Measured velocities of tidal currents in submarine canyons worldwide	Shepard *et al.* (1979)
45	Southard, J. B.	Recognized five types of bottom currents at the shelf break based on their origin. These currents are generated by (1) thermohaline differences, (2) wind forces, (3) tidal forces, (4) internal waves, and (5) surface waves.	Southard and Stanley (1976)
46	Stanley, D. J.	Submarine canyon and slope sedimentation The Selfbreak: Critical Interface Sedimentation in Submarine Canyons, Fans, and Trenches	Stanley (1971) Stanley and Moore (1983) Stanley and Kelling (1978)
47	Stow, D. A. V.	Contourite facies and the facies model with five divisions	Stow and Faugères (2008)
48	Walker, R. G.	Facies models	Walker (1992)
49	Wüst, G.	A pioneer in oceanography of North Atlantic bottom currents	Wüst (1933)
50	Zenk, W.	Provided clarity on the fact that bottom currents in the Gulf of Cadiz are not genuine contour currents	Zenk (2008)

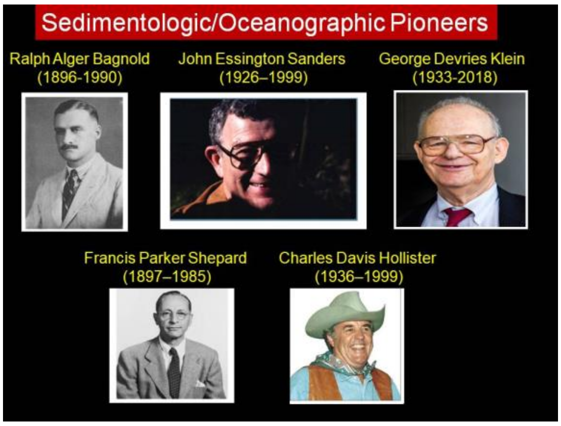

Fig. 12 Sedimentologic / Oceanographic Pioneers.

5. Depositional Environments

As a process sedimentologist, I have studied a wide range of depositional environments and related processes (Fig. 13). Published examples are::

1) Subaerial and submarine landslides (Shanmugam, 2015).
2) Braided fluvial channel reservoir, Alaska (Shanmugam and Higgins, 1988)
3) Rainforests, New Zealand (Shanmugam, 1985a)
4) Fan deltas and braid deltas (McPherson, Shanmugam, and Moiola, 1987).
5) Bute Inlet, British Columbia, Canada (Shanmugam, 2022f).
6) Hyperpycnites (Shanmugam, 2018a).
7) Elwha River plume, Washington, USA (Shanmugam, 2019a).
8) Estuarine facies, Ecuador (Shanmugam et al., 2000)
9) Slope deposits, Norway (Shanmugam et al., 1994)
10) Submarine Canyon, KG Basin, India (Shanmugam, Shrivastava, and Das, 2009)
11) Submarine fans (Shanmugam and Moiola, 1988; Shanmugam, 2016a).
12) Basin-floor fans, North Sea (Shanmugam et al., 1995)
13) Contourites (Shanmugam, 2017b).
14) Hybrid flows, Gulf of Mexico (Shanmugam et al., 1993)
15) Internal waves and tides (Shanmugam, 2013).
16) Tsunami deposits (Shanmugam, 2006b, 2012b).
17) Climate Change and CO_2 (Shanmugam, 2023b).

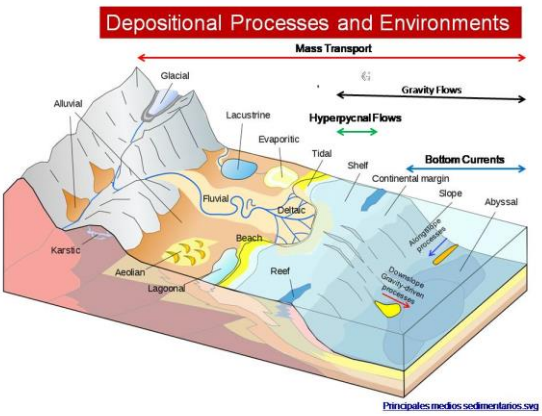

Fig. 13 Depositional Processes and Environments.

6. Fan deltas and Braid deltas

For the first time, McPherson, Shanmugam, and Moiola (1987) provided the much needed conceptual clarity by introducing a new type of coarse-grained delta called “Braid delta” (Fig. 14). Their contribution is summarized below.

Two types of coarse-grained deltas are recognized: fan-deltas and braid deltas. Fan-deltas are gravel-rich deltas formed where an alluvial fan is deposited directly into a standing body of water from an adjacent highland. They occupy a space between the highland (usually a fault-bounded margin) and the standing body of water. In contrast, *braid deltas* (here introduced) are gravel-rich deltas that form where a braided fluvial system progrades into a standing body of water. Braid deltas have no necessary relationship with alluvial fans, as exemplified by fluvioglacial braid deltas. Braid deltas have previously been classified as fan-deltas even though the geomorphic and sedimentologic settings of the two systems can be vastly different. Braid deltas are a common present-day geomorphic feature and are abundant in the geological record.

Fan-deltas and braid deltas can be distinguished in the rock record by distinctive subaerial components of these depositional systems; the shoreline and subaqueous components of both are similar. Fan-delta sequences have a subaerial component that is an alluvial-fan facies comprising interbedded sheetflood, debris-flow, and braided-channel deposits. Fan-deltas produce small (a few tens of square kilometers), wedge-shaped bodies of sediment, and commonly displaying high variability in paleocurrent patterns and abrupt changes in facies. The deposits are generally very coarse grained (with large out-sized clasts), very poorly sorted, matrix-rich, polymictic, heterolithic, partially cemented by penecontemporaneous carbonate, and have low porosity and permeability. Braid-deltas, in contrast, have a subaerial component consisting entirely of braided-river or braidplain facies. Their deposits display better sorting, roundness, and clast orientation than do fan-delta sediments; they lack a muddy matrix; they display size grading and bar migration; they commonly have a sheet geometry with high lateral continuity (tens to hundreds of square kilometers); and they exhibit moderate to high porosity and permeability. Valuable paleogeographic and tectonic information concerning the proximity of highlands and major fault zones may be misinterpreted or lost if these two coarse-grained deltaic systems are not differentiated.

Fig. 14 A. Distinction between fan deltas and braid deltas. After McPherson, Shanmugam, and Moiola, 1987). B. Fan delta. C. Braid delta. B and C photographs are courtesy of John. G. McPherson.

7. Estuarine Facies, Oriente Basin, Ecuador

Figures 15 to 24 illustrate concepts, modern examples, and sedimentological characteristics of estuaries and estuarine facies. A case study of petroleum-producing ancient estuarine facies in Ecuador was published by Shanmugam et al. (2000) in the AAPG Bulletin. The Sacha field (Fig. 25) is a prolific producer of hydrocarbons from the Cretaceous Hollin and Napo formations in the Oriente basin, Ecuador. To understand the depositional origin of these reservoirs, a detailed sedimentological study using 516 ft (157 m) of conventional core from seven wells was carried out. This study reveals seven lithofacies (Shanmugam et al., 2000): (1) cross-bedded sandstone with erosional base (fluvial channels), (2) heterolithic facies with erosive-based, cross-bedded sandstone (tidal channels), (3) heterolithic facies with cross-bedded sandstone showing full-vortex structures, crinkled laminae, sandy rhythmites, and double mud layers (Fig. 26) (tidal sand bars) (Fig. 27), (4) heterolithic facies with flaser-bedded sandstone (tidal sand flats), (5) muddy rhythmites with silty lenticular beds and double mud layers (subtidal mud flats), (6) bioturbated glauconitic sandstone (sandy shelves), and (7) bioturbated and laminated mudstone (muddy shelves).

Based on the presence of mud drapes on bed forms, heterolithic facies, double mud layers, bidirectional (i.e., herringbone) cross-bedding, sandy rhythmites, thick-thin alternations of silt and clay layers showing cyclicity (muddy rhythmites), crinkled laminae, and deepening-upward (i.e., transgressive) successions, it was interpreted that the cored intervals of the Hollin and Napo formations represented tide-dominated estuarine facies (Fig. 28). Previous interpretations that the Hollin and Napo formations represent fluvio-deltaic environments were not supported by this study.

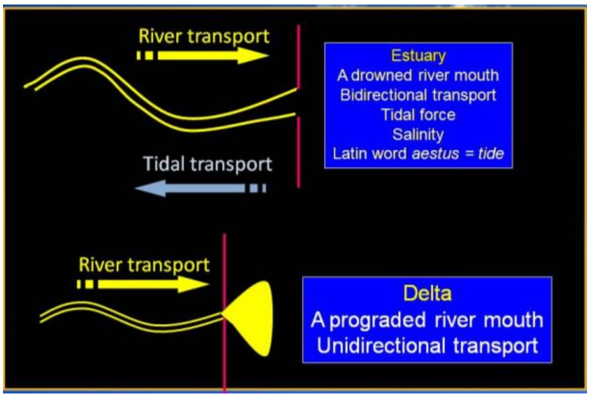

Fig. 15 Distinction between Estuary vs. Delta.

Fig. 16 Modern Rio de la Plata Estuary, Argentina and Uruguay. NASA

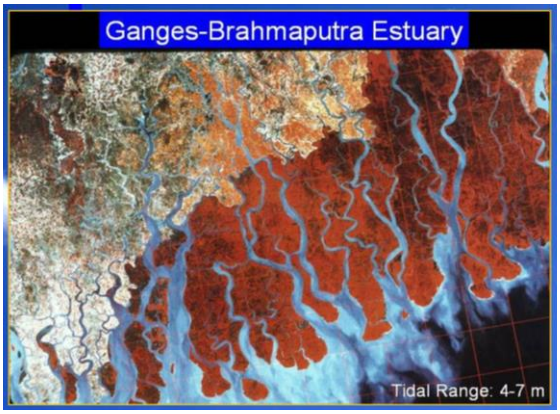

Fig. 17 Modern Ganges-Brahmaputra Estuary. NASA

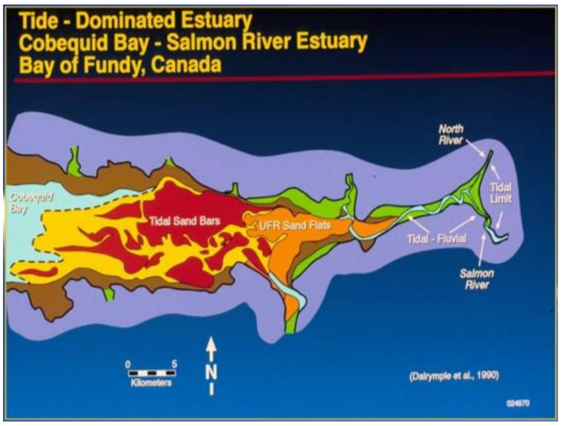

Fig. 18 Modern Tide─dominated estuary, Bay of Fundy, Canada. From Dalrymple et al. (1990).

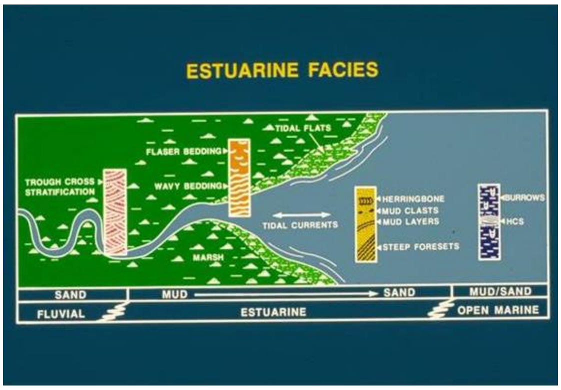

Fig. 19 Conceptual diagram shoeing Estuarine Facies.

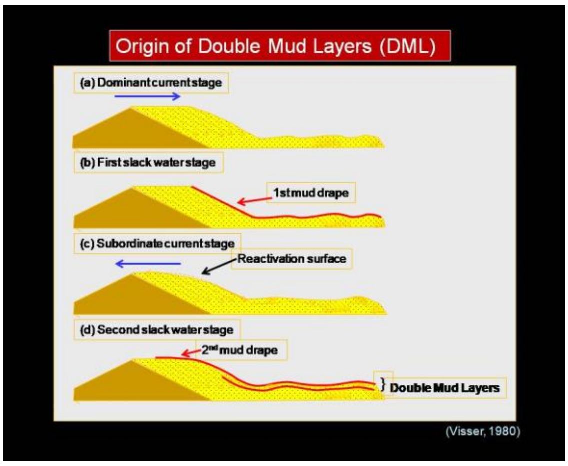

Fig. 20 Origin of Double Mud Layers (Visser, 1980).

Fig. 21 Core photograph showing Double Mud Layers (arrows), West Africa. Courtesy R. D. Kreisa.

Fig.22 Outcrop photograph showing Herringbone Cross Stratification, Miocene, France.

Fig. 23 Outcrop photograph showing Sjgmoidal Tidal bundle, Cretaceous, Saudi Arabia.

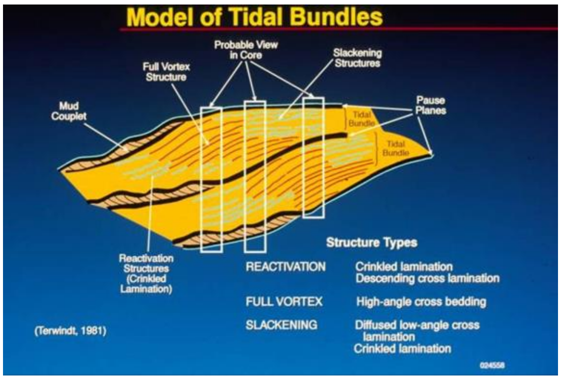

Fig.24 —A model for tidal bundles. The term "mud couplet" refers to double mud layers. Core photograph (e.g. Fig. 21) in this paper may be compared with the probable view in core outlined by the three boxes above. Simplified from Terwindt (1981) and Banerjee (1989).

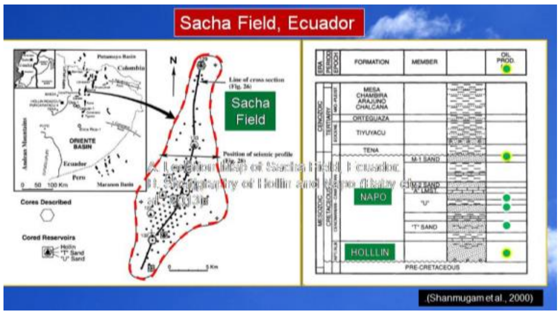

Fig. 25 A. Location Map of Sacha Field, Ecuador. B. Stratigraphy of Hollin and Napo Formations. From Shanmugam et al. (2000).

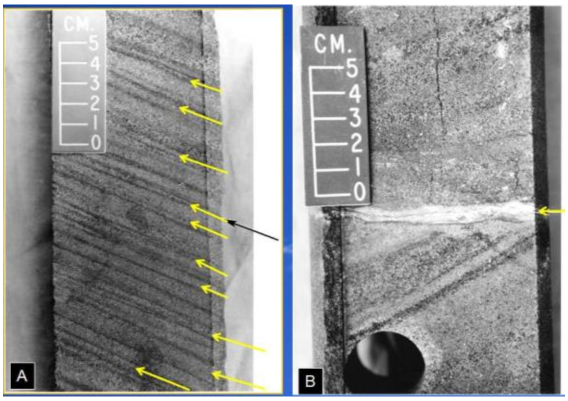

Fig. 26 A—Core photograph of heterolithic facies showing cross-bedded sandstone with double mud layers (arrows). Note rhythmic alternation of thick and thin sand layers. Each mud layer represents a period of slack-water deposition. Tidal cyclicity is poorly developed because of merging of mud layers (black). Tidal sand bar facies. From Shanmugam et al. {2000). B—Core photograph showing sandstone with mud-draped reactivation surface (arrow). Note steeply dipping cross-stratification below reactivation surface. Tidal sand bar facies. Upper Hollin, 9887 ft (3015.5 m), Sacha 130 well. From Shanmugam et al.(2000).

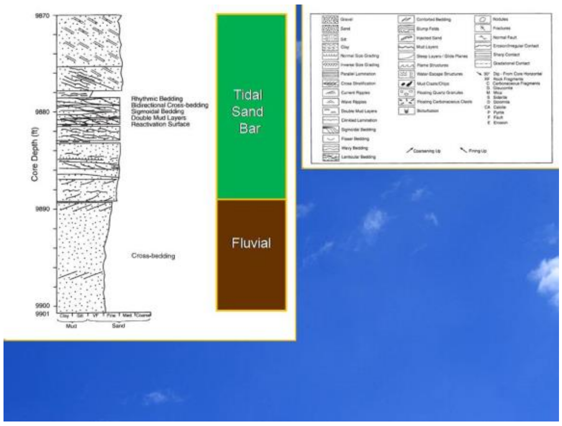

Fig. 27 — Sedimentological log of core from the Sacha130 well showing tidal sand bar facies overlying fluvial channel facies, indicative of a transgressive phase. Lower to upper Hollin. From Shanmugam et al. (2000).

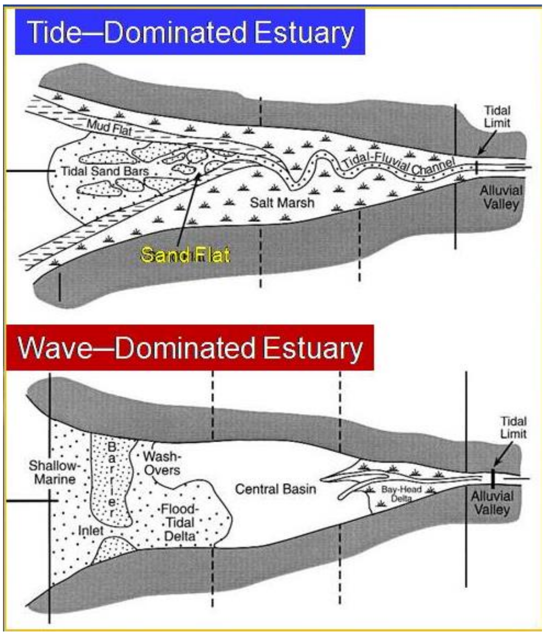

Fig. 28 Two end members of estuarine facies models. After Dalrymple et al. (1992). Hollin and Napo cores are interpreted as tide- dominated estuary and fluvial facies by Shanmugam et al. (2000).

8. The hyperpycnite problem

Bates (1953) 0riginally suggested three types of sediment plumes at river mouths (Fig. 29): (1) hypopycnal plume for floating river water that has lower density than basin water (Fig. 29a); (2) homopycnal plume for mixing river water that has equal density as basin water (Fig. 29b); and (3) hyperpycnal plume for sinking river water that has higher density than basin water (Fig.29c). Mulder et al. (2003) expanded the applicability of the concept of hyperpycnal plumes from shallow water (deltaic) to deep-water (continental slope and abyssal plain) environments (Fig. 30). He also proposed the facies model with internal erosional surface (Fig. 31). However, sequences with internal erosional surfaces are unqualified for stratigraphic correlations because they do not obey the Walther's Law (Middleton, 1973).

In a critical review, Shanmugam (2018a) discussed the problems associated with hyperpycnites (Figs. 31, 32 and 33). Sedimentologic, oceanographic, and hydraulic engineering publications on hyperpycnal flows claim that (1) river flows transform into turbidity currents at plunge points near the shoreline, (2) hyperpycnal flows have the power to erode the seafloor and cause submarine canyons, and, (3) hyperpycnal flows are efficient in transporting sand across the shelf and can deliver sediments into the deep sea for developing submarine fans. Importantly, these claims do have economic implications for the petroleum industry for predicting sandy reservoirs in deep-water petroleum exploration. However, these claims are based strictly on experimental or theoretical basis, without the supporting empirical data from modern depositional systems (Shanmugam, 2018a).

This topic generated lively debate (Van Loon et al., 2019; Zavala, 2019; Shanmugam, 2019b).

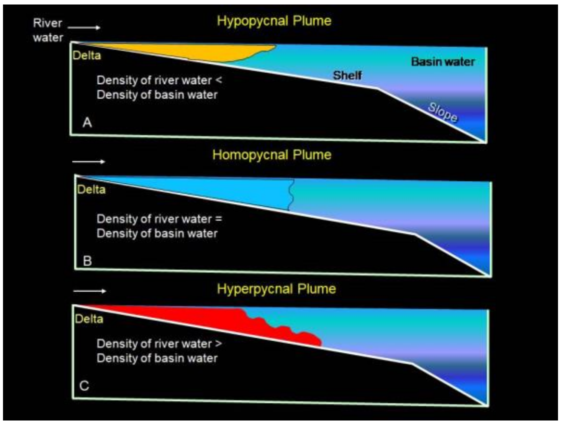

Fig.2 9 Three types of river-mouth plumes (Bates, 1953).

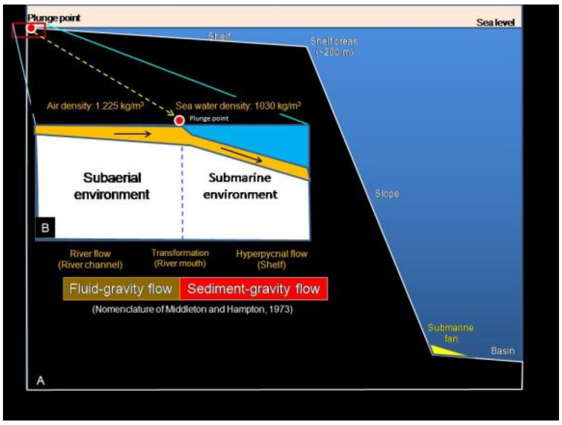

Fig. 30 Hyperpycnal flow at Plunge Point (Shelf). There is no documented case of Hyperpycnal flows in the deep sea.

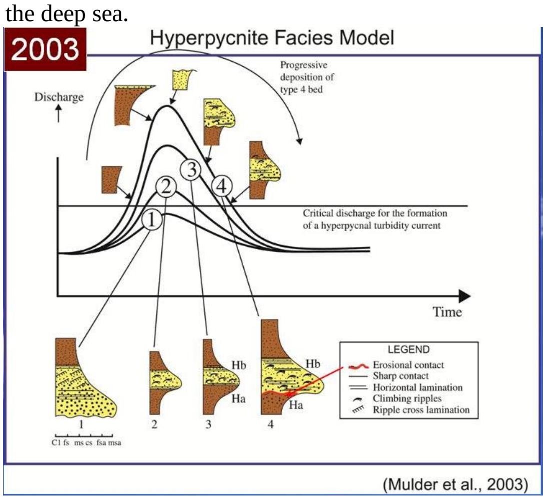

Fig. 31 Hyperpycnite facies model with internal erosional contact shown by a red arrow. Modified after Mulder et al., (2003).

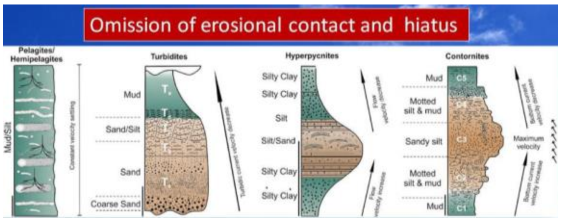

Fig. 32 Omission of internal erosional contact from the hyperpycnite facies model and omission of Internal hiatus from the contourite facie model. Compare with Fig. 80 for the original hyperpycnite facies model. From Rodriguez-Tovar (2022).

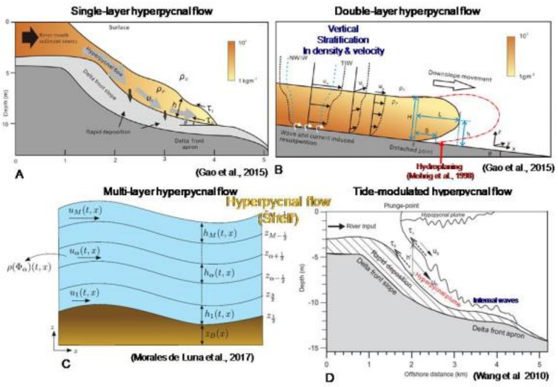

Fig. 33 Four types of Hyperpycnal flows. See Shanmugam (2018a).

9. A global satellite survey of density plumes

On the basis of "A global satellite survey of density plumes at river mouths and at other environments: Plume configurations, external controls, and implications for deep-water sedimentation" (Figs. 34 to 40), Shanmugam (2018c) concluded the following. The U. S. National Aeronautics and Space Administration (NASA) has archived thousands of satellite images of density plumes in its online publishing outlet called 'Earth Observatory' since 1999. Although these images are in the public domain, there has not been any systematic compilation of configurations of density plumes associated with various sedimentary environments and processes. This article, based on 45 case studies covering 21 major rivers (e.g., Amazon, Betsiboka, Congo [Zaire], Copper, Hugli [Ganges], Mackenzie, Mississippi, Niger, Nile, Rhone, Rio de la Plata, Yellow, Yangtze, Zambezi, etc.) and six different depositional environments (i.e., marine, lacustrine, estuarine, lagoon, bay, and reef), is the first attempt in illustrating natural variability of configurations of density plumes in modern environments. There are, at least, 24 configurations of density plumes. An important finding of this study is that density plumes are controlled by a plethora of 18 oceanographic, meteorological, and other external factors. Examples are: 1) Yellow River in China by tidal shear front and by a change in river course; 2) Yangtze River in China by shelf currents and vertical mixing by tides in winter months; 3) Rio de la Plata Estuary in Argentina and Uruguay by Ocean currents; 4) San Francisco Bay in California by tidal currents; 5) Gulf of Manner in the Indian Ocean by monsoonal currents; 6) Egypt in Red Sea by Eolian dust; 7) U.S. Atlantic margin by cyclones; 8) Sri Lanka by tsunamis; 9) Copper River in Alaska by high-gradient braid delta; 10) Lake Erie by seiche; 11) continental margin off Namibia by upwelling; 12) Bering Sea by phytoplankton; 13) the Great Bahama Bank in the Atlantic Ocean by fish activity; 14) Indonesia by volcanic activity; 15) Greenland by glacial melt; 16) South Pacific Ocean by coral reef; 17) Carolina continental Rise by pockmarks; and 18) Otsuchi Bay in Japan by internal bore. The prevailing trend in promoting a single type of river-flood triggered hyperpycnal flow is flawed because there are 16 types of hyperpycnal flows. River-flood derived hyperpycnal flows are muddy in texture and they occur close to the shoreline in inner shelf environments. Hyperpycnal flows are not viable transport mechanisms of sand and gravel across the shelf into the deep sea. The available field observations suggest that they do not form meter-thick sand layers in deep water settings. For the above reasons, river-flood triggered hyperpycnites are considered unsuitable for serving as petroleum reservoirs in deep-water environments until proven otherwise.

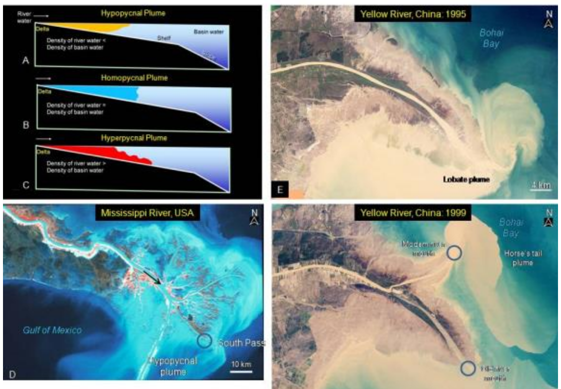

Fig. 34 Types of plumes.

Fig. 35 Zambezi River Delta, Central Mozambique

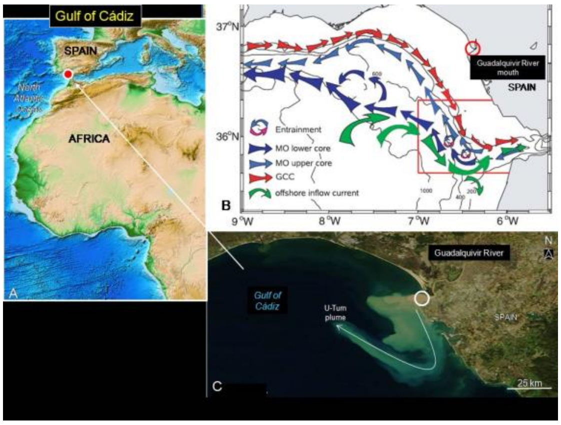

Fig. 36 U─Turn plume, Gulf of Cádiz.

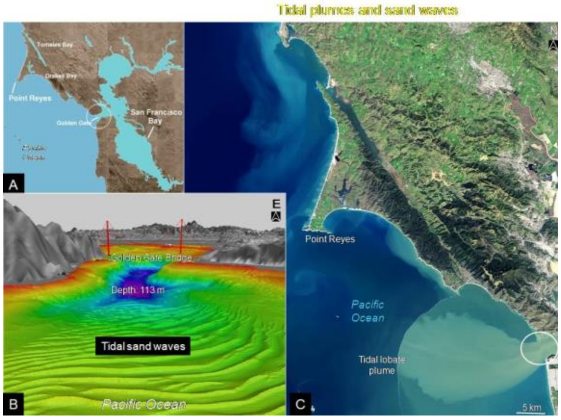

Fig. 37 Tidal sand waves, Golden Gate Bridge, California

Environment	Composition	Provenance	External Control	Type
1. Marine	1. Siliciclastic	1. River flood	1. Tidal shear front	1. Simple lobe
2. Lacustrine	2. Calciclastic	2. Common delta	2. Winter season	2. Horse's tail
3. Estuarine	3. Volcaniclastic	3. Braid delta	3. Ocean current	3. Deflecting
4. Lagoon	4. Planktonic	4.Tidal estuary	4. Tidal current	4. Dissipating
5. Bay	5. Hydrogen sulfide	5. Subglacial	5. Monsoonal current	5. U-Turn
6. Reef	6. Gas hydrate	6. Eolian	6. Eolian	6. Swirly
		7. Volcanic	7. Cyclone	7. Cloudy
		8. Planktonic	8. Tsunami	8. Massive
		9. Carbonate platform/Reef	9. Braid delta	9.Tidal lobe
		10. Hydrogen sulfide	10. Seiche	10. Cascading
		11. Gas hydrate	11. Upwelling	11. Backwash
			12. Phytoplankton	12. Meltwater
			13. Fish activity	13. Coalescing irreg.
			14. Volcanism	14. Blanketing
			15. Glacial melt	15. Linear
			16. Coral reef	16. Anastomosing
			17. Pockmarks	17. Coalescing lobe
			18. Internal waves and tides	18. Whitings
				19. Ring
				20. Tendril
				21. Eolian dust
				22. Feathery
				23. Volcanic ash
				24. Gas hydrate

Fig.38 24 Types of plumes

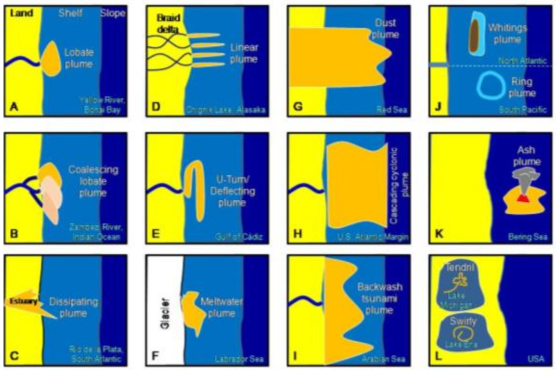

Fig.39 Summary diagram showing 14 general types of plumes that include 12 marine examples and twolacustrine examples. From Shanmugam (2018c).

In a companion study "Global significance of wind forcing on deflecting sediment plumes at river mouths: Implications for hyperpycnal flows, sediment transport, and provenance", Shanmugam (2019a) observed the following (Figs. 40 to 43). A review, based on sediment plumes at the mouths of 29 rivers worldwide, has revealed that sediment (density) plumes are commonly deflected away from the normal downslope direction in 18 out of 29 cases. These deflected sediment plumes have been documented at the mouths of Brisbane, Congo, Connecticut, Dart, Ebro, Eel, Elwha, Fonissa, Guadalquivir, Krishna-Godavari, Mississippi, Monros, Rio de la Plata, Pearl, Rhone, Tiber, Yellow, and Yangtze rivers. As a consequence, current directions change drastically and sediment distribution occurs on only one side of river mouths. In these cases, sediment transport is diverted by a plethora of 22 oceanographic, meteorological, and other external factors. Empirical data show that wind forcing is the most dominant factor. Other influencing factors are tidal currents, ocean currents, and coastal upwelling. Deflection of sediment plumes defies the conventional use of paleocurrent directions in determining sediment transport and provenance in the ancient sedimentary record. Failure to recognize deflected sediment plumes in the rock record could result in construction of erroneous depositional models with economic implications for reservoir prediction in petroleum exploration.

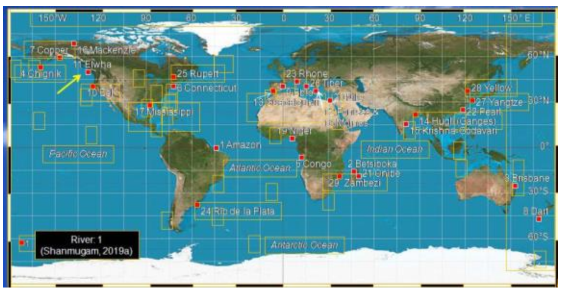

Fig. 40 Location map of sediment plumes around the globe. Note Elwha River plume (arrow)

Fig. 41 Deflecting sediment plume at the mouth of Elwha Ruver. See Shanmugam (2019a). Photo courtesy of Tom Roorda, Roorda Aerial, Port Angeles, WA.

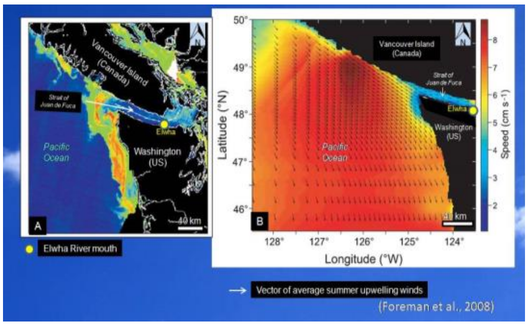

Fig. 42 Wind forcing. Foreman et al. (2008). See Shanmugam (2019a).

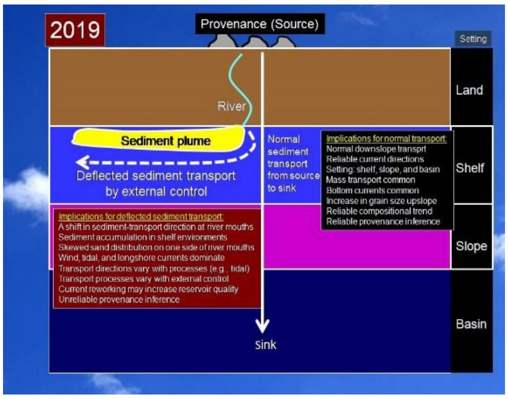

Fig. 43 Deflected sediment transport vs. conventional source to sink downslope transport. From Shanmugam (2019a).

10. MASS TRANSPORT

Mass-transport deposits (MTD) have been documented not only on Earth but also on other planets, such as Mars and Jupiter (Fig. 44). The general term "mass transport" (Fig. 45) (i.e., slides, slumps, and debris flows) represents the failure, dislodgement, and downslope movement of either sediment or glacier under the influence of gravity (Fig. 46). Mass transport is much more efficient in transporting large volumes of sediment of all sizes into the deep sea than turbidity currents (Fig. 46). In soil mechanics (Duncan and Wright, 2005), a stable slope can be maintained only when the factor of safety for slope stability (F) is larger than or equal to 1 (Fig. 47). The sliding motion of failed soil mass commences along the shear surface when the factor of safety (F) is less than 1 (Fig. 47).

$$F = \frac{S}{\tau} = \frac{\text{Shear strength of the soil}}{\text{Shear stress required for equilibrium}} \geqslant 1$$

where

S = Available shear strength, which depends on the soil weight, cohesion, friction angle, and pore-water pressure.

τ = Equilibrium shear stress, which is the shear stress required to maintain a just-stable slope. It depends on the soil weight, pore-water pressure, and slope angle.

On the modern U. S. Atlantic Continental Slope (Fig. 48) most slides occur on gentle slopes of less than 4^0 (Fig. 49) (Booth et al., 1993). On the modern seafloor (Fig. 50), fan-like distribution of MTD has been documented using Multibeam bathymetric images (Greene et al., 2006). MTD is ubiquitous on both land and undersea worldwide (Fig. 51). Examples are shown in Figures 52 to 56. Planar fabric of clasts are a useful criterion for interpreting laminar flow of debris flows in outcrop and core (Fig. 57.

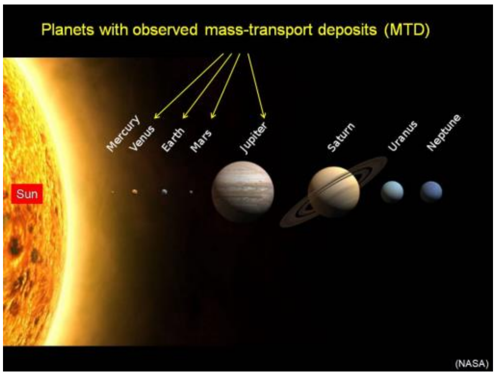

Fig.44 Planets with observed mass-transport deposits (MTD). From Shanmugam (2021a). Elsevier and NASA.

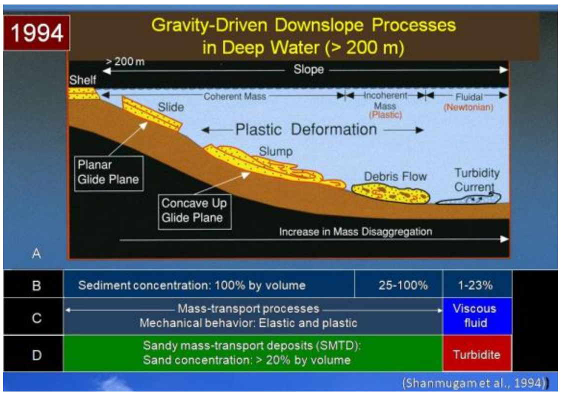

Fig. 45 Gravity-driven downslope processes in deep-marine (> 200 m) environments. From Shanmugam et al. (1994).

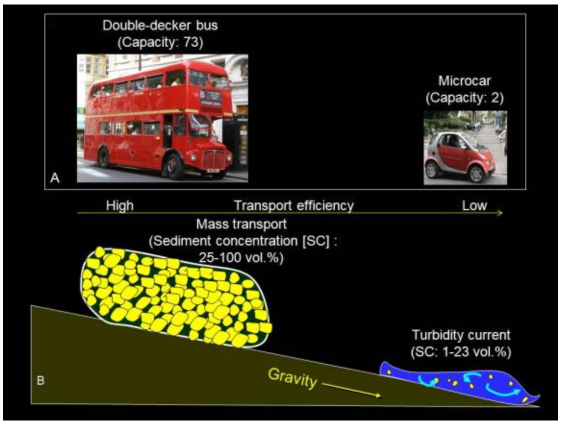

Fig. 46 Comparison of human transport on land (A) with gravity-driven sediment transport under water (B). From Shanmugam (2015).

Fig. 49 Histogram showing frequency distribution of submarine slides with increasing slope angle, U.S. Atlantic Continental Slope. Note most slides occur on

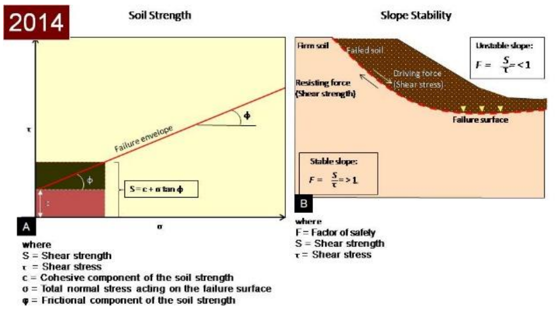

Fig. 47 A. Plot showing that the shear strength of the soil (s) is composed of frictional (ϕ) and cohesive (c) components. B. Conceptual diagram showing that a stable slope can be maintained only when the factor of safety for slope stability (F) is larger than or equal to 1 (Duncan and Wright, 2005). The sliding motion of failed soil mass commences along the shear surface when the factor of safety (F) is less than 1. From Shanmugam (2015).

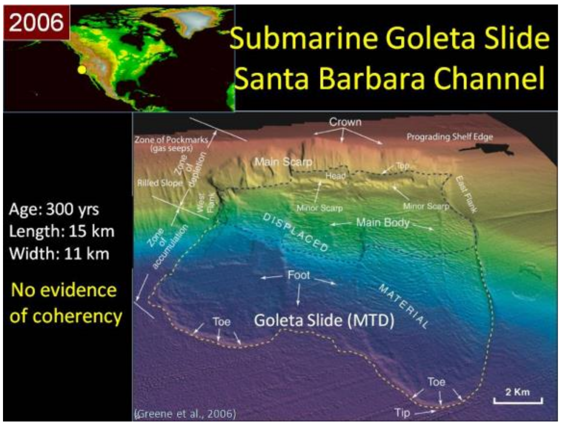

Fig. 50 EM300 Multibeam bathymetric image showing fan-shaped MTD. From Greene et al. (2006).

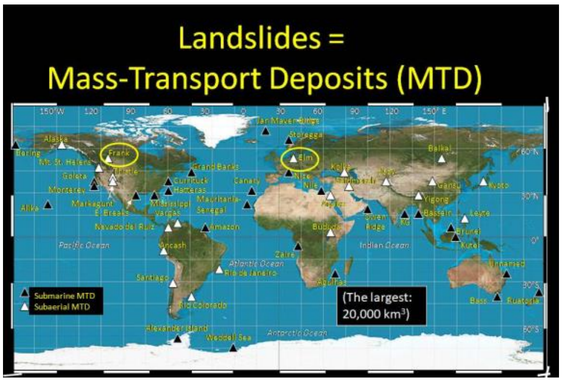

Fig. 51 Locations of Mass─transport deposit (MTD) worldwide. MTD refers to the failure, dislodgement, and downslope movement of either sediment or glacier under the influence of gravity. From Shanmugam (2015).

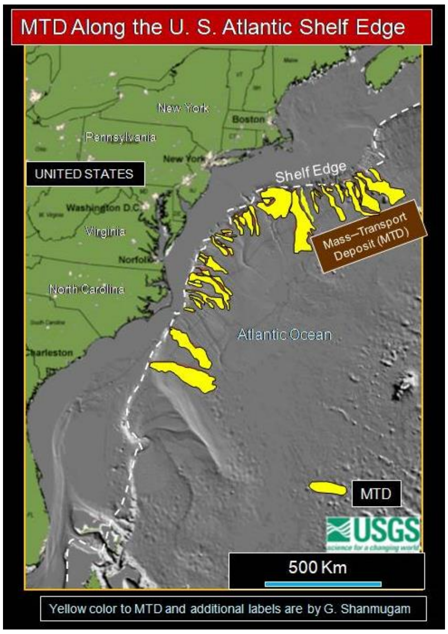

Fig.48 Mass ─Transport Deposits (MTD) on the U. S. Atlantic Margin. These MTDs are mostly composed of muddy types. See ODP Core photo from this area in Fig. 209. Yellow color to MTD and other additional labels are added by G. Shanmugam. Original map by USGS.

Fig. 52 The 2005 La Conchita MTD, California. (Photo: Mark Reed, USGS, NOAA-USGS Debris Flow Task Force, 2005).

Fig. 53 Nevado del Huila, Colombia, 1994 MTD.

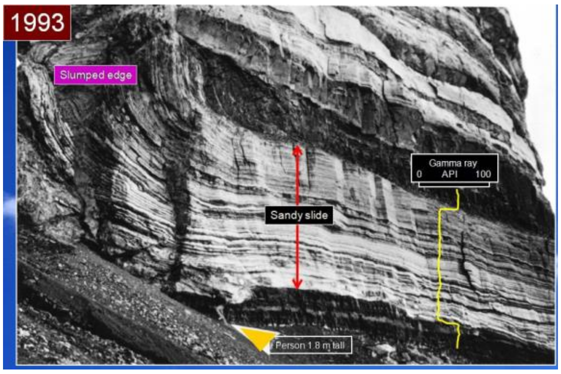

Fig. 54 Outcrop photograph showing sheet-like geometry of an ancient sandy submarine slide (1000 m long and 50 m thick) encased in deep-water mudstone facies. Note the large sandstone sheet with rotated/slumped edge (left). Ablation Point Formation, Kimmeridgian (Jurassic), Alexander Island, Antarctica. Photo courtesy of D.J.M. Macdonald. From Macdonald, et al. {1993). Gamma ray motif and other labels by G. Shanmugam.

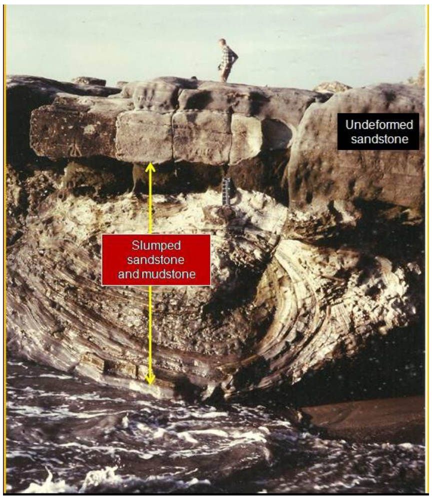

Fig. 55 Outcrop photograph showing slump-folded heterolithic facies (arrow) overlain by undeformed deep-water sandstone, Eocene, La Jolla, California. Source: After Shanmugam (2006a).

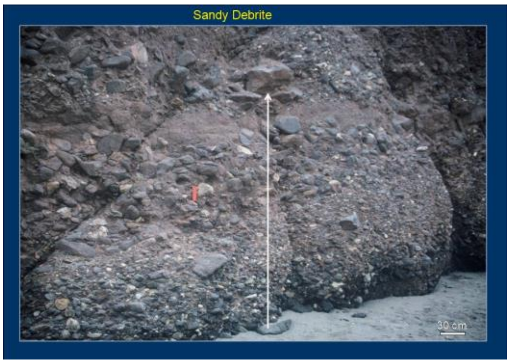

Fig. 56 Outcrop photograph showing inverse grading with floating boulder-size clasts Near the top of sandstone unit (arrow), Middle Miocene, San Onofre Breccia, Dana Point, California.This lithofacies has been interpreted to be sandy debrite.

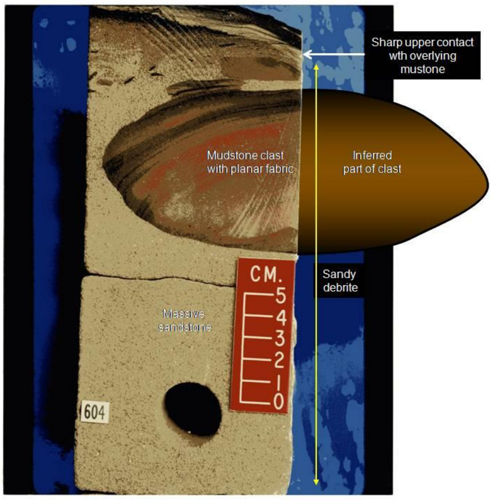

Fig. 57 Core photograph showing a floating mudstone clast near the top of a sand unit, Paleocene, North Sea. Planar fabric, indicative of laminar flow, and sharp upper contact, indicative of flow freezing, are considered evidence for deposition from debris flows. Source: Published in Shanmugam (2012a).

11. Gravity Flows

This review covers 139 years of research on gravity flows since the first reporting of density plumes in the Lake Geneva, Switzerland by Forel (1885). Six basic types of gravity flows have been identified in subaerial and suaqueous environments Shanmugam (2020). They are: (1) hyperpycnal flows, (2) turbidity currents, (3) debris flows, (4) liquefied/fluidized flows, (5) grain flows, and (6) thermohaline contour currents. The first five types are flows in which the density is caused by sediment in the flow, whereas in the sixth type, the density is caused by variations in temperature and salinity. Although all six types originate initially as downslope gravity flows, only the first five types are truly downslope processes, whereas the sixth type eventually becomes an alongslope process. (1) Hyperpycnal flows are triggered by river floods in which density of incoming river water is greater than the basin water. These flows are confined to proximity of the shoreline. They transport mud, and they do not transport sand into the deep sea. There are no sedimentological criteria yet to identify hyperpycnites in the ancient sedimentary record. (2) A turbidity current is a sediment-gravity flow with Newtonian rheology and turbulent state in which sediment is supported by flow turbulence and from which deposition occurs through suspension settling. Typical turbidity currents can function as truly turbulent suspensions only when their sediment concentration by volume is below 9% or C < 9%. This requirement firmly excludes the existence of 'high-density turbidity currents'. Turbidites are recognized by their distinct normal grading in deep-water deposits. (3) A debris flow (c. 25-100%) is a sediment-gravity flow with plastic rheology and laminar state from which deposition occurs through freezing *en masse*. The terms debris flow and mass flow are used interchangeably. General characteristics of muddy and sandy debrites are floating clasts, planar clast fabric, inverse grading, etc. Most sandy deep-water deposits are sandy debrites and they comprise important petroleum reservoirs worldwide. (4) A liquefied/fluidized flow (>25%) is a sediment-gravity flow in which sediment is supported by upward-moving intergranular fluid. They are commonly triggered by seismicity. Water-escape structures, dish and pillar structures, and SSDS are common. (5) A grain flow (c. 50-100%) is a sediment-gravity flow in which grains are supported by dispersive pressure caused by grain collision. These flows are common on the slip face of aeolian dunes. Massive sand and inverse grading are potential identification markers. (6) Thermohaline contour currents originate in the Antarctic region due to shelf freezing and the related increase in the density of cold saline (i.e., thermohaline) water. Although they begin their journey as downslope gravity flows, they eventually flow alongslope as contour currents. Hybridites are deposits that result from intersection of downslope gravity flows and alongslope contour currents. Hybridites mimic the "Bouma Sequence" with traction structures (Tb and Tc). Facies models of hyperpycnites, turbidites, and contourites are obsolete. Of the six types of density flows, hyperpycnal flows and their deposits are the least understood.

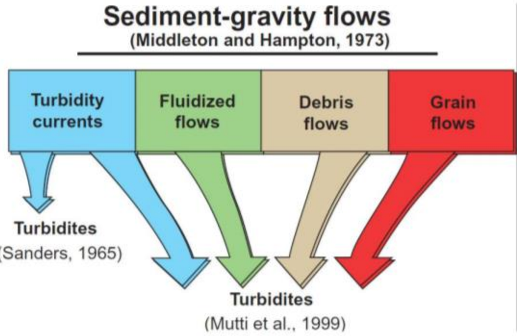

Fig. 58 Two different classification of turbidites. In this article, the term "turbidite" represents deposits of turbidity currents following the definition of Sanders (1965).

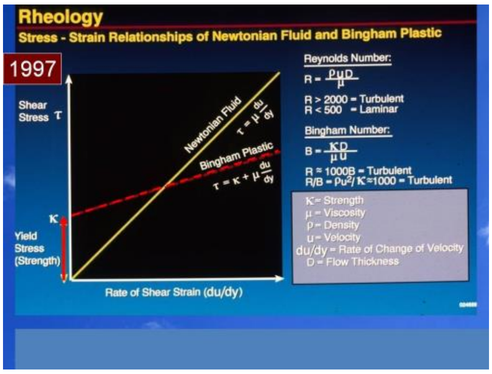

Fig. 59 Rheology (stress-strain relationships) of Newtonian fluids and Bingham plastics. Graph shows that the fundamental rheological difference between debris flows (Bingham plastics) and turbidity currents (Newtonian fluids) is that debris flows exhibit strength, whereas turbidity currents do not. Reynolds number is used for determining whether a flow is turbulent (turbidity current) or laminar (debris flow) in state. From Shanmugam (1997).

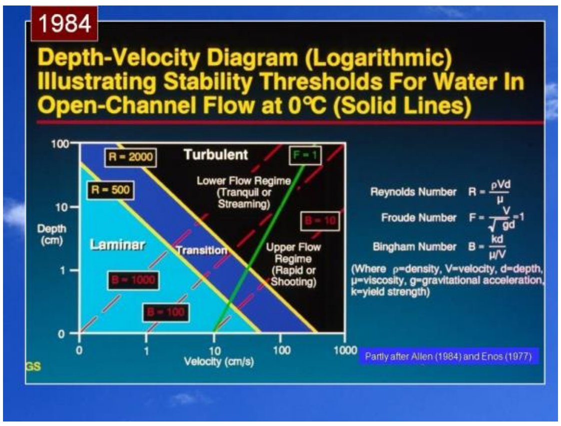

Fig. 60 Depth-velocity diagram showing laminar and turbulent fields of fluids (partly after Allen, 1984; Enos, 1977). From Shanmugam (2012a). Elsevier.

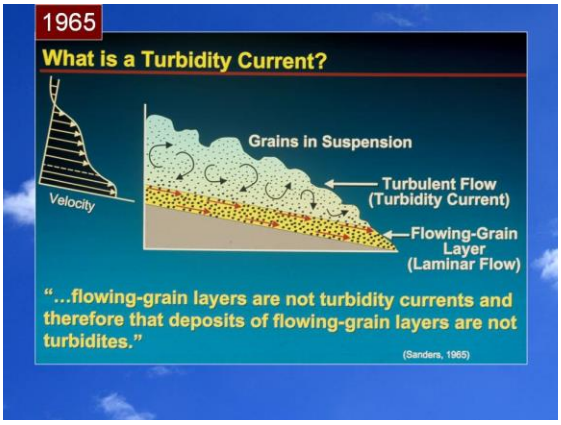

Fig. 61 Turbidity currents are truly turbulent in state in which grains are in suspension (upper part). However, the basal flowing-grain layers are laminar in state and they are not turbidity currents (Sanders, 1965). Sanders' definition is adopted in this article.

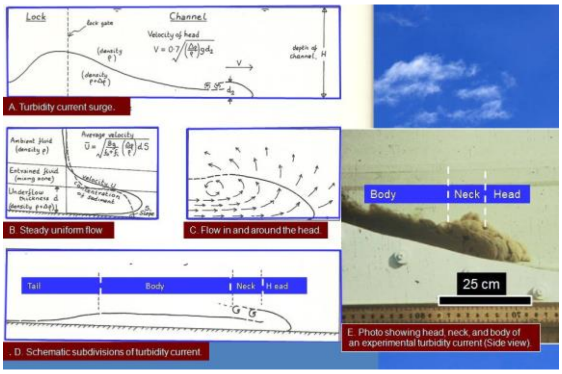

Fig. 64 Hydraulics of experimental turbidity currents. A. Turbidity current surge. B. Steady uniform flow. C. Flow in and around the head. D. Schematic subdivisions of turbidity current. E. Photo showing head, neck, and body of an experimental turbidity current. Credit: A, B, C, and D From Middleton and Hampton (1973). E from experiments by M. L. Natland. Photo courtesy of G. C. Brown.

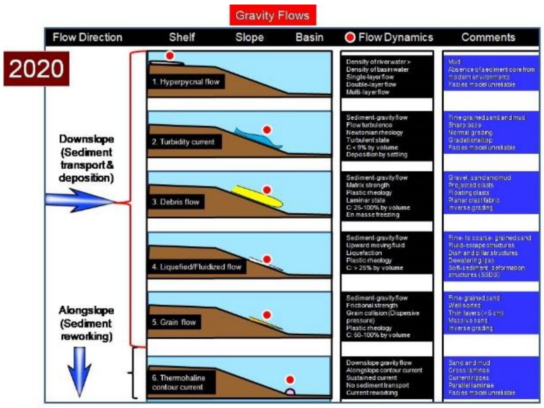

Fig. 62 Types of gravity flows. From Shanmugam (2020).

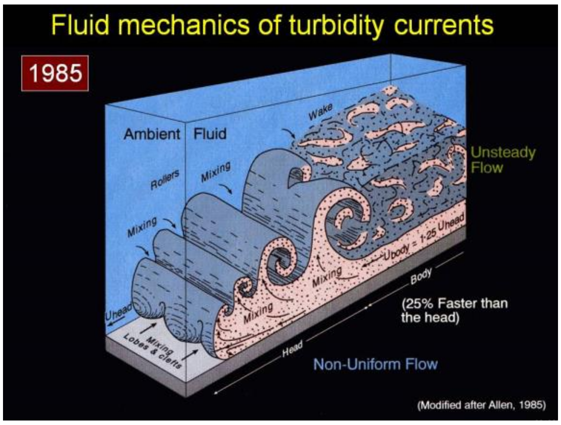

Fig. 65 Turbidity currents. Modified after Allen (1985).

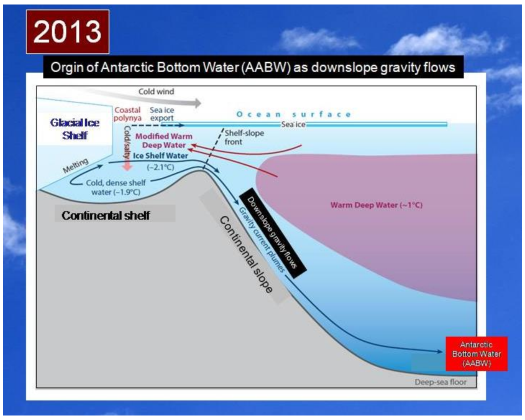

Fig. 63 Origin of Antarctic Bottom Water (AABW) as downslope gravity flows. Modified after Gordon (2013) and Purkey et al. (2018).

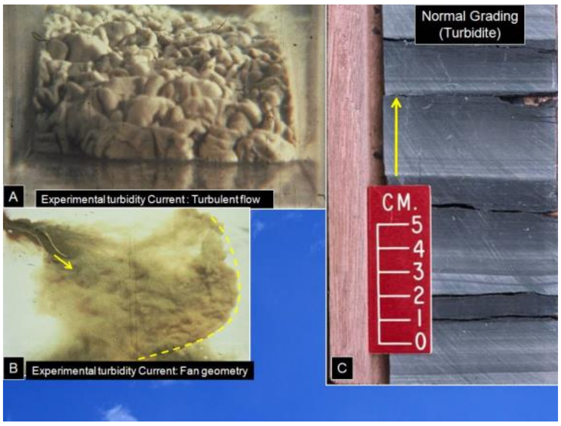

Fig. 66 A. Front view of experimental turbidity current showing turbulent state. B. Map view showing fan geometry. Arrow = Channel mouth. C, Core photo of silty turbidite layers showing normal grading (arrow). Experiments in A and B by M. L. Natland. Photos of turbidity currents courtesy of G.C. Brown. Core photo by G. Shanmugam.

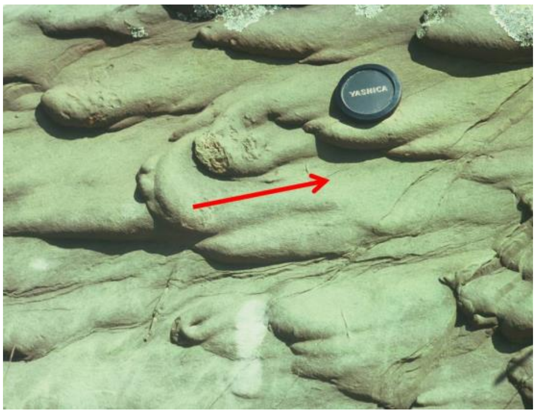

Fig. 67 Flute casts as sole marks in the Jackfork Group (Oklahoma) have been used as evidence for Turbidity currents. However, bottom currents could also generate such sole marks (Klein, 1966). Arrow shows transport direction. Photo by G. Shanmugam.

Fig. 68 Basin-plain turbidites, Zumaya Beach, Northern Spain

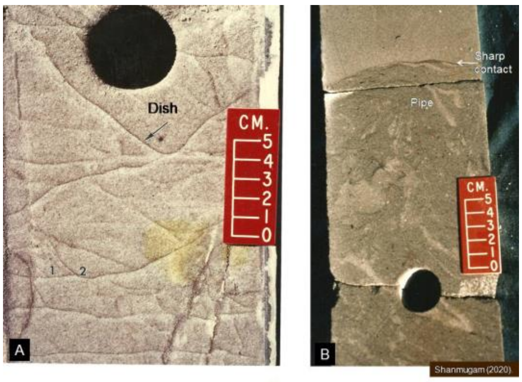

Fig. 69 (A)-Core photograph showing water-escape dish structures by liquidization. B. Pipe. From Shanmugam (2020).

12. High ─density turbidity currents

Turbidity currents are characterized by low sediment concentration, commonly below 9% sediment concentration by volume (Fig. 71A) (Bagnold, 1962). Experimental concentrations that exceed this limit cannot be considered normal turbidity currents. They are commonly mass flows or sandy debris flows (Shanmugam, 1996). Therefore, experiments on "high─density turbidity currents" (Fig. 71B) by Postma et al. (1988) is a diversion because their concept represents sandy debris flows (Shanmugam, 1996). Sanders (1965) recognized the importance of density-stratified gravity flows with basal laminar and upper turbulent layers (Fig. 61). Our flume experiments on sandy debris flows confirmed Sanders' concept by developing density-stratified flows (Fig. 72) (Shanmugam, 2000; Marr et al., 2001). Such flows are mislabeled as "high─density turbidity currents" by other researchers (Fig. 72). My paper on sandy debris flows (Shanmugam, 1996), which provided clarity to the long-standing,confused concept of "high─density turbidity currents" (Figs. 73─76), became the single most cited paper among three top sedimentological journals (Fig. 77).

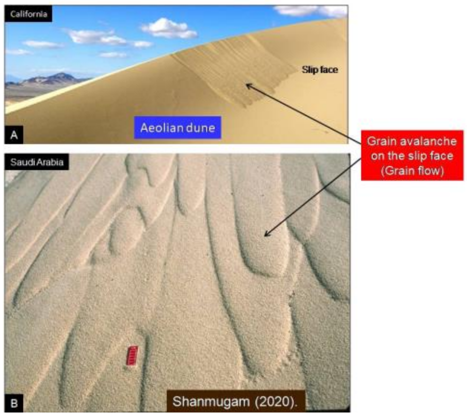

Fig. 70 Grain flows. From Shanmugam (2020).

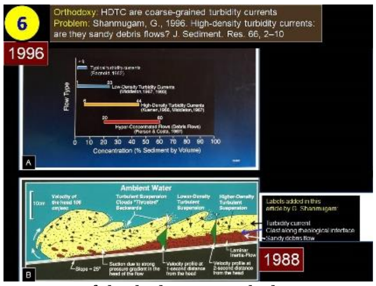

Fig. 71 Problems with the concept of high-density turbidity currents (HDTC). A. Overlapping sediment concentration. From Shanmugam (1996). B. Stratified flows with laminar layer at the base, From Postma et al. (1988).

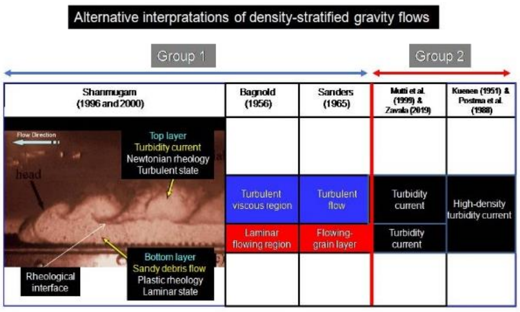

Fig. 72 Fig. 2 Alternative interpretations of density-stratified gravity flows. From Shanmugam (2019b).

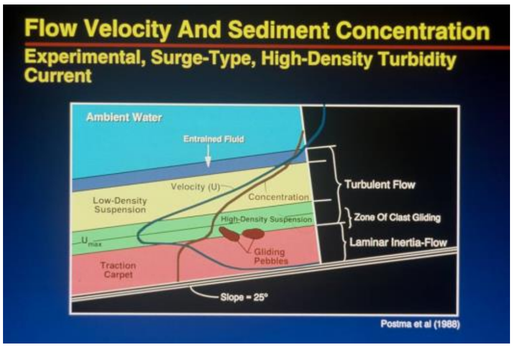

Fig. 73 Origin of mudstone clasts along rheological interface between underlying laminar-inertia flow and upper turbulent flow. Source: Postma, G., Nemec, W., Kleinspehn, K.L., (1988).

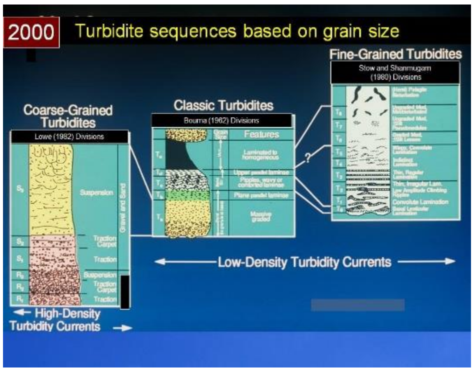

Fig. 74 Three major types of turbidite facies models based on grain size. From Shanmugam (2000).

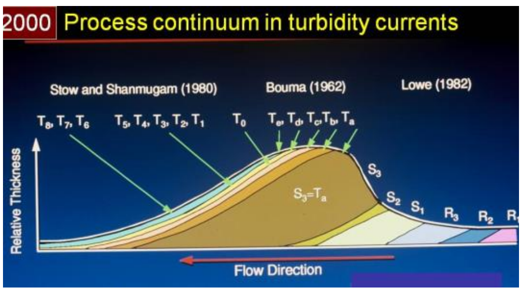

Fig. 75 Process continuum in turbidity currents and related divisions. Modified after Lowe (1982). From Shanmugam (2000).

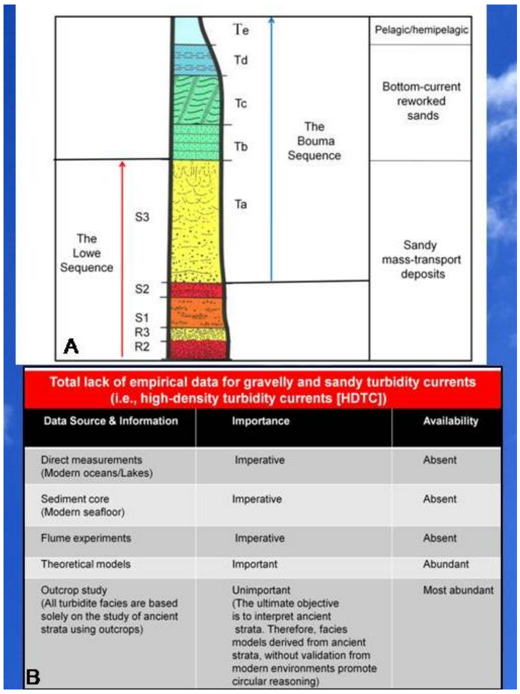

Fig. 76 Problems with HDTC concept

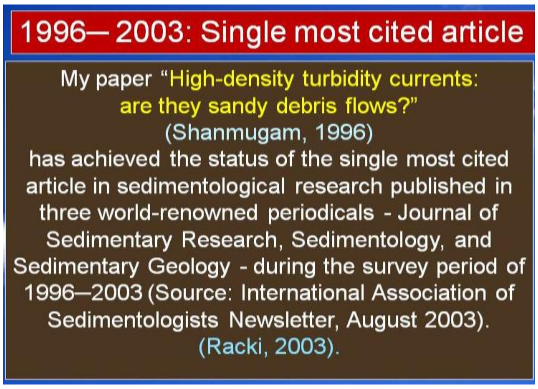

Fig. 77 IAS Survey results showing the importance of the controversy surrounding the concept of "High-density turbidity currents"(Racki, 2003).

13. Flume experiments on sandy debris flows

In verifying the concept of sandy debris flows with low clay content\ experiments were conducted on subaqueous sandy debris flows at St. Anthony Falls Laboratory of the University of Minnesota "(Shanmugam 2000; Marr et al., 2001). The following summary is from Marr et al. (2001). Deep-water deposits consisting mainly of massive sand are commonly identified as deposits of turbidity currents (i.e., turbidites). Speculation has risen in recent years as to whether some of these massive sandy deposits could have instead been deposited by debris flows. This possibility is explored here by examining the flow mechanics of sand-rich subaqueous gravity flows by means of laboratory experiments. In these experiments, sandy gravity flows were generated when well-mixed slurries of sand, clay, and water were released into a tank filled with tap water and allowed to flow under gravity over a slope that declined from 4.6° to 0.0°. The observed flow mechanics and resulting depositional features were strongly tied to the "coherence" of the debris flows (i.e., the ability of the slurry to resist being eroded and broken apart by the shear and pressure undergone by the flow). Low water content and high clay content resulted in strongly coherent debris flows, whereas high water content and low clay content resulted in weakly coherent flows. As little as 0.7 to 5 wt% of bentonite clay or 7 to 25 wt% of kaolinite clay at water contents ranging from 25 to 40 wt% was required to generate coherent gravity flows. Weakly coherent and moderately coherent flows produced significant, low-concentration subsidiary turbidity currents, and their deposits developed coarse- tail grading, water-escape structures, and minor increases in thickness at the base of the slope. Strongly coherent debris flows commonly hydroplaned and generated only minor subsidiary turbidity currents. Their deposits were structureless and ungraded, commonly showing tension cracks, compression ridges, water-escape structures, detached slide blocks, and a significant increase in thickness at the base of the slope. Application of distorted geometric scaling suggests that many aspects of these experiments appropriately scale up to the field scale of natural submarine debris flows. Our flume experiments on sandy debris flows (Shanmugam, 2000; Marr et al., 2001) have been a major achievement in process sedimentology. This is because finally it provided clarity to the long-standing, confused concept of "high─density turbidity currents" (Figs. 78─88).

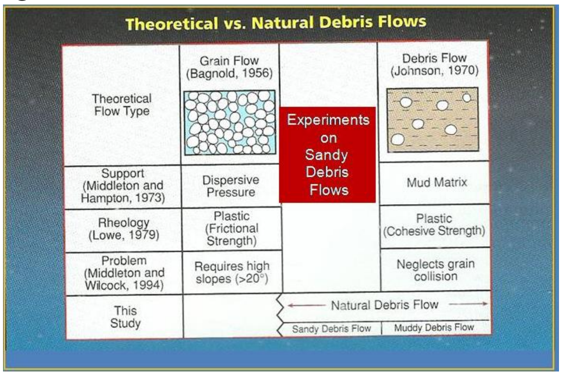

Fig. 78 Region of flume experiments on Sandy Debris Flows (Shanmugam, 2000; Marr et al., 2001).

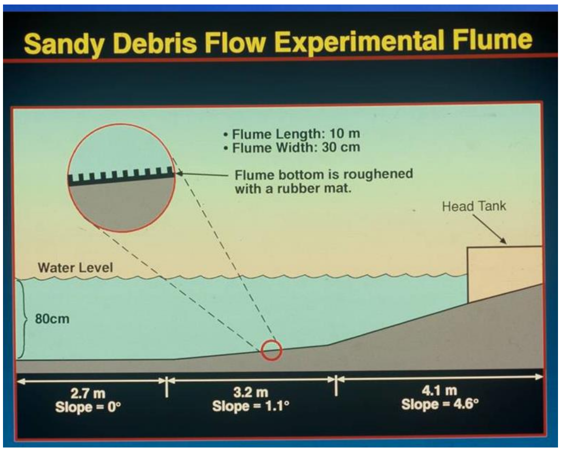

Fig.79. Dimensions of flume used in experiments on Sandy Debris Flows (Shanmugam, 2000; Marr et al., 2001).

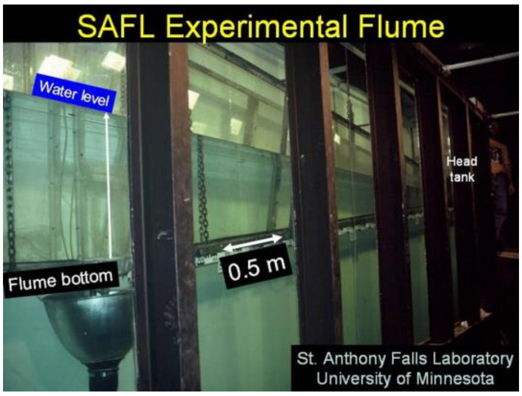

Fig. 80 Flume used in the generation of Sandy debris flows in a laboratory experiment.

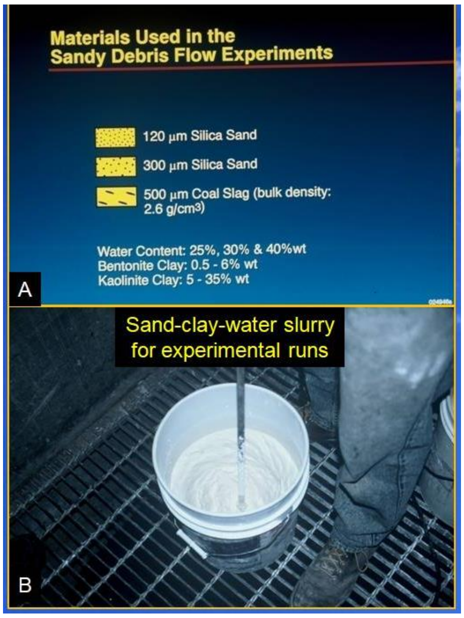

Fig. 81 Materials used in flume experiments on Sandy Debris Flows. (Shanmugam, 2000; Marr et al., 2001).

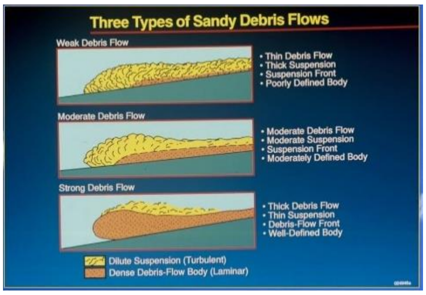

Fig. 82 Three types if sandy debris flows

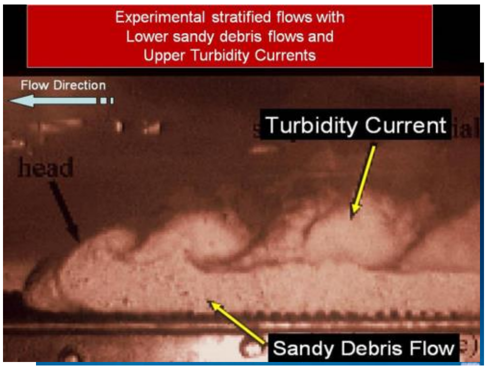

Fig. 83 Experimental stratified flow with lower Sandy debris flow and upper Turbidity current.

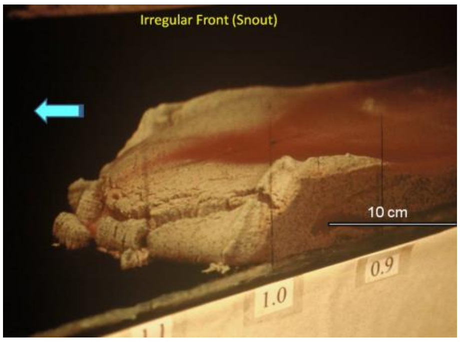

Fig. 84 Experimental flow with irregular snout, typical of debris flows

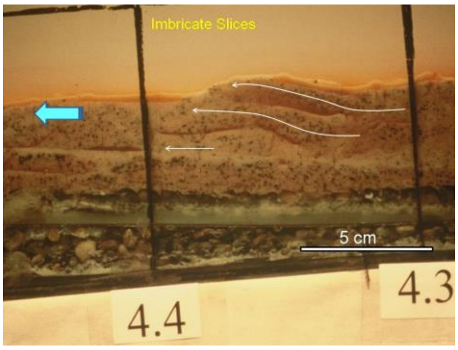

Fig. 85 Experimental flow showing imbricate slices, analogous to sigmoidal deformation structures (Shanmugam et al., 1988).

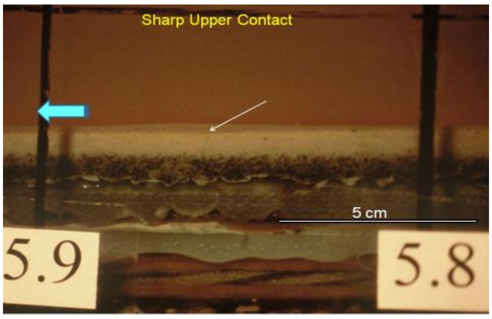

Fig. 86 Experimental deposit showing sharp upper contact

14. Bottom Currents

The four basic types of deep-marine bottom currents are (Southard and Stanley, 1976;

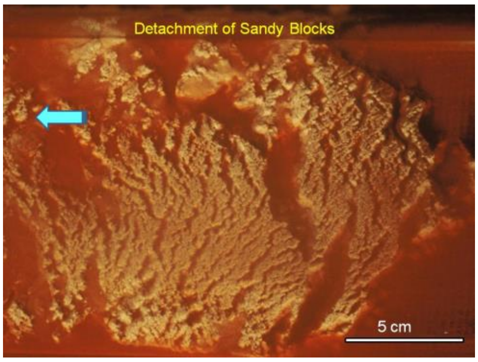

Fig. 87 Experimental deposits showing detachment of sandy blocks

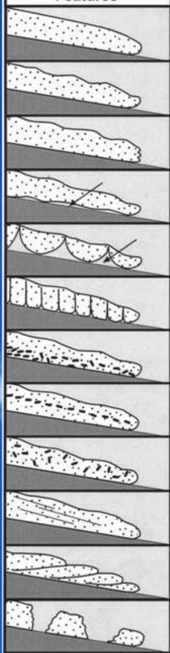

Features	Observation	Interpretation
	Sharp Upper Contact	Freezing of Flow and Plastic Rheology
	Irregular Upper Contact and Lateral Pinch-out Geometry	Freezing of Primary Relief and Plastic Rheology
	Irregular Front (Snout)	Freezing of Primary Relief and Plastic Rheology
	Non-Erosive Base and Water Entrapment (↙)	Laminar Flow and Hydroplaning
	Dish Structures and Water Entrapment (↙)	Hydroplaning and Water Escape
	Vertical Pipes	Hydroplaning and Water Escape
	Grain Segregation and Normal Grading	Grain Settling from Weak Flow
	Planar Fabric and Inverse Grading	Laminar Flow and Flow Strength
	Random Fabric	Flow Strength and Freezing of Flow
	Internal Layers	Mass Movement and Secondary Glide Planes
	Imbricate Slices	Mass Movement and Compression
	Isolated Blocks	Mass Movement and Tension
Flow Direction →	120 µm Silica Sand; 500 µm Coal Slag (bulk density: 2.6 g/cm3)	

Fig. 88 Summary diagram showing experimental observations and interpretations. From Shanmugam (2000).

Shanmugam, 2008b): (1) thermohaline-induced geotropic contour currents (Heezen et al., 1966), (2) wind-driven bottom currents (Pequegnat, 1972), (3) tide-driven bottom currents (mostly in submarine canyons) (Shepard et al., 1979), and (4) internal wave/tide-driven baroclinic currents (Gill, 1982) (Figs. 89─100). Traction structures are common in deposits of all four types of bottom currents (Fig. 93), including the Atlantic contourites (Fig. 94). In the Gulf of Mexico with wind-driven Loop Current (Fig. 95), there are traction deposits both on the modern seafloor (Fig. 96) and in the subsurface (Fig. 97). However, there are no diagnostic sedimentological or seismic criteria for distinguishing ancient contourites from the other three types. Double mud layers are a reliable criterion for recognizing deep-marine tidalites in cores and outcrops (Visser, 1980). Shanmugam et al. (1993) have documented the importance of bottom-current reworking and related traction structures in the Ewing Bank area, Gulf of Mexico. In this review, the original definition of "Contourites" by Hollister (1967) for deposits of thremohaline-induced contour currents is adopted (Fig. 98). The contourite facies model (Fig. 99) developed from the Gulf of Cadiz (Fig. 100) is obsolete because of complicating factors associated with Gulf of Cadiz (Fig. 100) (Shanmugam, 2016b, 2017b; Zenk, 2008). On a positive note, the IODP Expedition 339 in the Gulf of Cadiz (Hernández-Molina et al., , 2013) has resulted in some realistic observation of sedimentary structures indicative of traction processes (de Castro et al., 2020).

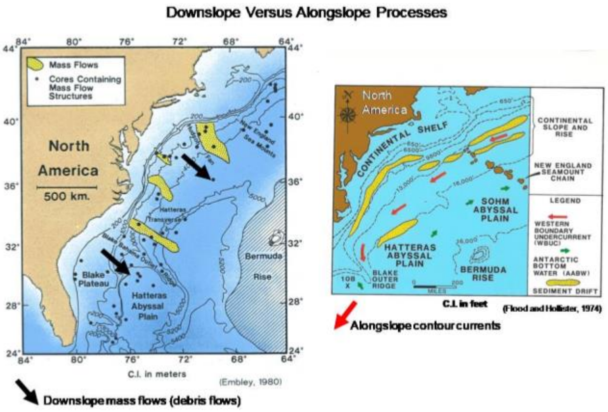

Fig. 89 Downslope Versus Alongslope Processes. From Shanmugam (2017b).

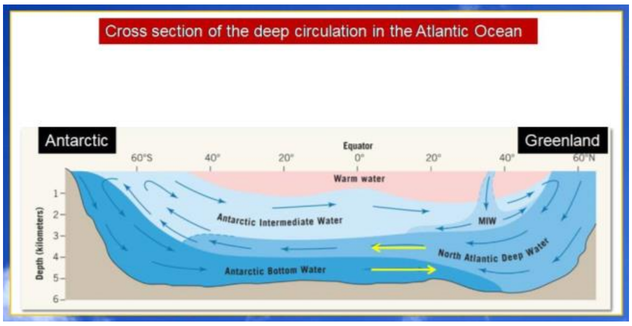

Fig. 90 Cross section of the deep circulation in the Atlantic Ocean. https://www.chegg.com/homework-help/questions-and-answers/figure-1212d-cross-section-atlantic-ocean-use-complete-following-figure-1212-cross-section-q36799777

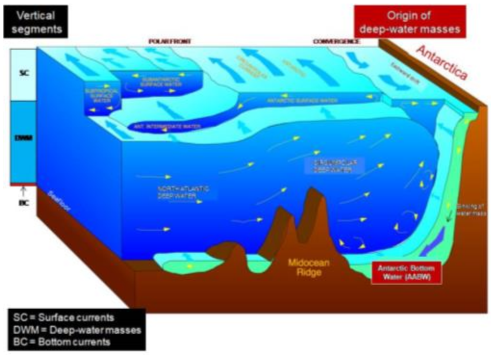

Fig. 91 A conceptual model of the Southern Ocean showing three vertical segments, composed of the upper surface currents, the middle deep-water masses, and the lower bottom currents, forming a vertical continuum (left). Note the origin of Antarctic Bottom Water (AABW) as a gravity flow (right). From Shanmugam (2012a). Modified after Hannes Grobe, April 7, 2000. http://en. wikipedia.org/wiki/File:Antarctic _bottom_water_hg.png (accessed 18.05.11.)

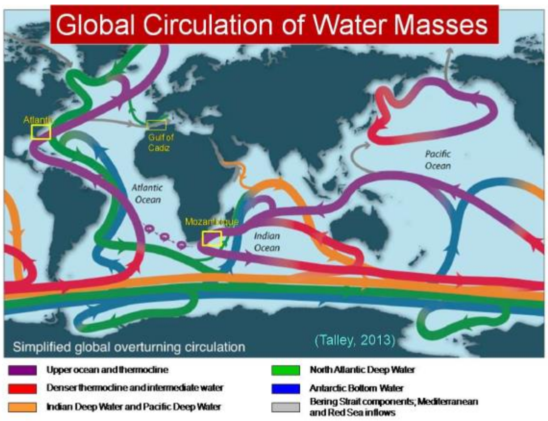

Fig. 92 Map showing the global overturning circulation (GOC). Talley (2013).

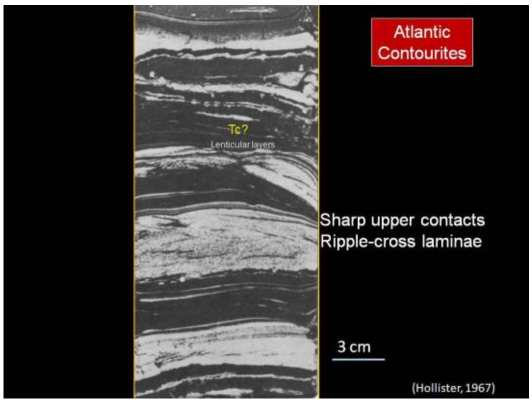

Fig. 93. Traction structures in Atlantic Contourites. From Hollister (1967).

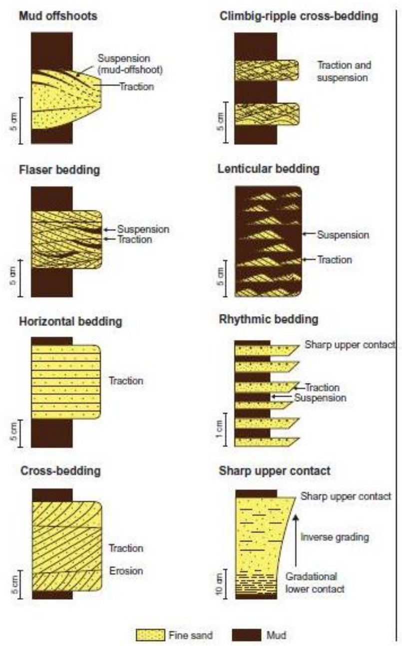

Fig. 94 Types of traction structures in Bottom–current reworked sands (BCRS). From Shanmugam et al. (1993).

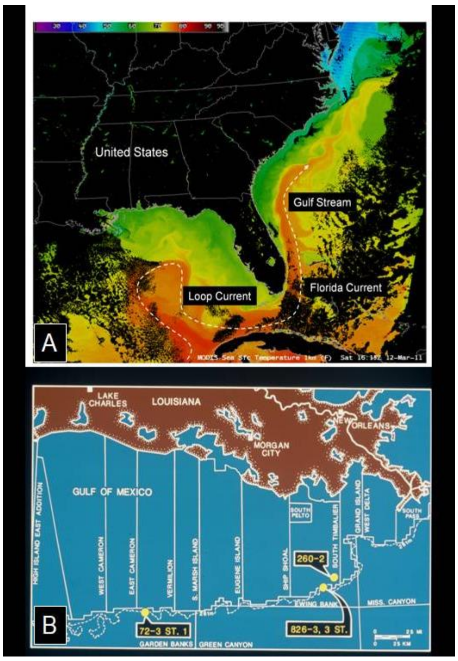

Fig. 95 (A) Sea surface temperature (SST) image showing the Loop Current in the Gulf of Mexico and the axis of the Gulf Stream in the Atlantic Ocean along the U.S. Continental margin on March 12, 2011. (B) Location map of Ewing Bank area. From Shanmugam (2012a).

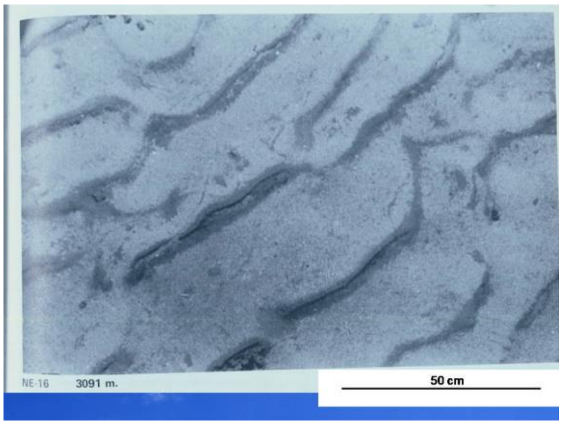

Fig. 96 Underwater photograph showing ripples on the seafloor. Gulf of Mexico. From Pequegnat (1972).

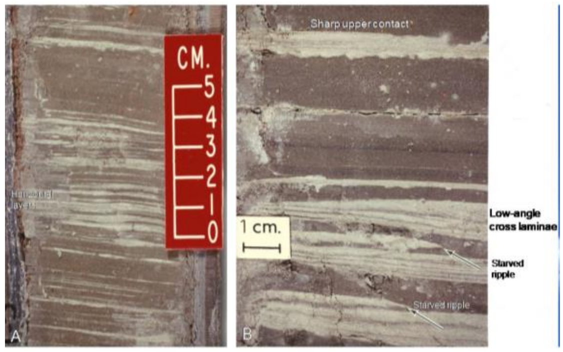

Fig. 97. Core photograph showing rhythmic layers of sand and mud. Middle Pleistocene, Gulf of Mexico. (B) Core photograph showing discrete thin sand layers with sharp upper contacts (top arrow). Traction structures include horizontal laminae, low-angle cross-laminae, and starved ripples. Dip of cross-laminae to the right suggests current from left to right. Note rhythmic occurrence of sand and mud layers. Middle Pleistocene, Gulf of Mexico. Source: (A) From Shanmugam (2012a). (B) Shanmugam et al. (1993).

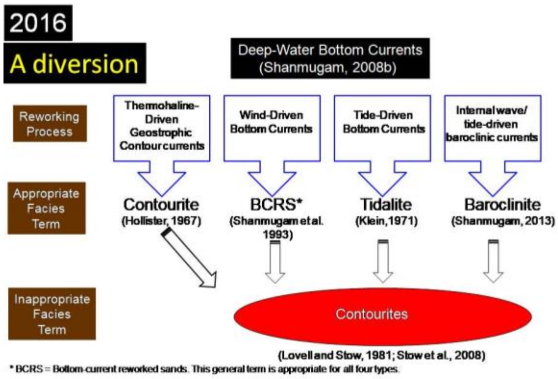

Fig. 98 I follow the original definition of "Contourites" for exclusively deposits of thermohaline–induced geostrophic contour currents proposed by Hollister (1967). Note alternative nomenclature used for contourites by Lovell and Stow (1981). Modified after Shanmugam (2016b).

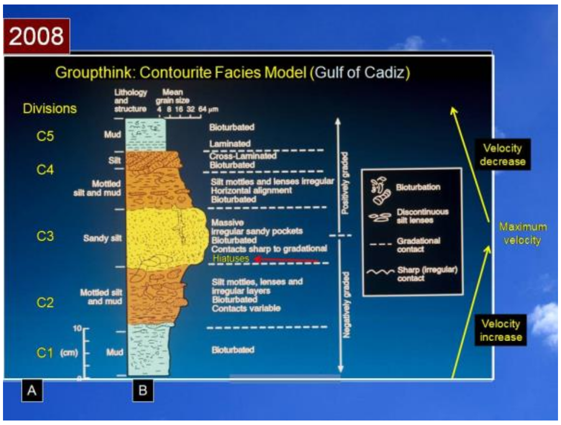

Fig. 99 A. Revised contourite facies model with five divisions (C1_C5) proposed by Stow and Faugères (2008). B. Original contourite facies model from Gulf of Cadiz by Faugères et al. (1984).

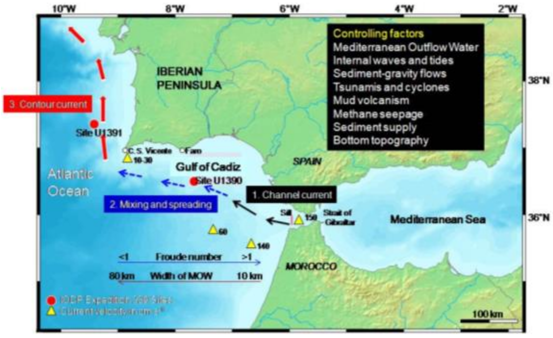

Fig. 100 Schematic diagram showing the location of Gulf of Cadiz and complex transport nature of the Mediterranean Outflow Water (MOW). From Shanmugam (2016b).

15. The Kelvin ─ Helmholtz waves

The Kelvin-eHelmholtz instability defines a fluid instability in nature. It occurs when there is velocity shear in a single continuous fluid or in a velocity difference across the interface between two fluids. Kelvin-Helmholtz instabilities are visible as billow clouds in the atmospheres of planets, such as in cloud formations on Earth (Fig. 101). They also develop waves in the oceans.

In a recent study (Fig. 102), Ge et al. (2022) stated that "Here, we demonstrate, on the basis of a high-resolution advanced numerical CFD (computational fluid dynamics) simulation and rock-record examples, that the depositional event in reality involves many brief episodes of non─deposition. The reason is inherent hydraulic fluctuations of turbidity current energy driven by interfacial Kelvin-Helmholtz waves." What is the practical significance of these "turbidites with hiatuses" associated with Kelvin-Helmholtz waves? Conventionally, a genetic facies model is designed for a single depositional event, without internal hiatuses.

A classic example is the turbidite facies model or the Bouma Sequence" (Bouma, 1962) (Fig. 25). According to Middleton (1973), Walther's Law is not meaningful for sequences with internal hiatuses. In other words, Walther's Law is not meaningful for these "turbidites with hiatuses" discussed by Ge et al. (2022). Importantly, these turbidites are problematic in stratigraphic correlations (Shanmugam, 2022f).

Fig. 101 Kelvin-Helmholtz clouds look like ocean waves. Photo taken on M5, south of Birmingham/Black country driving towards Worcester (UK) on March 28, 2022 around sunset by Erms Hammersley. Photo credit: EarthSky and Matty Hammersley.

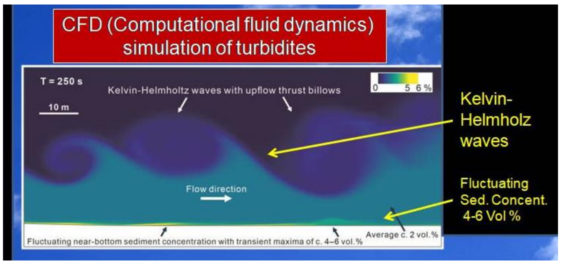

Fig. 102 Image of Kelvin-Helmholtz waves and bottom sediment layer. From Ge et al. (2022). Additional labels by G. Shanmugam (2022f).

16. Internal waves

Detailed accounts of internal waves and tides were provided by Gill (1982) and Apel (1987, 2000, and 2002). Jackson *2004) compiled a comprehensive atlas of modern internal waves in the world's oceans. For the benefit of petroleum geologists, Shanmugam (2013) reviewed the topic of "Modern internal waves and internal tides along oceanic pycnoclines: challenges and implications for ancient deep-marine baroclinic sands. Thus far, the subject of deep-marine sands emplaced by baroclinic currents associated with internal waves and internal tides as potential reservoirs has remained an alien topic in petroleum exploration. Internal waves are gravity waves that oscillate along oceanic pycnoclines. Internal tides are internal waves with a tidal frequency. Internal solitary waves (i.e., solitons), the most common type, are commonly generated near the shelf edge (100–200 m [328–656 ft] in bathymetry) and in the deep ocean over areas of sea-floor irregularities, such as mid-ocean ridges, seamounts, and guyots. Empirical data from 51 locations in the Atlantic, Pacific, Indian, Arctic, and Antarctic oceans reveal that internal solitary waves travel in packets. Internal waves commonly exhibit (1) higher wave amplitudes (5–50 m [16–164 ft]) than surface waves (<2 m [6.56 ft]), (2) longer wavelengths (0.5–15 km [0.31–9 mi]) than surface waves (100 m [328 ft]), (3) longer wave periods (5–50 min) than surface waves (9–10 s), and (4) higher wave speeds (0.5–2 m s^{-1} [1.64–6.56 ft s^{-1}]) than surface waves (25 cm s^{-1} [10 in. s^{-1}]). Maximum speeds of 48 cm s^{-1} (19 in. s^{-1}) for baroclinic currents were measured on guyots. However, core-based sedimentologic studies of modern sediments emplaced by baroclinic currents on continental slopes, in submarine canyons, and on submarine guyots are lacking. No cogent sedimentologic or seismic criteria exist for distinguishing ancient counterparts. Outcrop-based facies models of these deposits are untenable. Therefore, potential exists for misinterpreting deep-marine baroclinic sands as turbidites, contourites, basin-floor fans, and others. Economic risks associated with such misinterpretations could be real.

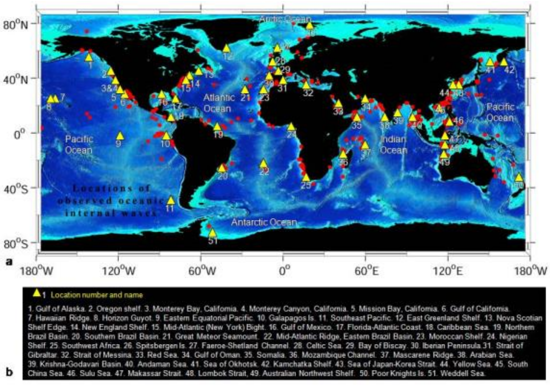

Fig. 103 Locations of 51 examples of internal waves. From Shanmugam (2013).

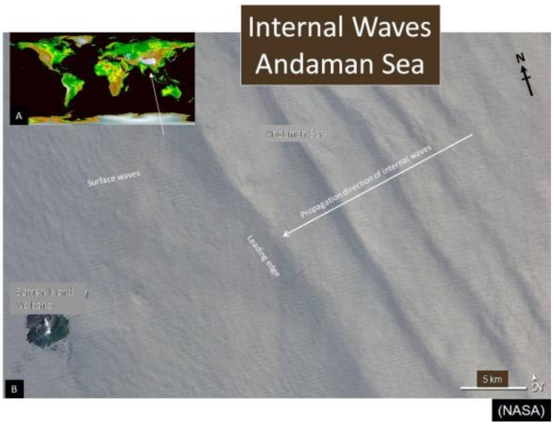

Fig. 104. A. Index map. B. Satellite image of internal waves, Andaman Sea. From Shanmugam (2021a). NASA

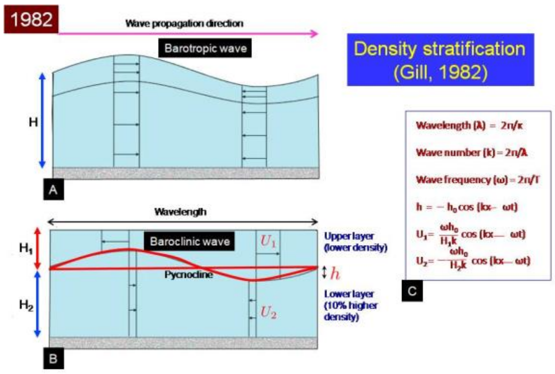

Fig. 105 A. Barotropic waves. B. Baroclinic waves. C. Explanation. A theoretical progress was made by Gill (1982) who proposed that density stratifications in the world's oceans could be used to explain baroclinic waves along pycnoclines. From Shanmugam (2013).

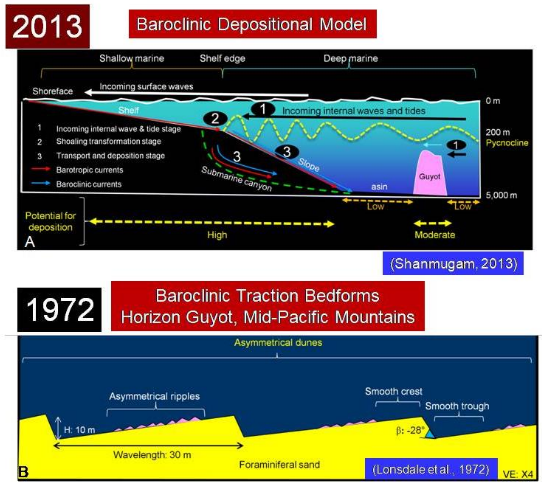

Fig. 106 Baroclinic Depositional Model (A) and ripple bedforms (B) associated with internal waves and tides. From Shanmugam (2013).

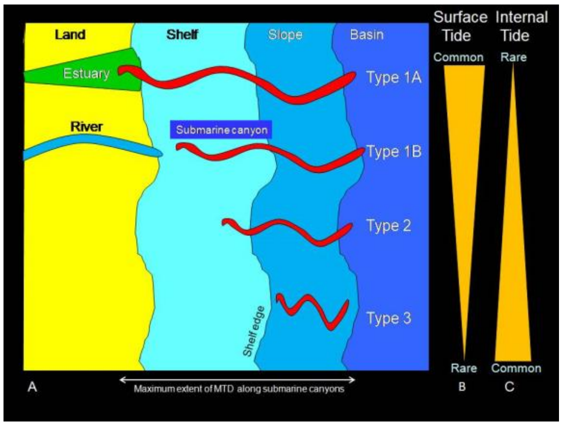

Fig. 107 Types of submarine canyons and internal waves. Canyon types modified after Harris and Whiteway (2011). From Shanmugam (2021a).

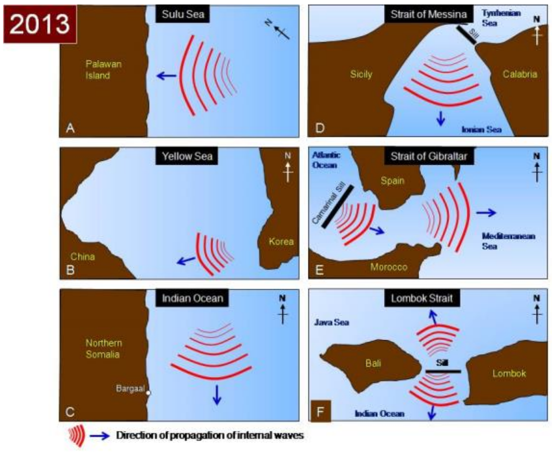

Fig. 108 Maps showing the variable directions of propagation of internal waves. From Shanmugam (2013).

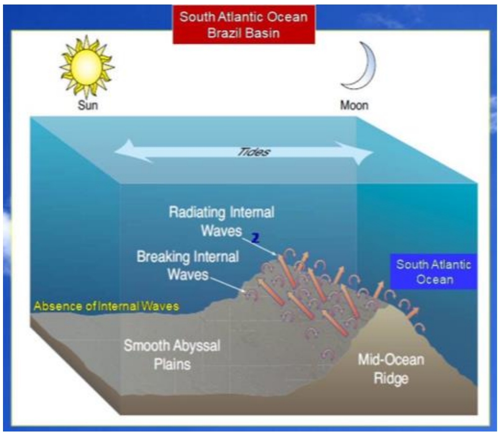

Fig. 109 Internal waves breaking over the Mid-Ocean Ridge, Brazil Basin. Note absence of internal waves over the smooth abyssal plains. Modified after St. Laurent et al. (2012).

17. Hybrid flows: Ewing Bank, Gulf of Mexico

According to the Cambridge Dictionary, the term "hybrid" represents the hybrid offspring byproducts of two different plants, animals, or other entities (https://dictionary.cambridge.org/ dictionary / learner-english/hybrid, accessed June 2, 2020). Accordingly, the term "hybrid flows" is defined in this book to represent the intersection of two different processes, such as alongslope bottom currents (e.g., contour currents) intersecting with downslope sediment-gravity flows (e.g., sandy debris flows, turbidity currents, etc.) in deep-water environments (e.g., continental slope (Fig. 110). Such an interaction commonly results in bottom-current-reworked sands with traction structures, which were documented in the Ewing Bank area, Gulf of Mexico (Shanmugam et al., 1993a).

In recent years, the concept of hybrid flows has been misapplied to flow transformation (Figs. 111 and 112).

The term "Hybridite" represents an amalgamated offspring deposit of two hydrodynamically different flow types, such as sandy debris flows and contour currents (i.e., hybrid flows).

Recently, a diversion was caused by Rodrigues et al. (2022, their Fig. 18) by introducing the term "mixed system" for intersecting down-slope turbidity currents and along-slope bottom currents. Rodrigues et al. (2022) assumed bottom current is a single process. However, bottom currents are composed of four processes that include tidal currents which do not flow along-slope (Shanmugam, 2008b). Shanmugam (2022c) debated this issue.

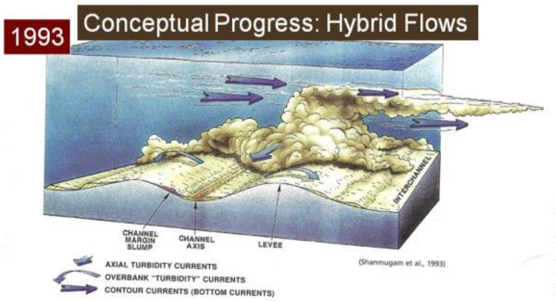

Fig. 110 Hybrid flows originally proposed by Shanmugam et al. (1993).

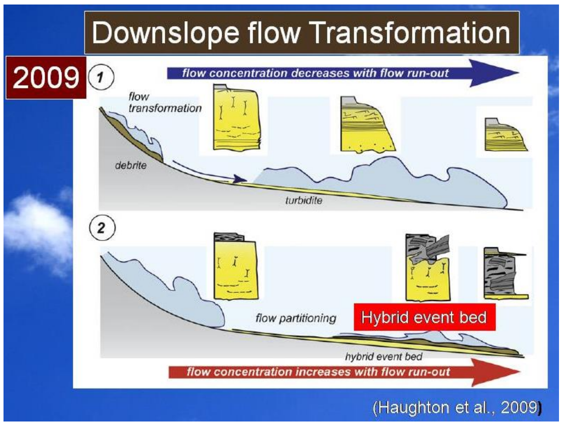

Fig. 111 Misapplication of hybrid-flow concept to downslope flow transformation by Haughton et al. (2009).

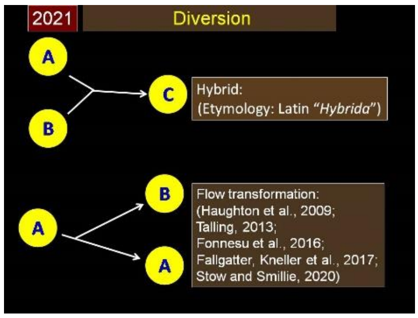

Fig. 112 Hybrid flows do not represent flow transformation. Modified after Shanmugam (2021a).

18. Tidalites: The Krishna─Godavari Basin, Bay of Bengal

The eastern continental margin of India Eigs. 113 and 114), along the western region of the Bay of Bengal, is composed of four major sedimentary basins from north to south: (1) the Bengal, (2) the Mahanadi, (3) the Krishna–Godavari (KG), and (4) the Cauvery (Subrahmanyam and Chand 2006). Sediments in these basins have been supplied by the four major river systems, namely the Ganges–Brahmaputra (two rivers), the Mahanadi, the Krishna–Godavari (two rivers), and the Cauvery (Fig. 115A), respectively. Operator Reliance Industries Limited

Fig. 113 Location map of Krishna-Godavari (KG) Basin, India. From Bastia et al. (2006).

and Niko Resources discovered gas in Pliocene deep-water siliciclastic reservoirs of the Krishna–Godavari Basin in 2002 (Shirley 2003). These reservoir sands and the processes that deposited them are the focus of our paper (Shanmugam, Shrivastava, and Das, 2009), sponsored by the Reliance Industries Ltd. The primary objective of our paper was to develop a depositional model to understand the distribution of Pliocene sand in our

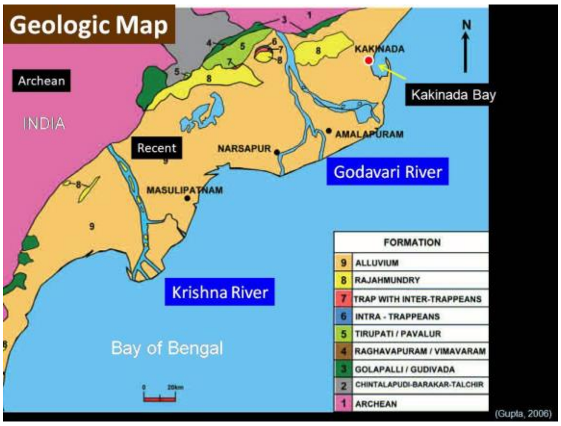

Fig. 114 Grologic map of KG Basin (Gupta, 2006). Additiobal labels and symbols by G. Shanmugam. See Fig. 122 for Photo of DML from a trench in Kakinada Bay

study area using conventional cores from three wells in Block KG-D6 of the offshore Krishna–Godavari Basin (Fig. 115C). Below is a summary (Figs. 116-125)

A depositional model is proposed for deep-water petroleum reservoir sands (Pliocene) in the Krishna–Godavari Basin, Bay of Bengal, India. Based on examination of 313 m of conventional cores from three wells, five depositional facies have been interpreted: (1) sandy debrite, sandy slump, sandy slide, and sandy cascading flow, (2) muddy slump and debrite, (3) sandy tidalite, (4) muddy tidalite, and (5) hemipelagite. Debrites and slumps constitute up to 99% in one well. Sand injectites are common. Pliocene environments are interpreted to be comparable to the modern upper continental slope with widespread mass-transport deposits and submarine canyons in the Krishna–Godavari Basin. Frequent tropical cyclones, tsunamis, earthquakes, shelf-edge canyons with steep-gradient walls of more than 30u, and seafloor fault scarps are

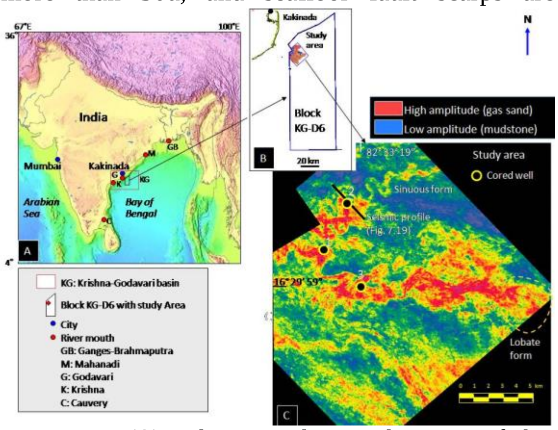

Fig. 115 (A) Index map showing locations of the Krishna-Godavari (KG) Basin and the KG-D6 block (offshore, State of Andhra Pradesh) on the eastern continental margin of India. (B) Map showing location of our study area in the Block KG-D6. (C) Root mean square (RMS) seismic amplitude map of our study area showing locations of cored wells 1, 2, and 3. RMS map represents the entire reservoir (400 ms time window). Amplitude color code: bright red, high amplitude (gas-charged sandy lithologies); yellow, intermediate amplitude (mixed lithologies); blue-to-dull green, low amplitude (non sandy or muddy lithologies). Sinuous and lobate planform geometries are present. Note position of well 2 in a sinuous form. The seismic profile, which passes through well 2, represents an oblique strike section across a sinuous form (submarine canyon) Source: (A─C) From Shanmugam, G., Shrivastava, S.K., Das, B., (2009). Sandy debrites and tidalites of Pliocene reservoir sands in upper-slope canyon environments, offshore Krishna-Godavari Basin (India): implications. J. Sediment. Res. 79, 736─756, with permission from SEPM.

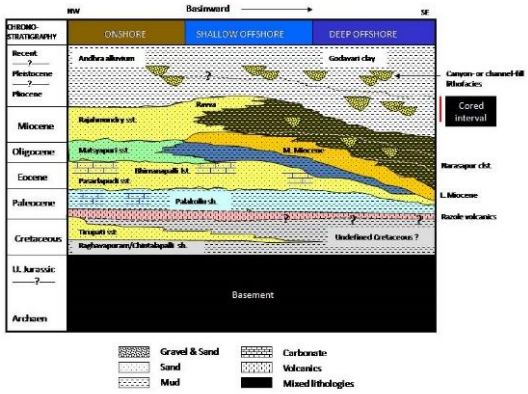

Fig. 116.Stratigraphic chart of the KG Basin showing cored interval. From Shanmugam, G., Shrivastava, S.K., Das, B., (2009).

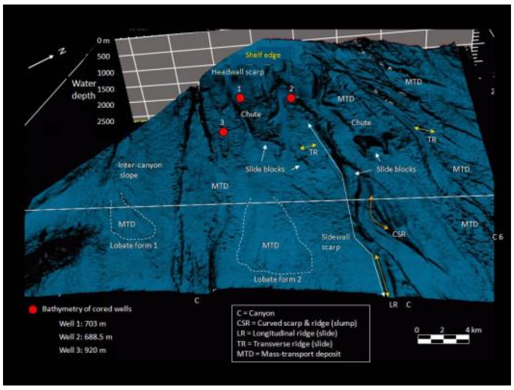

Fig. 117 Bathymetric image showing cored wells and submarine canyons. From Shanmugam et al. (2009)

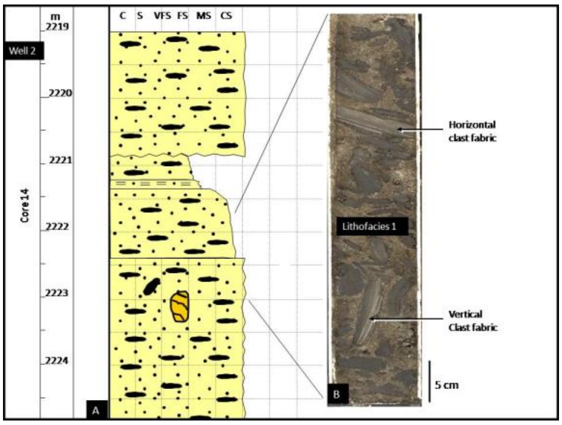

Fig. 118 (A) Sedimentological log of core 14 m in well 2 showing floating mudstone clasts in amalgamated massive sand. (B) Core photograph showing horizontal (planar fabric) and vertical (random fabric) positions of floating mudstone clasts (arrows) in massive sand (after Shanmugam et al., 2009). Source: With permission from SEPM.

considered to be favorable factors for triggering mass movements. Pliocene canyons are sinuous, exhibit 90u deflections, at least 22 km long,

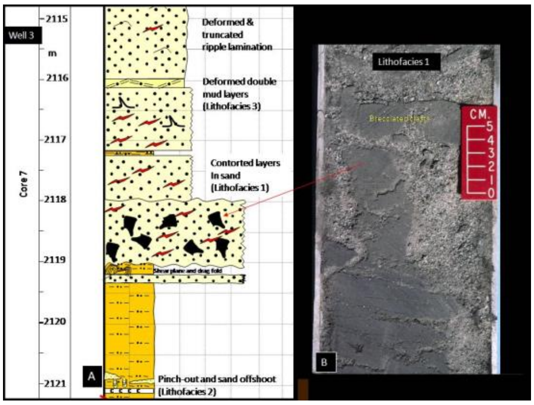

Fig. 119 (A) Sedimentological log showing massive sand with floating brecciated mudstone clasts, deformed double mud layers, and truncated ripples in massive sand (lithofacies 1 and 3). (B) Lithofacies 1 core photograph showing brecciated mudstone clasts. Arrow shows stratigraphic position of photograph (after Shanmugam et al., 2009). Source: With permission from SEPM.

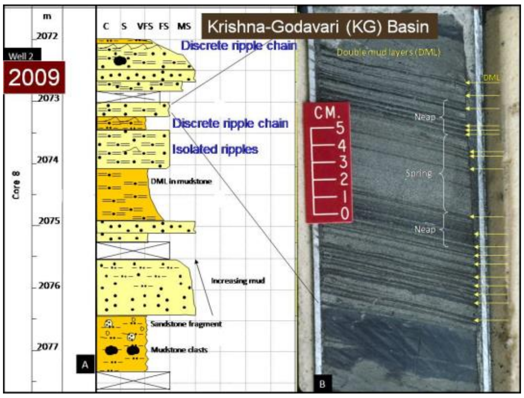

Fig. 120 (A) Sedimentological log of core 8 for the interval 2072_2077.5 m in well 2 showing alternation of sand (lithofacies 3) and mudstone (lithofacies 4) intervals with continuous presence of double mud layers (DML). Note floating sandstone rock fragments and mudstone clasts in a basal mudstone interval (lithofacies 2). The cored interval represents core 8 of canyon-fill deposits in seismic profile (Fig. 3.36). (B) Lithofacies 3 core photograph showing rhythmic bedding (rhythmites) and double mud layers (DML, arrows) in sand. N 5 Neap (thin)bundle; S 5 Spring (thick) bundle (after Shanmugam et al., 2009). Source: With permission from SEPM.

relatively narrow (500–1000 m wide), deeply incised (250 m), and asymmetrically walled. Sandy debrites occur as sinuous canyon-fill massive sands, inter-canyon sheet sands (1750 m long or wide and 32 m thick), and canyon-mouth slope-confined lobate sands (3 km long, 2.5 km wide, and up to 28 m thick). Canyon-fill facies are characterized by the close association of sandy debrites and tidalites.

Reservoir sands, composed mostly of amalgamated units of sandy debrites, are thick (up to 32 m), low in mud matrix (less than 1% by volume), and high in measured porosity (35–40%) and permeability (850–18,700 mD). Because upper-slope sandy debrites mimic base-of-slope turbidite channels and lobes in planform geometries, use of conventional submarine fan models as a template to predict the distribution of deep-water sand is tenuous.

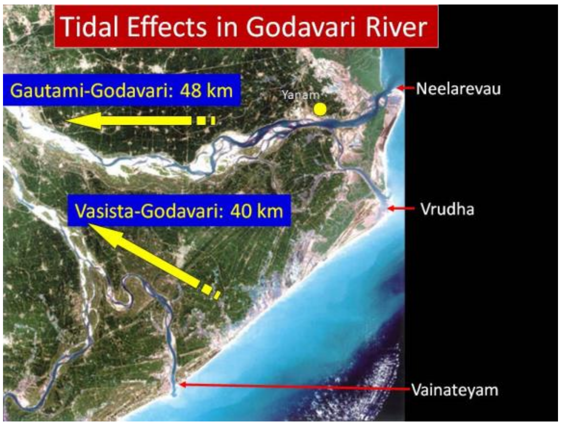

Fig. 121 Tidal effects in modern Godavari River. http://www.isro.org/rep2007/40.jpg Double mud layers were 0bserved in trenches in Kakinada Bay, which is located just north of the Godavari River.

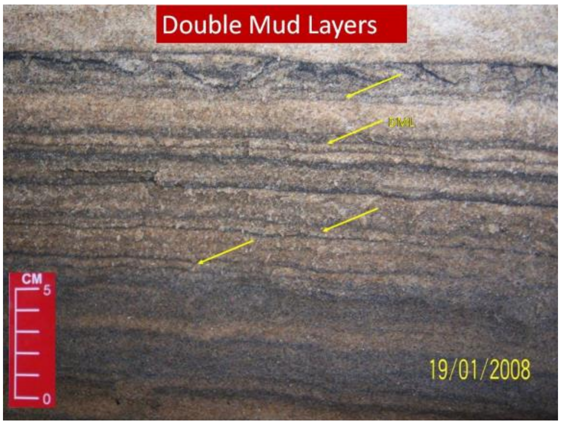

Fig. 122 Double Mud Layers (DML) (arrows) in fine-grained sand, Kakinada Bay. These DMLs were observed in trenches that were excavated along walls of creeks connected to the Kakinada Bay (see Fig. 114) during a Field Trip organized by G. Shanmugam for Reliance geoscientists on January 19, 2008. The significance of these DMLs is that the principle of “Uniformitarianism” (Present is the key to the Past) is best exemplified in the KG Basin in terms of tidal processes in both modern and ancient sediments.

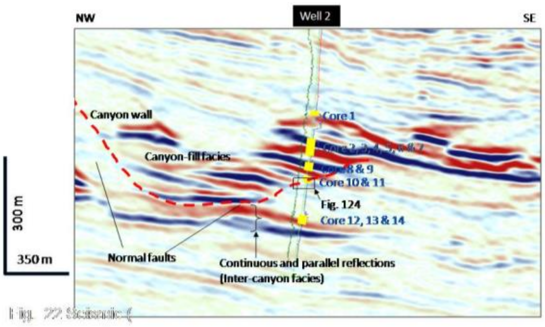

Fig. 123 Seismic profile showing boundaries of a major erosional feature of Pliocene age, which we have interpreted as a submarine canyon on the upper-slope environment. Cored intervals are shown by yellow bars on the wireline log of well 2. The southeast canyon wall, which corresponds to the contact between cores 10 and 11, is characterized by slump folds, sand injections, and other sediment deformation in core. Both walls of the canyon are aligned in trend with underlying normal faults. Immediately beneath the canyon, a seismic unit (with cores 12, 13, and 14) exhibits continuous and parallel reflections. This seismic unit, which is 1750 m long or wide, is composed primarily of sandy debrites in core in the inter-canyon environments. This NW-SE seismic profile represents an oblique strike section across a sinuous canyon with well 2 (after Shanmugam et al., 2009). Source: With permission from SEPM.

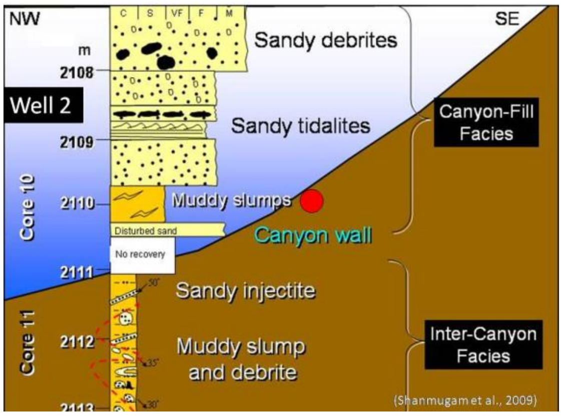

Fig. 124 The canyon-fill facies is composed of sandy debrites, sandy tidalites, and muddy slumps. The inter-canyon facies is composed of muddy slumps and debrites with sand injectites in core. Severe sediment deformation is evident both below and above the canyon wall. The lack of core recovery at the canyon wall may be due to extreme sediment deformation (after Shanmugam et al., 2009). Source: With permission from SEPM.

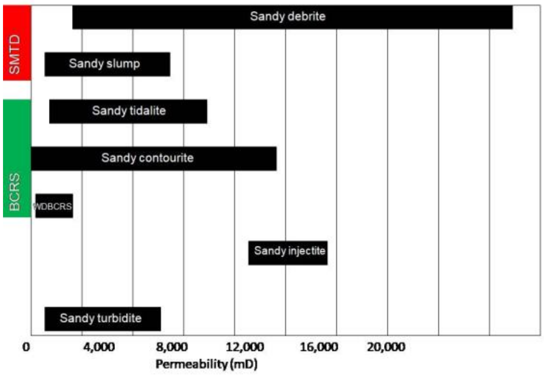

Fig. 125 Reservoir quality of KG reservoirs. SMTD = Sandy mass transport deposit. BCRS = Bottom current reworked sands

19. Turbidite Groupthink: Bute Inlet, British Columbia, Canada

Shanmugam (2022f) used a case study in illustrating how turbidite groupthink functions, without sound scientific methods, on the basis of published information on modern turbidity currents in Bute Inlet (fjord and estuary), British Columbia, Canada (Fig. 126). The claim of modern turbidity currents in Bute Inlet by Pope et al.(2022) remains unproven. They have provided no scientific data to establish the true nature of submarine flows in the Inlet and their work consists of a lot of speculation and conjecture. It is suggested that the reasoning behind the conclusions reached by Pope et al. (2022) is that of a turbidite groupthink (Fig. 127) in which all alternative interpretations have been filtered out of the consideration, such as strong tidal influence (Fig. 128).

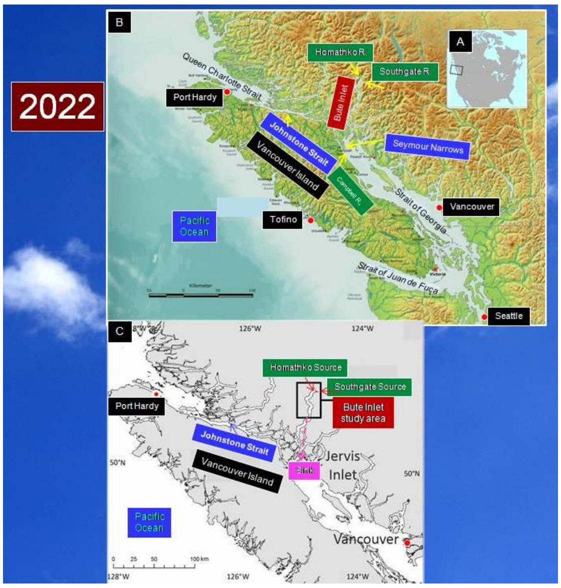

Fig. 126 A. Index map of North America showing Vancouver Island in British Columbia, Canada. B. Map showing Bute Inlet with Homathko and Southgate Rivers in the mainland Canada. Note Seymour Narrows (Spring tidal range: 5.1 m} and Campbell River (Spring tidal range: 4.6 m) near the mouth of Bute Inlet. Tofino: Spring tidal range: 4.1 m. Port Hardy: Spring tidal range: 5.6 m. Entire map area represents marcro-tidal environment. Tidal range data from Thomson (1981). Map credit: Wikipedia. Color labels by G. Shanmugam. C. Map showing Bute Inlet study area by Pope et al. (2022). Note source and sink are outside of the study area. Map from Pope et al. (2022). Color labels by G. Shanmugam.

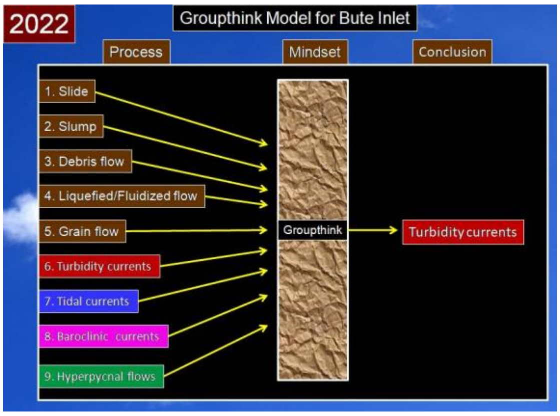

Fig. 127 Groupthink model for Bute Inlet showing the pre-conceived conclusion of turbidity currents, irrespective of alternative processes (Shanmugam, 2022f). Mass transport = Slide, Slump, and Debris flow (Shanmugam et al., 1994).

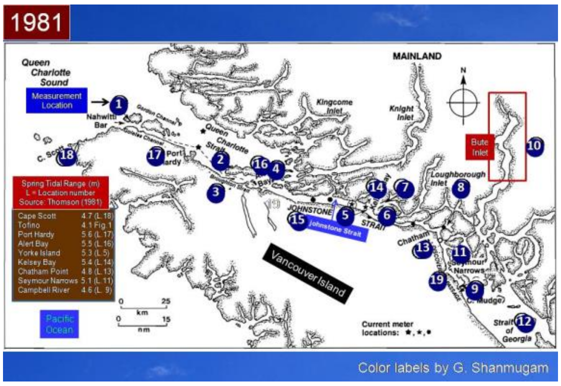

Fig. 128 Spring tidal range of Johnstone Strait region, Canada: 1. Bull Harbour; 2. Malcolm Island; 3. Port McNeill; 4. Wevnton Passage; 5. Hardwicke and Yorkc Islands; 6. Hclmcken Island; 7. Sunderland Channel; 8. Nodales Channel; 9. Duncan Bay and Campbell River area. 10. Bute Inlet study area (rectangle) covered by Pope et al. (2022. their Fig. 1B); 11. Seymour Narrows; 12. Strait of Georgia; 13. Chatham Pt.,14. . Kelsey Bay, 15. Johnstone Strait,16. Alert Bay, 17. Port Hardy,18. Cape Scott, and 19. Discovery Passage. Tofino is located on the west Coast of Vancouver Island (Fig. 1B). Tidal range table: L.18 = Location 18. Broken line in Queen Charlotte Strait gives sounding line for bottom profiles. Map and tidal range data are from Thomson (1981). Additional labels by G Shanmugam.

20. Submarine canyons

Shepard and Dill (1966) provided a comprehensive account of submarine canyons.

Submarine canyon is a steep-sided valley that incises into the continental shelf and slope. V-shaped profile of submarine canyons is common (Fig.129), although U-shaped profiles have also been observed. Canyons serve as major conduits for sediment transport from land and the shelf to the deep-sea environment worldwide (Figs 130-135.). Smaller erosional features on the continental slope are commonly termed gullies in modern environments; however, there are no standardized criteria to distinguish canyons from gullies in the rock record. Similarly, the distinction between submarine canyons and submarine erosional channels is not straightforward. Thus alternative terms such as gullies, channels, troughs, trenches, fault valleys, and sea valleys are in use for submarine canyons in the published literature. Normark and Carlson (2003) compared submarine canyons and their cross sections near the shelf edge and reported that the Zhemchug Canyon from the North American Margin of the Bering Sea has the largest cross section (Fig.136).

Zhemchug Canyon has a volume of 5800 km^3 (Carlson and Karl, 1988). The Bering Canyon has the largest area of all canyons studied (Table 2). The importance of mass movements in shaping large submarine canyons in the Beringian continental margin has been discussed by Carlson et al. (1991). Dimensions of selected modern submarine canyons are listed in Table 3. The Great Bahama Canyon has the world's highest wall relief of 14,060 ft. (4285 m) (Fig. 137).

Aspects of submarine canyons have been discussed in great details by many researchers (Shepard and Dill, 1966; Inman et al., 1976; Shepard et al., 1979; Twichell and Roberts, 1982; Normark and Carlson, 2003; Shanmugam, 2003; Paull et al., 2005; Normark et al., 2009; Harris and Whiteway, 2011, among others). De Leo and Ross (2019) compiled an atlas of "Large Submarine Canyons of the United Ocean Energy Management".

Harris and Whiteway (2011), based on ETOPO1 bathymetric grid, compiled the first inventory of 5849 separate large submarine canyons in the world's oceans. They classified canyons into three basic types:

Type 1: shelf-incising canyons having heads with connection to a major river or estuarine system (Fig. 138);

Type 2: shelf-incising canyons with no clear connection to a major river or estuarine system (Fig. 139);

Type 3: slope-incising blind canyons with their heads confined to the continental slope (Fig. 139).

Active debris flows (Fig. 140), cascading sand fall (Fig. 141), and tidal currents (Fig. 142) (Shepard et al. (1979) were documented using underwater photographs and velocity measurements in modern submarine canyons. In A variety of deposits, such as slumps (Fig. 143), tidalites with double mud layers (Fig. 144), and sandy debrites (Fig. 145) were documented in cores from submarine canyons (Shanmugam, 2003). Section 18 describes a case study of canyon─fill sandy debrites and tidalites from the Krishna─Godavari Basin in the Bay of Bengal, India.

Table 2 Area of submarine canyons. From several sources. Compiled from Normark and Carlson (2003). See cross sections of these canyons in Figure 136.

Serial Number	Canyon	Area (km^2)
1	Zhemchug	11,350
2	Bering	30,800
3	Navarin	14,600
4	Monterey	2380
5	La Jolla	33
6	Horizon Channel	No data.
7	Swatch of No Ground	9000
8	Swatch	1700
9	Amazon	2250
10	Zaire (Congo)	4470
11	Laurentian Fan Valley	No data

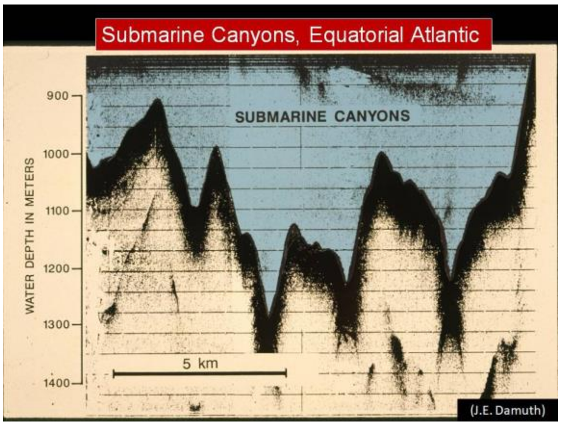

Fig. 129 V─shaped cross sections of submarine canyons. Courtesy J. E. Damuth.

Table 3 Dimensions of selected modern submarine canyons. After Shepard and Dill (1966), Shepard (1973) ans Carlson and Karl (1988)

Serial Number	Modern canyon	Length mi (km)	Gradient ft/mi (m/km)	Wall relief ft (m)
1	Bering, Bering Sea	929 (1495)	42 (7.9)	6,036 (1,829)
2	Great Bahama, North Atlantic Ocean	140 (225)	300 (60.0)	14,060 (4,285)
3	Zaire (Congo), South Atlantic Ocean	138 (222)	51 (9.5)	4,023 (1,219)
4	Pribilof, Bering Sea	99 (159)	106 (20.9)	7,042 (2,134)
5	Monterey, Pacific Ocean	292 (470)	138 (26.2)	6,035 (1,829)
6	Hudson, North Atlantic Ocean	58 (93)	117 (21.9)	4,023 (1,219)
7	Hydrographer, North Atlantic Ocean	30 (50)	200 (37.5)	3,016 (914)
8	Rhone, Mediterranean Sea	17 (28)	287 (53.9)	2,013 (610)
9	La Jolla, Pacific Ocean	9 (14)	203 (38.1)	1,007 (305)
10	Halawai, Pacific Ocean	7 (11)	478 (89.8)	1,007 (305)

`

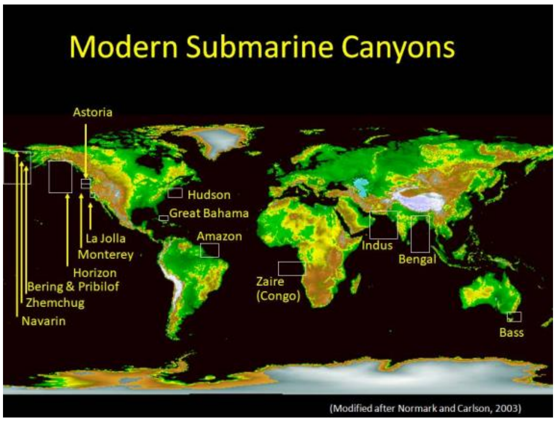

Fig. 130 Locations of Modern Submarine Canyons. Modified after Normark and Carlson, (2003).

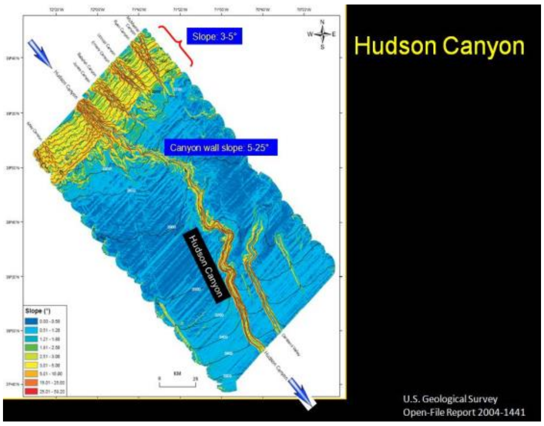

Fig. 132 Hudson Canyon, U. S. Atlantic Margin. U.S. Geological Survey Open-File Report 2004-1441

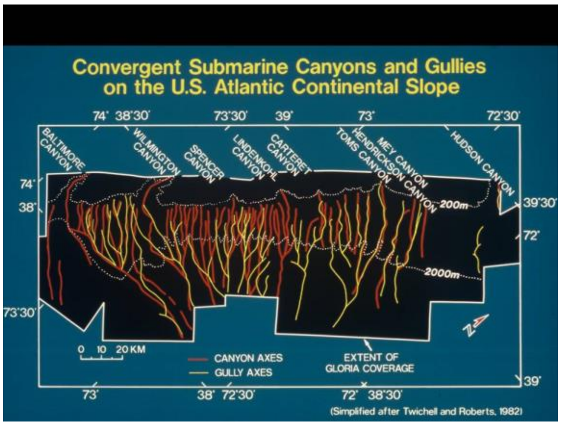

Fig. 131 Submarine Canyons and Gullies, U. S. Atlantic Margin. From Twichell and Roberts (1982).

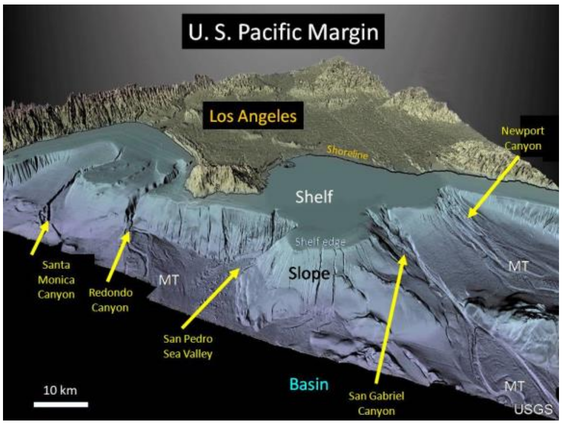

Fig. 133 Submarine Canyons, U.S. Pacific Margin. USGS. See Normark et al. (2009).

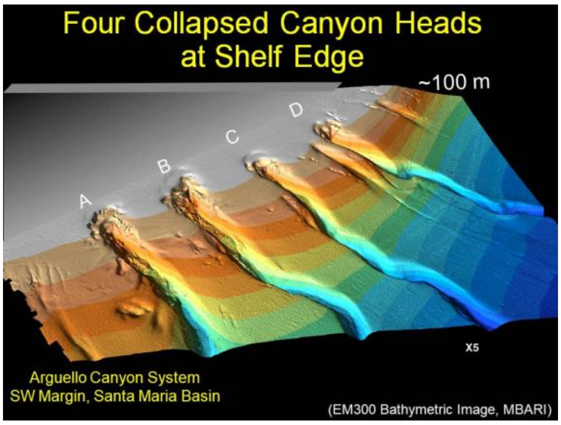

Fig. 134 EM300 Bathymetric Image showing a perspective from the west of f four Collapsed Canyon Heads of the Arguello Submarine Canyon System at the shelf edge at about 100 m water depth. Southwstern Margin of the Santa Maria Basin, U.S. Pacific Margin. Additional labels by G. Shanmugam. Courtesy MBARI (Monterey Bay Aquarium Research Institute). See related website: https://www.mbari.org/news/innovative-mbari-technology-reveals-processes-that-sculpt-submarine-canyons/ See also Marsaglia et al. (2019).

Fig. 135 Mississippi Canyon, Gulf of Mexico. From Shanmuham (2012a)

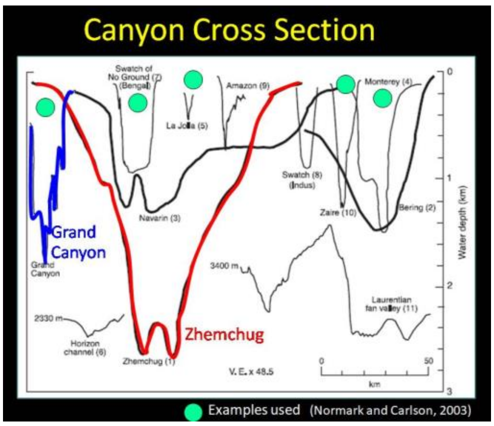

Fig. 136 Cross sections of Canyons. From Normark and Carlson (2003)

Fig. 137 Great Bahama Canyon. NASA.

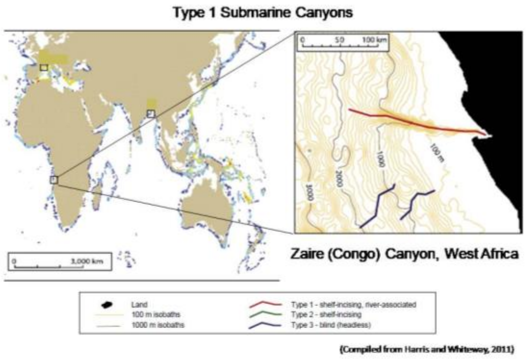

Fig. 138 Type 1 shelf-incising, river-associated Zaire (formerly Congo) Canyon. *Source:* Compiled from Harris, P.T., Whiteway, T., 2011. Global distribution of large submarine canyons: geomorphic differences between active and passive continental margins. Mar. Geol. 285, 69_86, with permission from Elsevier.

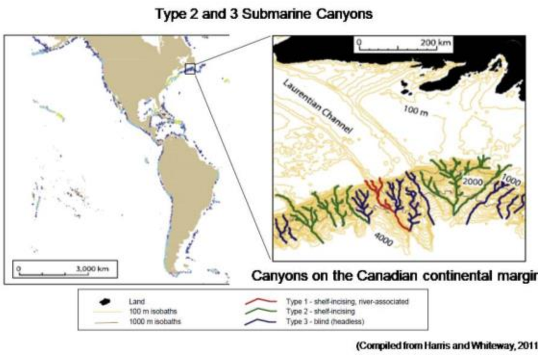

Fig. 139 Types 2 and 3 canyons near the Laurentian Channel, many of which incise the shelf, incised into the glacial trough mouth fan. *Source:* Compiled from Harris, P.T., Whiteway, T., 2011. Global distribution of large submarine canyons: geomorphic differences between active and passive continental margins. Mar. Geol. 285, 69_86, with permission from Elsevier.

Fig. 140 Underwater photograph showing a pocket of rounded cobbles up to 15 cm in diameter in massive sandy matrix at a depth of 130 m (427 ft) in Los Frailes Canyon, Baja California. Photo by R.F. Dill. From Shepard and Dill, 1966). Published in Shanmugam (2012a).

Fig. 141 Underwater photograph showing a cascading sand fall at a depth of 40 m (130 ft) in gully leading down into San Lucas Canyon, Baja California. Such pure sand falls would develop massive sand intervals in the rock record. Analogous to grain flows. Photo by R.F. Dill. From Shepard and Dill (1966). Published in Shanmugam (2012a).

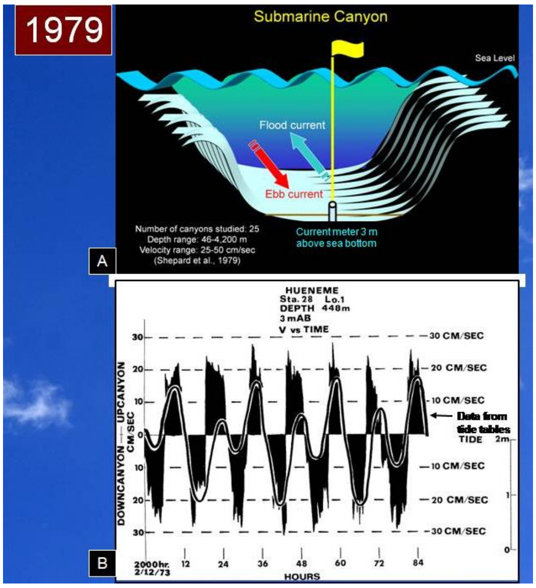

Fig. 142 A. Conceptual diagram showing a cross-section of a submarine canyon with ebb and flood tidal currents (opposing arrows). Shepard et al. (1979) measured current velocities in 25 submarine canyons at water depths ranging from 46 to 4200 m by suspending current meters commonly 3 m above the sea bottom. Measured maximum velocities commonly range from 25 to 50 cm/sec. From Shanmugam (2003). B. Time-velocity plot from data obtained at 448 m in the Hueneme Canyon, California, showing excellent correlation between the timing of up- and down canyon currents and the timing of tides obtained from tide tables (solid curve). 3mAB = Velocity measurements were made 3 m above sea bottom. From Shepard et al. (1979).

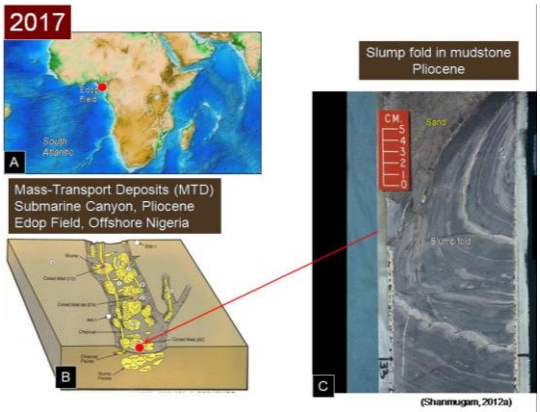

Fig. 143 Edop Field (A) with submarine canyon (B) filled with slump facies (C). From Shanmugam (2017a).

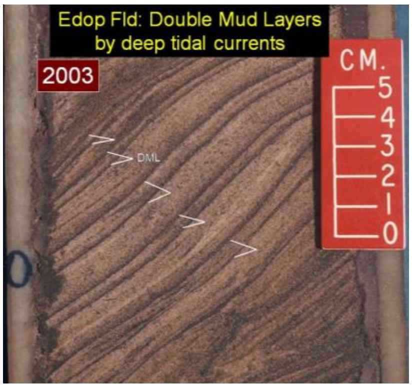

Fig. 144 Edop Field with submarine canyon filled with tidalite facies composed of double mud layers (DML). From Shanmugam (2003).

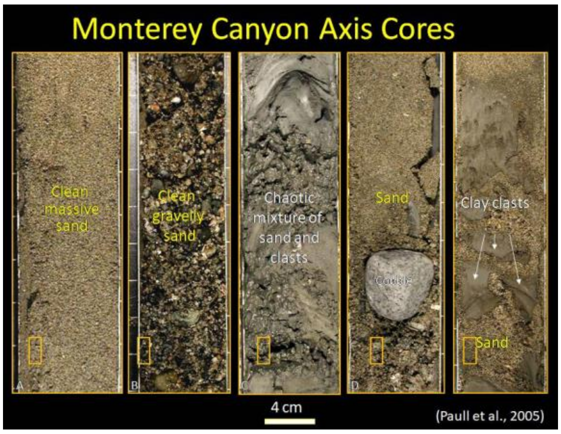

Fig. 145 Core photographs showing floating clasts in sand (Sandy debrites), Monterey Canyon. From Paull et al. (2005).

21. Submarine fans

Since their first review article 36 years ago on "Submarine fans" (Shanmugam and Moiola, 1988), Shanmugam (2016a) reminisced over the topic with the following observations. When we look back the contributions on submarine fans during the past 65 years (1950-2015), the empirical data on 21 modern submarine fans and 10 ancient deep-water systems, published by the results of the First COMFAN (Committee on FANs) Meeting (Boumaet al., 1985a), have remained the single most significant compilation of data on submarine fans. The 1970s were the "heyday" of submarine fan models. In the 21st century, the general focus has shifted from submarine fans to submarine mass movements, internal waves and tides, and contourites. The purpose of this review is to illustrate the complexity of issues surrounding the origin and classification of submarine fans. The principal elements of submarine fans, composed of canyons, channels, and lobes, are discussed using nine modern case studies from the Mediterranean Sea, the Equatorial Atlantic, the Gulf of Mexico, the North Pacific, the NE Indian Ocean (Bay of Bengal), and the East Sea (Korea). The Annot Sandstone (Eocene-Oligocene), exposed at Peira-Cava area, SE France, which served as the type locality for the "Bouma Sequence", was reexamined. The field details are documented in questioning the validity of the model, which was the basis for the turbidite fan link. The 29 fan-related models that are of conceptual significance, developed during the period 1970e2015, are discussed using modern and ancient systems. They are: (1) the classic submarine fan model with attached lobes, (2) the detached-lobe model, (3) the channel-levee complex without lobes, (4) the delta-fed ramp model, (5) the gully-lobe model, (6) the suprafan lobe model, (7) the depositional lobe model, (8) the fan lobe model, (9) the ponded lobe model, (10) the nine models based on grain size and sediment source, (11) the four fan models based on tectonic settings, (12) the Jackfork debrite model, (13) the basin-floor fan model, (14) supercritical and subcritical fans, and (15) the three types of fan reservoirs. Each model is unique, and the long-standing belief that submarine fans are composed of turbidites, in particular, of gravelly and sandy high-density turbidites, is a myth. This is because there are no empirical data to validate the existence of gravelly and sandy high-density turbidity currents in the modern marine environments. Also, there are no experimental documentation of true turbidity currents that can transport gravels and coarse sands in turbulent suspension. Mass-transport processes, which include slides, slumps, and debris flows (but not turbidity currents), are the most viable mechanisms for transporting gravels and sands into the deep sea. The prevailing notion that submarine fans develop during periods of sea-level lowstands is also a myth. The geologic reality is that frequent short-term events that last for only a few minutes to several hours or days (e.g., earthquakes, meteorite impacts, tsunamis, tropical cyclones, etc.) are more important in controlling deposition of deep-water sands than sporadic long-term events that last for thousands to millions of years (e.g., lowstand systems tract).

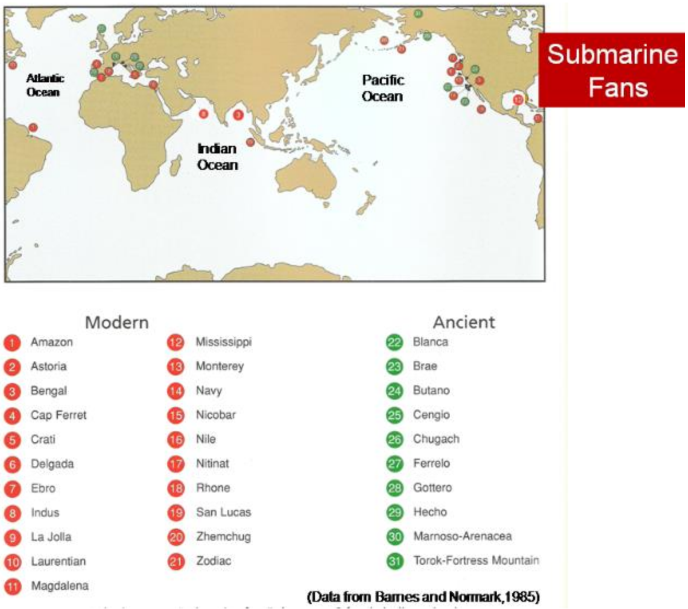

Fig. 146 Locations of modern and ancient deep-water systems, commonly known as submarine fans, From Bouma et al. (1985a).

Submarine fans are still in a stage of muddled turbidite paradigm because the concept of high-density turbidity currents is incommensurable. Selected Figures (146─160).

NAME	GEOGRAPHIC AREA	LENGTH, WIDTH [RADIUS] (Km)	AREA (Km^2)	MAXIMUM THICKNESS (m)
Modern				
1. Amazon	Brazilian Margin	700 min. 250-700	3.3×10^5	4200
2. Astoria	Oregon Margin, NE Pacific	250 min. 130	3.2×10^4	2200
3. Bengal	Bay of Bengal, NE Indian Ocean	2800, 1100	3×10^6	>5000
4. Cap Ferret	Bay of Biscay, NE Atlantic	[75]	1.6×10^3	1800
5. Crati	Gulf of Taranto, Southern Italian Margin	16, 4-5	60	30
6. Delgada	Central California Margin, NE Pacific	[>350]	4.4×10^4	3000
7. Ebro	Baleric Sea, Eastern Spain	100,50	5×10^3	370
8. Indus	Arabian Sea, NW Indian Ocean	1500, 960 max	1.1×10^6	>3000
9. La Jolla	Southern California Borderland, NE Pacific	40, 50	1200?	1600
10. Laurentian	Eastern Canadian Margin, NW Atlantic	500 min-1500 max 200-400	1.8×10^5 to 4.2×10^5	2000
11. Magdalena	Columbian Margin, SW Caribbean	[230]	5.3×10^4	3000
12. Mississippi	Gulf of Mexico	540, 570	$>3.0 \times 10^5$	4000
13. Monterey	Central California Margin, NE Pacific	400, 250	7.5×10^4	2000
14. Navy	Southern California Borderland, NE Pacific	[40]	560	900
15. Nicobar	East Central Indian Ocean	[2200]	1.5×10^5	3000
16. Nile	Egyptian Margin, Eastern Mediterranean	280, 500	7.0×10^4	>3000
17. Nitinat	Washington Margin, NE Pacific	260, 80	2.3×10^4	1000
18. Rhone	Gulf of Lions, Southern French Margin	440, 210	7×10^4	1500
19. San Lucas	Southern Baja California Margin, NE Pacific	[60]	5000	1000
20. Zhemchug	Central Bering Sea	>115m ?	?	2000
21. Zodiac	Aleutian Margin, Alaksa NE Pacific Ocean	?	1.1×10	1600
Ancient				
22. Blanca	Southern California Borderland, NE Pacific	215, 30	4×10^3	1000
23. Brae	North Sea	overlapping fans each [5-10]	20-50	600
24. Butano	Central California Coast Ranges	80, 40	3200	3000
25. Cengio	Piedmont Basin, NW Italy	6.4, 4.8	30	170
26. Chugach	Gulf of Alaska, Aleutian Alaska Margin	2000, 100	2.0×10^5	1000
27. Ferrelo	Southern California Borderland, NE Pacific	340, 65	$3.1\ 10^4$	1800
28. Gottero	Ligurian Apennines, NW Italy	[30, 60]	3500	1500
29. Hecho	Southern Pyrenees, Northern Spain	175, 40-50	8×10^3	3500
30. Marnoso-Arenacea	Northern Apennines, Italy	Major - 25-50, 6-15 Minor - 20-25, 4-10	150-7500	1000
31. Torok-Fortress Mtn.	North Slope, Alaska	150,300	4.5×10^5	3400

A

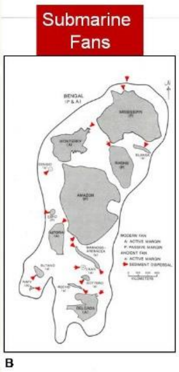

B

Fig. 147 Dimensions of modern and ancient deep-water systems, commonly known as submarine fans, Data from Barnes and Normark (1985). See Bouma et al. (1985a).

Fig. 149 Photo was taken during a Mobil Field Trip Organized by Prof. E. Mutti on "Classic submarine fans, Tertiary, Spanish Pyrenees". Photo by E. Mutti.

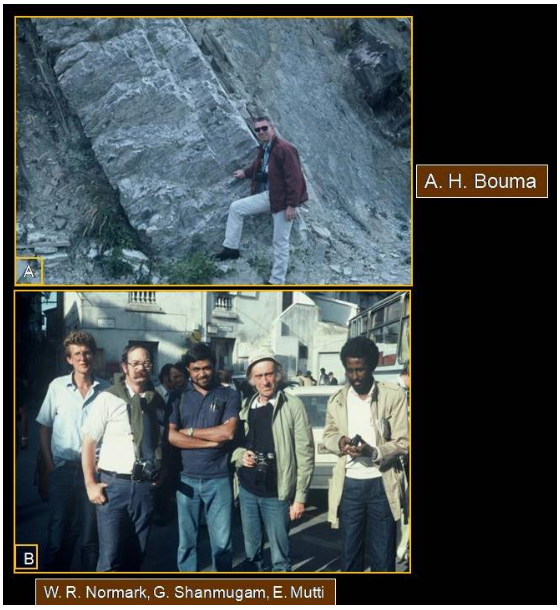

Fig. 148 A-The late A.H. Bouma (1932e2011) pointing to a "Bouma Sequence". Photo was taken during a field trip, associated with the COMFAN II Meeting held in Parma, Italy (1988), by G. Shanmugam; B-Photo showing (left to right) the late W.R. Normark (1943─2008), G. Shanmugam, Professor Emiliano Mutti. Photo was taken during a field trip associated with the NATO Advanced Study Institute Conference on "Reading Provenance from Arenites" held in Calabria, Italy (June 3e11, 1984).

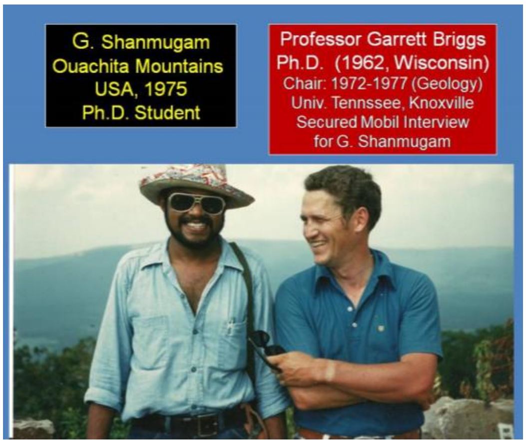

Fig. 150 Photo was taken during a Field Trip organized by Prof. Garrett Briggs to the Ouachita Mountains, Oklahoma.

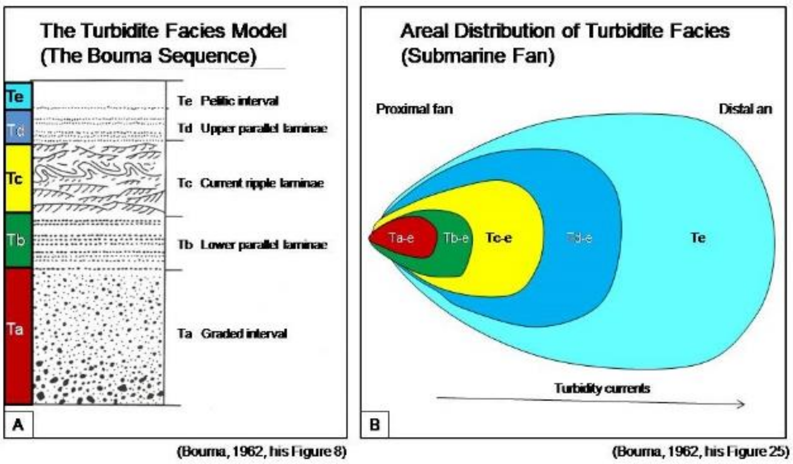

Fig. 151. The first turbidite-fan link proposed by Bouma (1962).

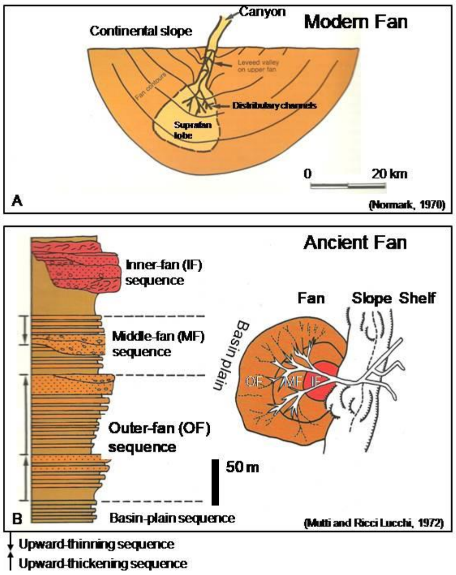

Fig. 152 Modern and Ancient Fan models.

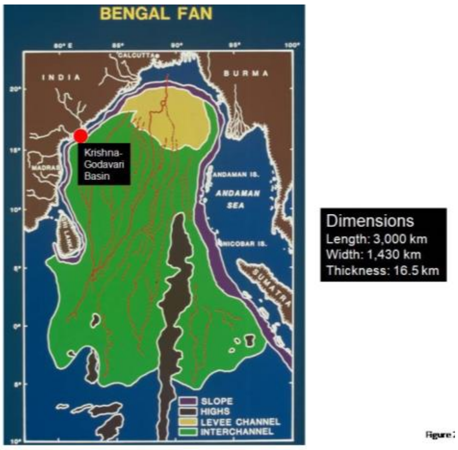

Fig. 153 The Bengal Fan, Bay of Bengal. After Curray and Moore (1974) and Curray et al. (2002)

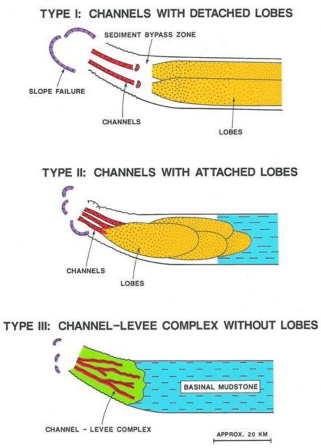

Fig. 154 Three types of turbidite systems based on depositional lobes. From Mutti (1985).

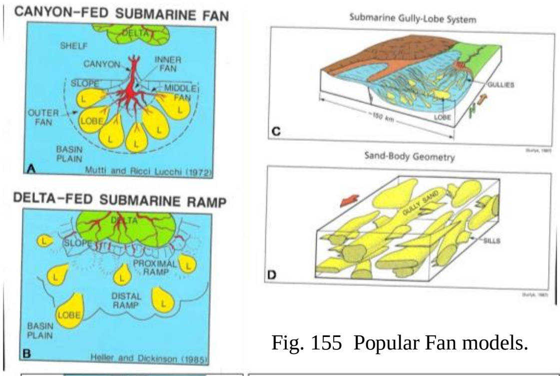

Fig. 155 Popular Fan models.

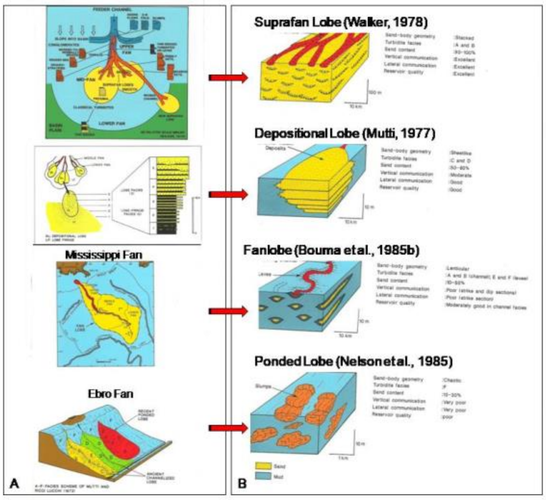

Fig. 156 Various Fan models.

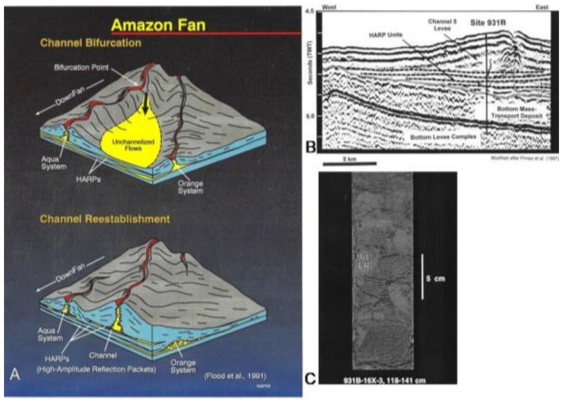

Fig. 157 A-Conceptual model showing that channel bifurcation through avulsion on a deep-sea fan can result in unchannelized sandy flows (top diagram) by breaching their confining levee through a crevasse and spreading out initially as unchannelized flows into a lower interchannel areas. New channel reestablishment over these sandy deposits (bottom diagram) can result in sheet-like geometry (Flood et al., 1995) that return high-amplitude reflections (HARPs) on seismic data (Flood et al., 1991). Sheet-like HARPs overlain by channel-levee complex (gull-wing geometry) are identical to basin-floor fan overlain by slope fan in a sequence-stratigraphic framework (see Fig. 44 in this article). However, there is a major difference between a basin-floor fan and HARP. For example, a basin-floor fan is formed by progradation during lowstands of sea level (allocyclic process), whereas HARPs are formed by channel bifurcation (autocyclic process). Therefore, caution must be exercised in interpreting seismic geometries in terms of processes. Original figure from Flood et al. (1991). Modified figure from Shanmugam (2000). B-Seismic profile showing HARP units (horizontal dashed lines) and overlying Channel 5 with levee units. Note position of Site 931B, Amazon Fan, modified after Pirmez et al. (1997); C-Core photograph showing floating mud clasts in silty matrix suggesting deposition from muddy debris flow. Site 931B, HARP unit, Leg 155, Site 931, Amazon Fan. See also Shipboard Scientific Party (1995, their Fig. 7B). Photo courtesy of J. E. Damuth. Figures B and C from Shanmugam (2006a).

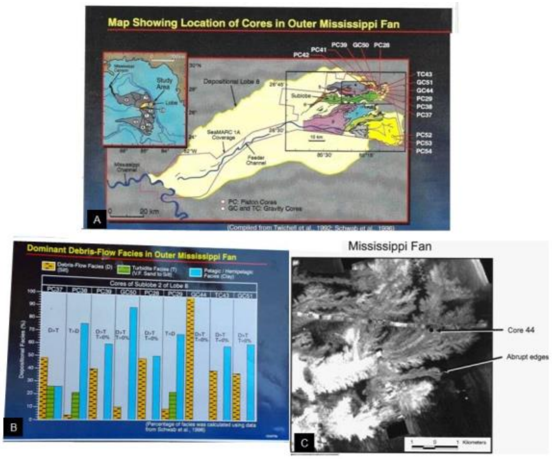

Fig. 158 A-Map showing location of piston and gravity cores taken from 'channelized lobes' in the outer Mississippi Fan, Gulf of Mexico. Compiled from Twichell et al. (1992) and Schwab et al. (1996). After Shanmugam (1997). B-Histograms showing dominance of debris-flow facies in cores from 'channelized lobes' in the outer Mississippi Fan. Percentages of facies were calculated by the author using published data from Schwab et al. (1996). Note that all nine cores contain debris flows, whereas only three cores comprise turbidites. In seven out of nine cores, the amount of debris-flow facies far exceeds the amount of turbidite facies. In core GC 44, debris-flow facies comprises 100%. This facies distribution has important implications for submarine fan models. After Shanmugam (1997). C-SeaMARC 1A sidescan-sonar image mosaic of 'depositional lobes' of the distal Mississippi Fan showing dendritic pattern with abrupt edges. Strong acoustic returns (high backscatter) are white and light grey; weak acoustic returns (light backscatter) are black and dark grey. Note position of core 44, which contains chaotic silt beds and floating clay clasts (see Twichell et al., 1995, their Fig. 41.4, p. 286), suggesting deposition from slumps and debris flows. Core 44 is composed of 100% debris flow (Fig. 25B). (Modified after Lee et al. (1996). Image courtesy of D. C. Twichell. Figure from Shanmugam (2006a).

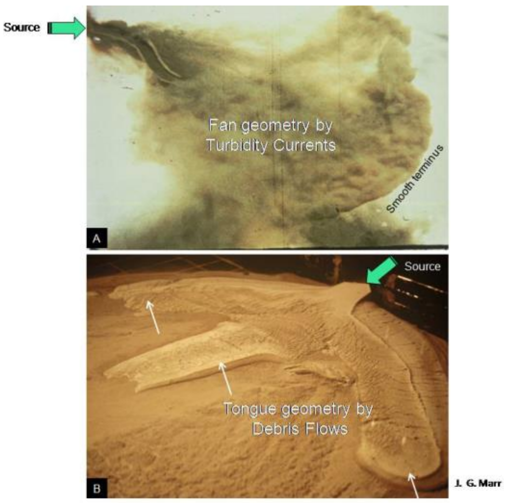

Fig. 159 Flume Experiments Showing differences in sediment geometry, Shanmugam (2016a).

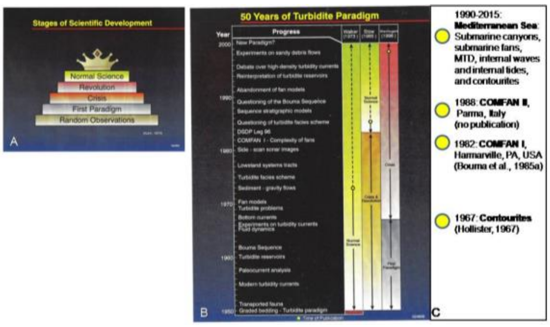

Fig. 160 Comparison of Kuhn's Stages of Scientific Development with Turbidite Paradigm. From Shanmugam; 2000)

22. The Annot Sandstone, Maritime Alps, SE France

The Annot Sandstone (Eocene-Oligocene), Peira Cava area, French Maritime Alps. SE France. Served as the type locality for developing the Bouma Sequence (Bouma, 1962), which is the seminal facies model for interpreting turbidites and predicting the distribution of turbidite facies of submarine fans (Fig. 151). In order for the Bouma Sequence to be useful, it must be continuous without internal hiatus (Fig. 161). Walther's Law of Facies (named after Johannes Walther [1860e1937]), states that the vertical succession of facies reflects their lateral changes in environment (Fig. 161). This law is applicable only to those sequences that represent continuous deposition without internal hiatus (Middleton, 1973). If a sequence contains hiatus, it cannot be used in stratigraphic correlations. Also, a sequence with hiatus is disqualified from being used

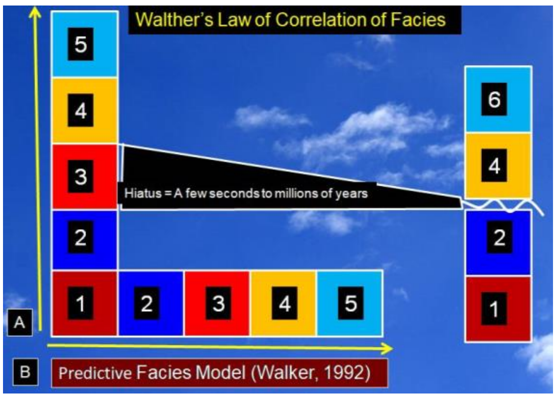

Fig. 161 A. Walther's Law of Facies: Vertical succession of facies reflects lateral changes in environment (No hiatus) (Middleton, 1973). If a sequence contains hiatus, it cannot be used in stratigraphic correlation. B. Sequence with hiatus is disqualified from being used as a predictive facies model (Walker, 1992).

as a predictive facies model (Walker, 1992). In other words, the popular Bouma Sequence (Fig. 161) is rendered useless if it contains internal hiatus. For example, the middle cutout Bouma Sequence (Walker, 1965) is disqualified as a facies model. Disappointingly, a reexamination of the Annot

Sandstone reveals that many field details of the Annot Sandstone do not validate the Bouma Sequence (Shanmugam, 2002a, 2022f) (Figs. 162–170).

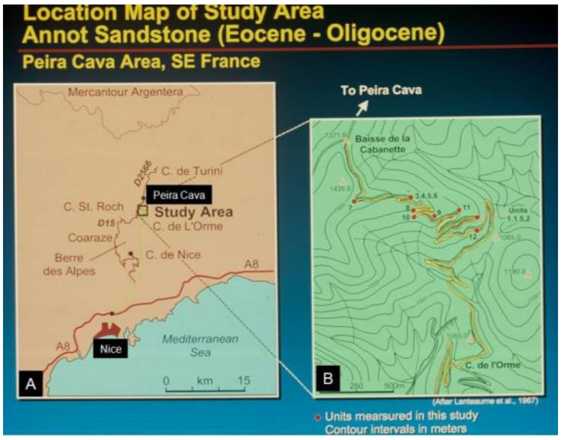

Fig. 162 Index map of Peira Cava north of Nice. B. Study sites for the Annot Sandstone in SE France.

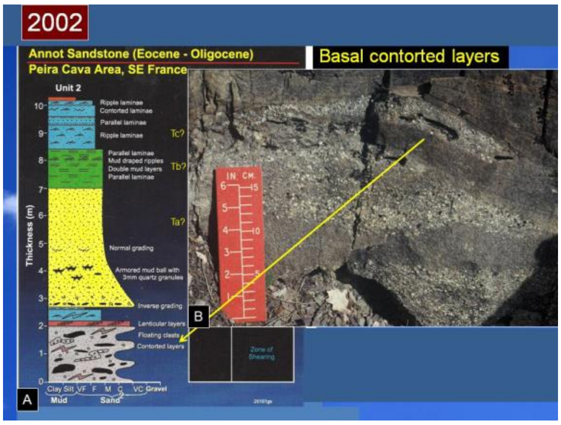

Fig. 163. A. Unit 2 with measured details of Unit 2. B. Outcrop photo showing contorted layers at the base. Peira Cava is the type locality for the Bouma Sequence in the Maritime Alps in SE France. From Shanmugam (2002a).

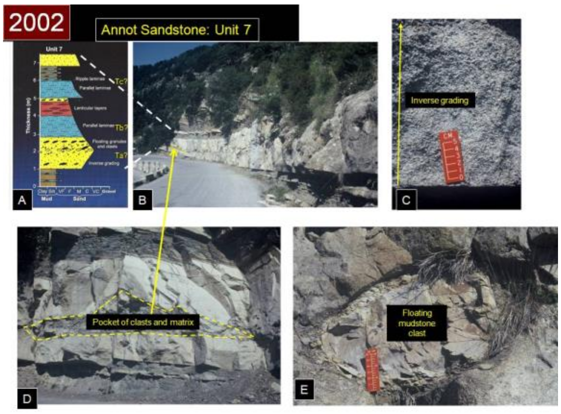

Fig. 164Annot Sandstone: Unit 7: Evidence for mass-transport deposit (MTD). From Shanmugam (2021a).

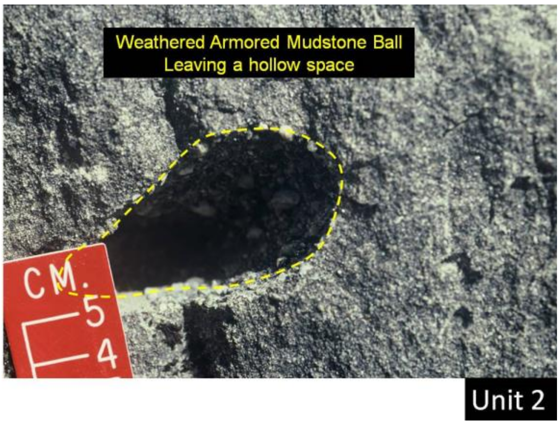

Fig. 165 Weathered Armored Mudstone Ball leaving a hollow space

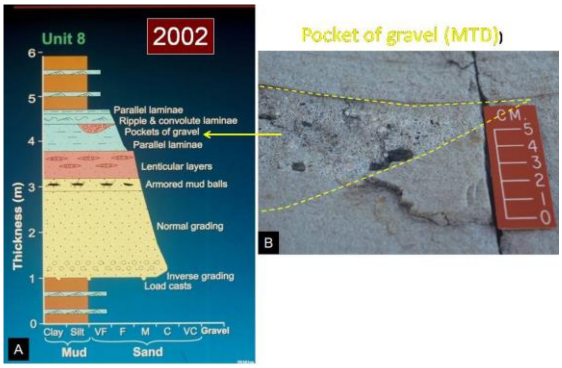

Fig. 166 A. Measured field details of Unit 8. B. Outcrop photo showing a pocket of gravel that is interpreted as MTD (sandy debrite). From Shanmugam (2002a).

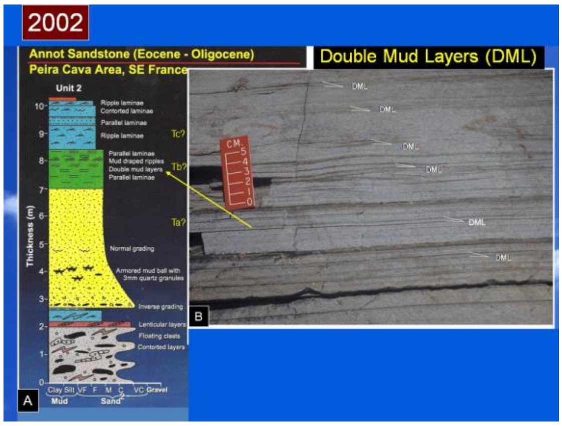

Fig. 167 A. Unit 2 with measured details of Unit 2. B. Outcrop photo showing double mud layers (DML). Peira Cava is the type locality for the Bouma Sequence in the Maritime Alps in SE France. From Shanmugam (2002a and 2021c). DML indicates tidal deposition (Visser, 1980).

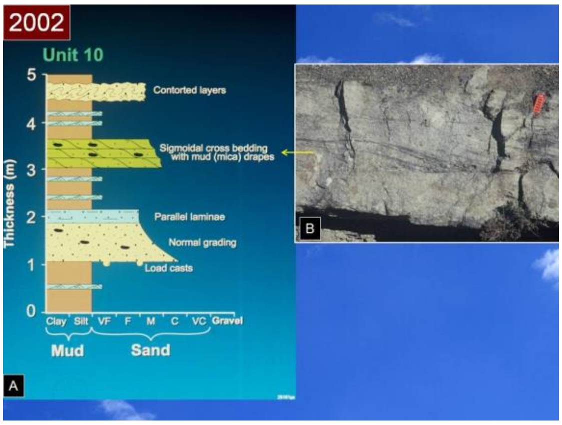

Fig. 168 (A) Sedimentological log of an amalgamated sandstone unit 10. (B) Outcrop photograph showing sigmoidal cross-bedding with mud (mica) drapes. Annot Sandstone (Eocene Oligocene), Peira Cava area, French Maritime Alps. From Shanmugam (2002a).

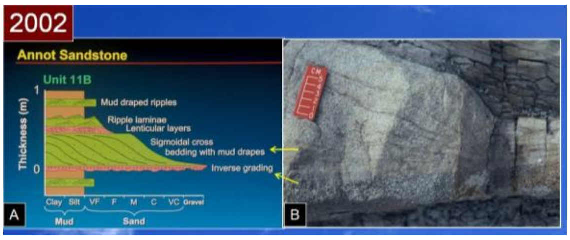

Fig. 169 (A) Sedimentological log of an amalgamated sandstone unit showing sigmoidal cross-bedding with tangential toe set. Note inverse grading below and lenticular layers above. (B) Outcrop photograph showing sigmoidal cross-bedding (top arrow) with tangential toe set in coarse- to granule-grade sandstone. Note mud/mica-draped (dark colored) stratification. Note inversely graded gravel layer below (bottom arrow). Arrows show stratigraphic position of photo, Annot Sandstone (Eocene Oligocene), Peira Cava area, French Maritime Alps. From Shanmugam (2002a).

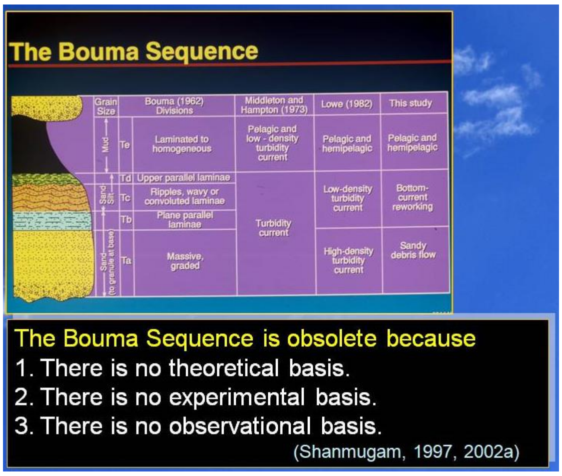

Fig. 170 The Bouma Sequence is obsolete (Shanmugam, 1997, 2002a).

23. The Ouachita Flysch, USA

Based on a rigorous ten─year research project at Mobil Oil Company (1984─1994), Shanmugam and Moiola (1995) published the following controversial findings on the Ouachita Flysch in the AAPG Bulletin.

The Pennsylvanian Jackfork Group in the Ouachita Mountains of Arkansas and Oklahoma has conventionally been interpreted by many workers, including us, as a classic flysch sequence dominated by turbidites in a submarine fan setting; however, normal size grading and Bouma sequences, indicative of turbidite deposition, are essentially absent in these sandstone beds. They appear massive (i.e., structureless) in outcrop, but when slabbed reveal diagnostic internal features. These beds exhibit sharp and irregular upper bedding contacts, inverse size grading, floating mudstone clasts, a planar clast fabric, lateral pinch-out geometries, moderate to high detrital matrix (up to 25%), sigmoidal deformation (duplex) structures, and contorted layers. All these features indicate sand emplacement by debris flows (mass flows) and slumps. Mud matrix in these sandstones was sufficient to provide cohesive strength to the flow. Discrete units of current ripples and horizontal laminae have been interpreted to represent traction processes associated with bottom-current reworking.

The dominance of sandy debris-flow and slump deposits (nearly 70% at DeGray Spillway section) and bottom-current reworked deposits (40% at Kiamichi Mountain section), and the lack of turbidites in the Jackfork Group have led us to propose a slope setting. Our rejection of a submarine fan setting has important implications for predicting sand-body geometry and continuity because deposits of fluidal turbidity currents in fans are laterally more continuous than those of plastic debris flows and slumps on slopes. A turbidite-dominated fan model would predict an outer fan environment with laterally continuous, sheet─like sandstones for the Jackfork Group in southern Oklahoma and western Arkansas, whereas a debris-flow/slump model would predict predominantly a slope environment with disconnected sandstone bodies for the same area.

Our (Shanmugam and Moiola, 1995) controversial reinterpretation had resulted in 42 printed pages of discussions and replies by some of the leading authorities in the field, which included the following:

- A.H. Bouma, M.B. DeVries, and C.G. Stone, (1997)
- J.L. Coleman, (1997)
- A.E. D'Agostino and D.W. Jordan (1997)
- D.R. Lowe (1997)
- R.M. Slatt, P. Weimer, and C.G. Stone (1997)

We promptly responded (Shanmugam and Moiola, 1997). These academic discussions had resulted in 42 printed pages in the AAPG Bulletin. It is worth noting that no other paper in the AAPG Bulletin history (1917─present) has generated this much controversy.

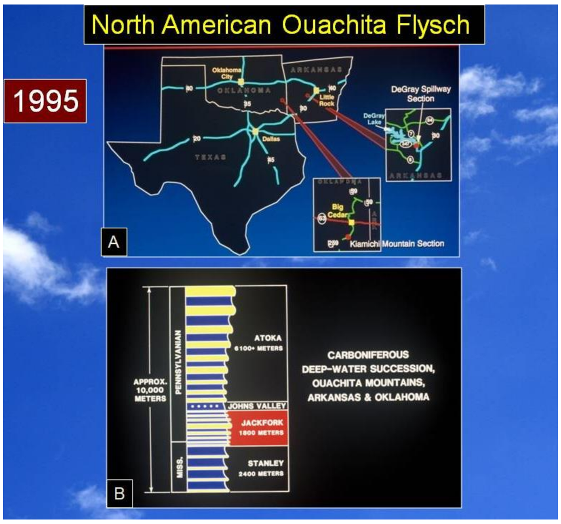

Fig. 171. A. Study locations of the Jackfork Group in Oklahoma and Arkansas, USA. From Shanmugam and Moiola (1995). B. Stratigraphy of the Jackfork Group.

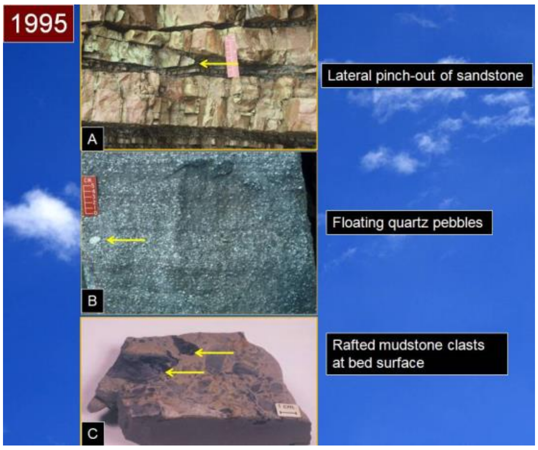

Fig. 172 Outcrop photographs showing (A) Lateral pinch-out of a sandstone bed, (B) floating quartzite pebble (arrow) in sandstone, and (C) rafted mudstone clasts at bed surface. These features are indicative of flow strength in debris flows. Pennsylvanian Jackfork Group. Ouachita Mountains. From Shanmugam and Moiola (1995).

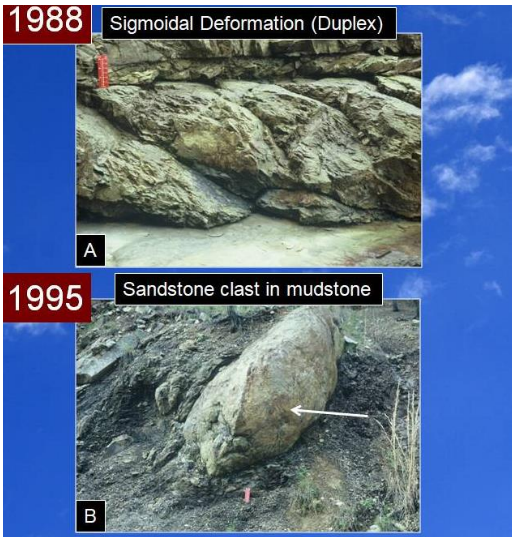

Fig. 173 A. Duplex-like structures in the Jackfork caused by synsedimentary slumping. From Shanmugam et al. (1988). B. Outcrop photograph showing sandstone clast (arrow) in mudstone, which is indicative of flow strength in debris flows. Pennsylvanian Jackfork Group. Ouachita Mountains. Red scale = 15 cm. From Shanmugam and Moiola (1995).

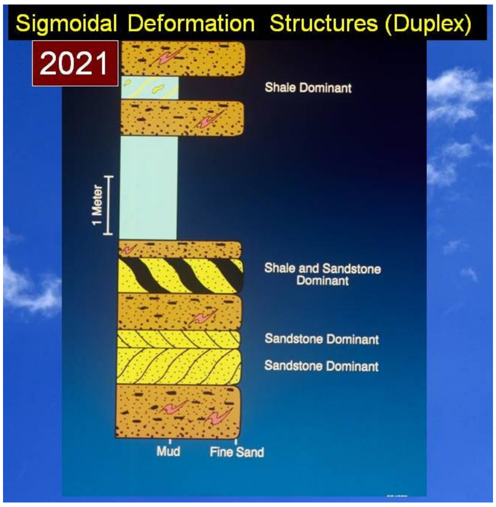

Fig. 174 Types of sigmoidal deformation structures (duplex) In the Jackfork Group. From Shanmugam (2021a).

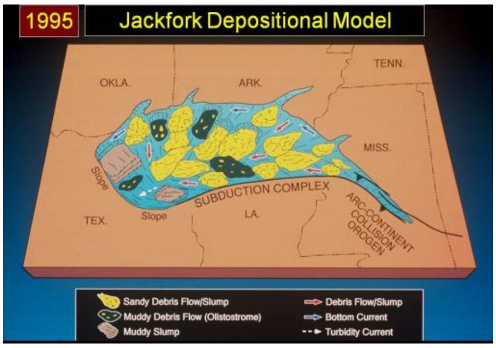

Fig. 175 An unconventional model. From Shanmugam and Moiola (1995).

24. Basin–floor fans: North Sea

Based on a five–year research project at Mobil Oil Company, an international group of geoscientists from the U.S., U.K., and Norway published the following controversial findings on Basin floor fans in the North Sea (Shanmugam et al., 1995).

Examination of nearly 12,000 feet (3658m) of conventional core from Paleogene and Cretaceous deep-water sandstone reservoirs cored in 50 wells in 10 different areas or fields in the North Sea and adjacent regions reveals that these reservoirs are predominantly composed of mass-transport deposits, mainly sandy slumps and sandy debris flows. Sedimentary features indicating slump and debris-flow origin include sand units with sharp upper contacts; slump folds; discordant, steeply dipping layers (up to 60{degrees}); glide planes; shear zones; brecciated clasts; clastic injections; floating mudstone clasts; planar clast fabric; inverse grading of clasts; and moderate-to-high matrix content (5-30%). This model predicts that basin-floor fans are predominantly composed of sand-rich turbidites with laterally extensive, sheet–like geometries. However, calibration of sedimentary facies in our long (400-700 feet) cores with seismic and wire-line-log signatures through several of these basin-floor fans (including the Gryphon-Forth, Frigg, and Faeroe areas) shows that these features are actually composed almost exclusively of mass-transport deposits consisting mainly of slumps and debris flows. Distinguishing deposits of mass-transport processes, such as debris flows, from those of turbidity currents has important implications for predicting reservoir geometry. Debris flows, which have plastic flow rheology, can form discontinuous, disconnected sand bodies that are harder to delineate and less economical to develop than deposits of fluidal turbidity currents, which potentially produce more laterally continuous, interconnected sand bodies. Process sedimentological interpretation of conventional core is commonly critical for determining the true origin and distribution of reservoir sands.

Our reinterpretation of massive sands in the North Sea had also resulted in a major discussion by R. N. Hiscott, K. T. Pickering, A. H. Bouma, B. M. Hand, B. C. Kneller, G. Postma, and W. Soh.(1997) and in a reply by Shanmugam et al. (1997). This debate was mostly about HDTCs. Importantly, Hiscott et al. did not examine the cores that we studied from released wells to the Public.

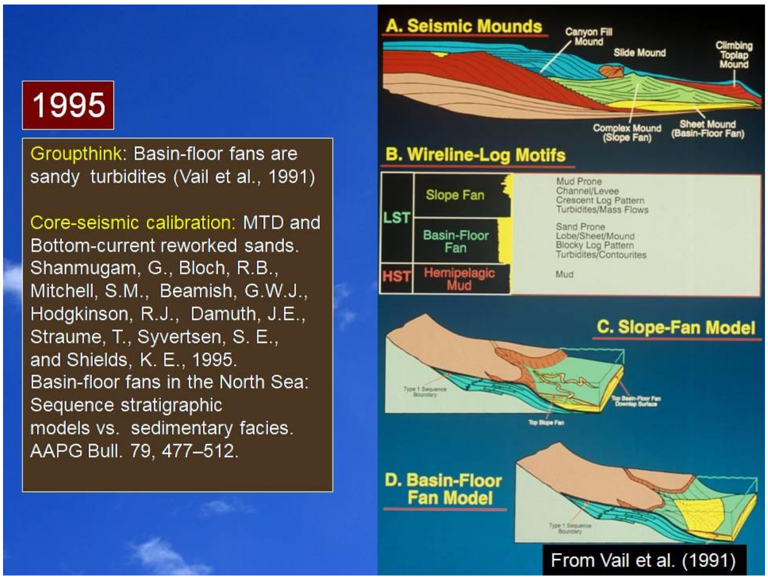

Fig. 176 Sequence-stratigraphic models for deep-water systems vs. Empirical data. From Shanmugam et al. (1995).

Fig. 177 Location map of the Faeroe Basin, West of the Shetland Islands.

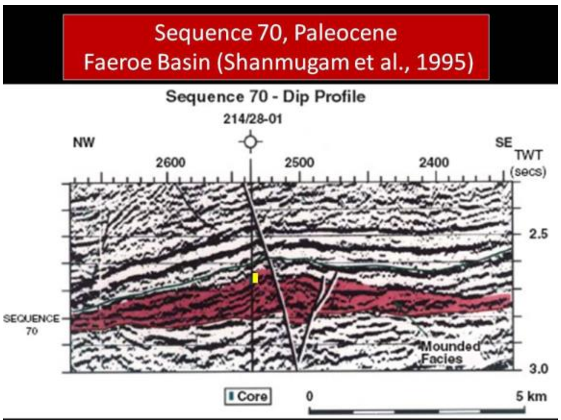

Fig. 178 Seismic profile showing mounded geometry with bidirectional downlap for Sequence 70, Paleocene, Faeroe Basin. Yellow bar represents cored interval in Well 214/28-01. From Shanmugam et al. (1995).

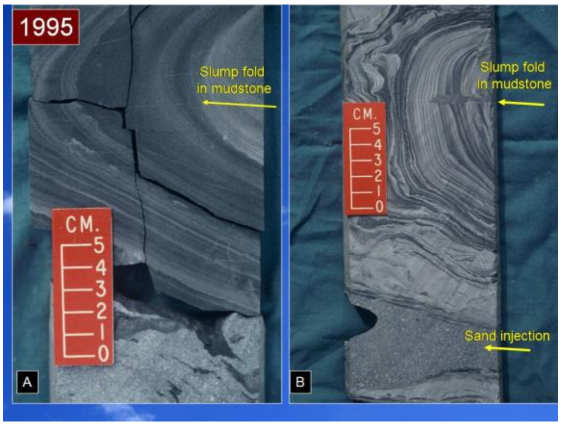

Fig. 179 A and B. Core photographs showing slump-folded heterolithic (sand and mud) facies and associated sand injection, Paleocene, Faeroe Basin, U.K. Continental Margin. From Shanmugam et al. (1995).

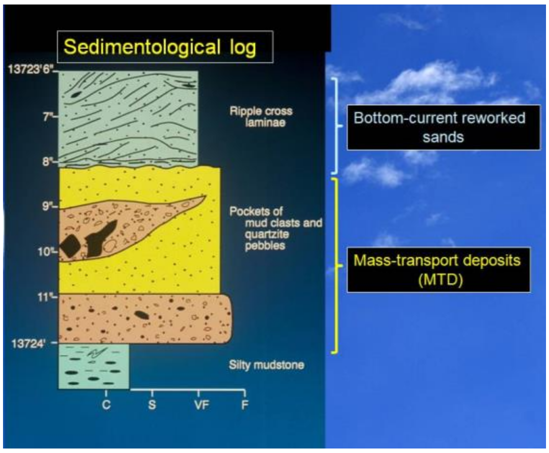

Fig. 180 Sedimentological log showing intervals of Mass-transport deposits (MTD) and Bottom-current reworked sands. Faeroe Basin, U.K. Continental Margin.

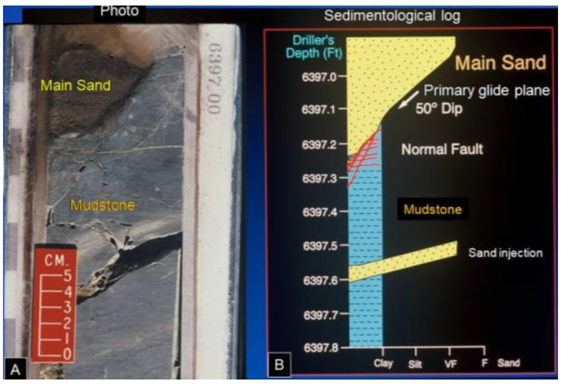

Fig. 181 Core photo (A) and sedimentological log (B) of a basal contact of a Tertiary sand showing evidence for shearing (i.e., slide). North Sea. Photo by G. Shanmugam.

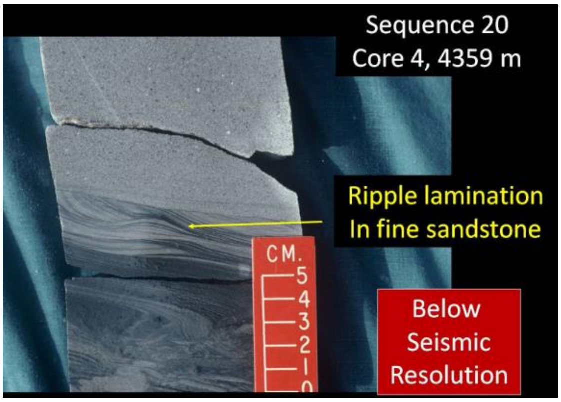

Fig. 182 Core photo showing Ripple lamination In fine sandstone, which is indicative of bottom-current reworking. These features are below seismic resolution. Faeroe Basin, U.K. Continental Margin.

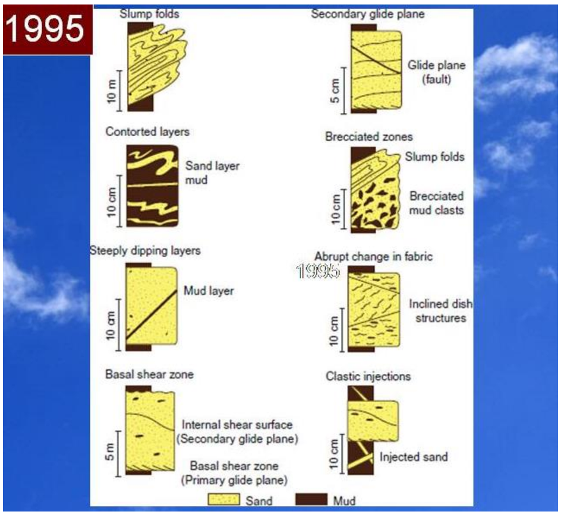

Fig. 183 Features associated with mass-transport deposits (MTD) in the North Sea cores. From Shanmugam et al. (1995).

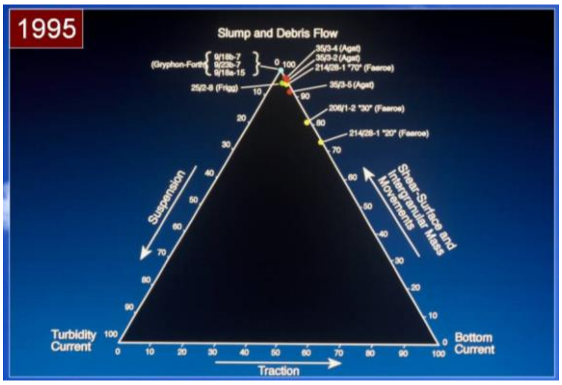

Fig. 184 Plot showing the abundance of slump and debris flow facies in the North Sea and North Atlantic cores. Note influence of bottom currents in the Faeroe cores. From Shanmugam et al. (1995).

25. Bioturbation and Trace Fossils

Bioturbation and trace fossils have been claimed to be an important attribute of deepwater contourites, turbidites, and hyperpycnites. However, these biogenic features have nothing to do with fluid mechanics of depositional processes of contour currents, turbidity currents, or hyperpycnal flows. Bioturbation can be both syn- and post-depositional in timing. Therefore, the presence of ichnological signatures in the ancient sedimentary record is irrelevant for interpreting deep-water deposits as a product of a specific process (Shanmugam, 2018b).

26. Oil from Coal: Gippsland Basin, Australia

Shanmugam (1985a) studied the significance of coniferous rain forests and related Organic matter in generating commercial quantities of oil, Gippsland basin, Australia. Contrary to the conventional belief that humic coal generates primarily gas, 3 billion bbl of recoverable oil has been discovered in the humic coaly succession of the fluviodeltaic Latrobe Group (Upper Cretaceous-Tertiary) that serves as both the reservoir and the source for hydrocarbons in the offshore Gippsland basin of southeastern Australia. Evidence for generation of liquid hydrocarbons from the coaly succession includes: (1) similarity of n-alkane distribution in the oil and in the coal extracts; (2) high wax content of oil (up to 27% by weight); (3) high ratio of pristane/phytane in oil (5-6); and (4) dominance of C_{29} steranes in the oil.

In the Gippsland basin, coniferous rain forests dominated by kauri vegetation flourished in a raised bog setting. Present temperate climate and kauri vegetation of New Zealand are considered to be the modern analog to the Gippsland basin. The coniferous vegetation provided large quantities of hydrogen-rich exinite macerals, such as cutinite and resinite, with potential to generate oil. High rainfall, raised ground-water level, low oxygen, high acidity, and low-nutrient conditions of a raised bog setting were suitable for preserving organic matter. A comparison of gas chromatograms of oils in the Gippsland basin with gas chromatograms of oils generated by hydrous pyrolysis in the laboratory from the immature source rocks suggests that the paraffinic fraction of the oil was derived from coal, and the naphthenic fraction was derived chiefly from resin.

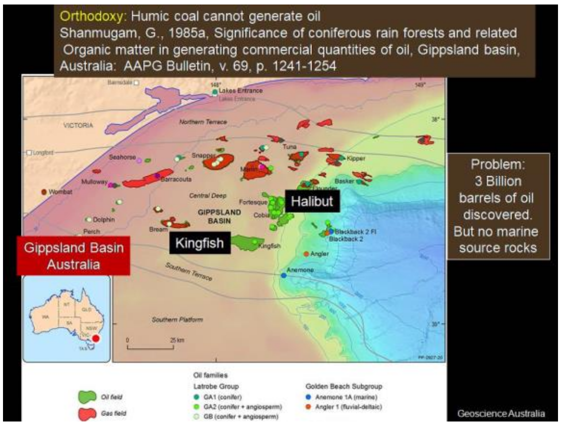

Fig. 185 Location map of Gippsland basin, Australia.

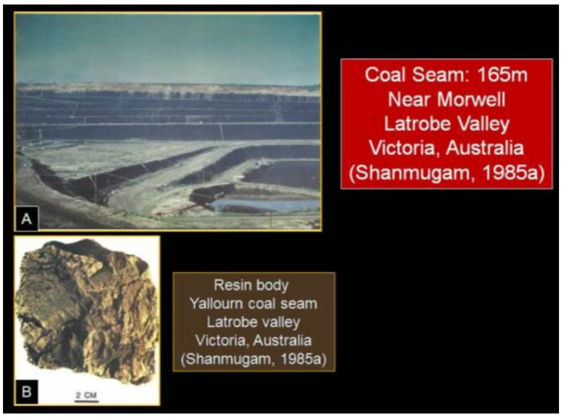

Fig. 186 Coal Seam: 165m, Near Morwell, Latrobe Valley, Victoria, Australia. B. Resin body from the coal seam. From Shanmugam (1985a).

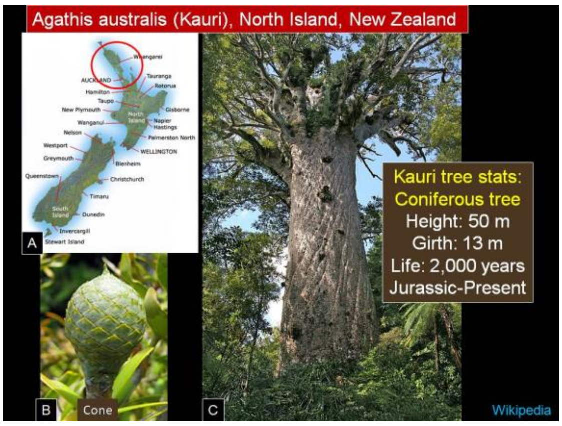

Fig. 187 A. Index map of New Zealand showing study area (circle). B. Kauri cone. C. Fully grown tree of Agathis australis (Kauri), North Island, New Zealand.

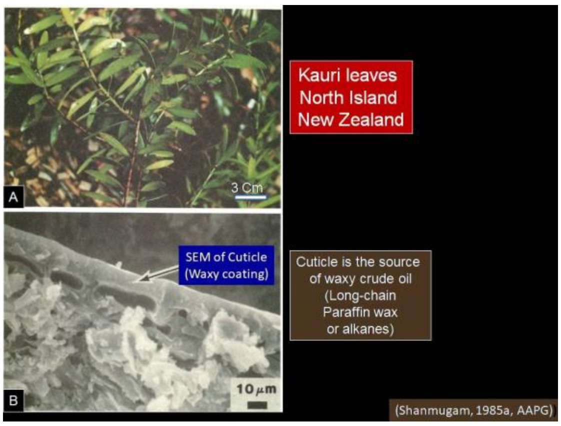

Fig. 188 A. Kauri leaves from an young tree, North Island, New Zealand. B. SEM photograph of Cuticle (Waxy coating). From Shanmugam (1985a).

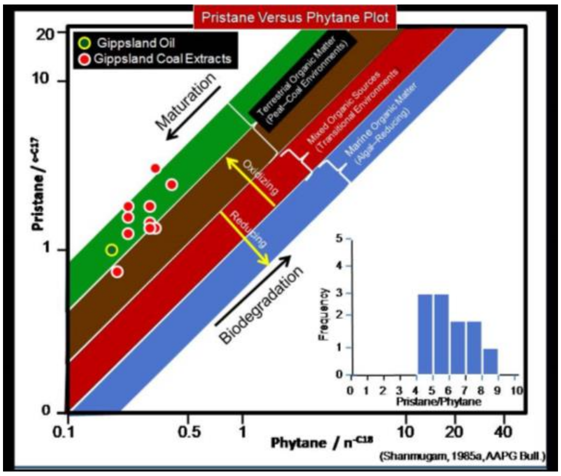

Fig. 189 Pristane Versus Phytane Plot sowing the origin of oil is from terrestrial organic matter. From Shanmugam (1985a).

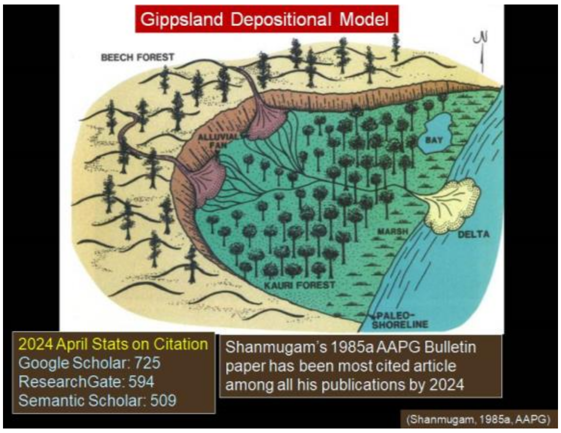

Fig. 190 Gippsland Depositional Model. From Shanmugam (1985a).

27. Appalachian Foredeep basins, USA

New stratigraphic data suggest that the diachronous evolution of the Ordovician foredeeps in the southern and central Appalachians was remarkably similar. Stratigraphic features that characterize the Middle Ordovician Sevier basin in Tennessee and the Middle and Late Ordovician Martinsbuirg basin in Pennsylvania are in identical ascending order: (1) disconformity on the Knox Group–Beekmantown Group, (2) shelf carbonates, (3) slope deposits, (4) submarine fan turbidites, and (5) contourites and muddy turbidites.

We propose that diachronous attempted subduction of the North American craton beneath southeastern microplates and/or volcanic arcs resulted in uplift and erosion of the western shelf followed by its rapid subsidence. Basinward migration of eastern and northeastern terrigenous source areas and associated submarine fan turbidites resulted from continued convergence and filled the basins. Finally, tectonic stabilization and lowering of the source area is recorded by contourites and muddy turbidites.

The evolutionary model proposed for the Sevier and Martinsburg basins closely resembles present-day tectonics of the Timor foredeep and the adjoining Sahul shelf north of Australia. Similar comparisons have also been made for Ordovician basins in the northern Appalachians. Analogous tectonic mechanisms, therefore, appear to have operated diachronously along the eastern margin of North America from Tennessee to New England and possibly to Newfoundland during Ordovician time.

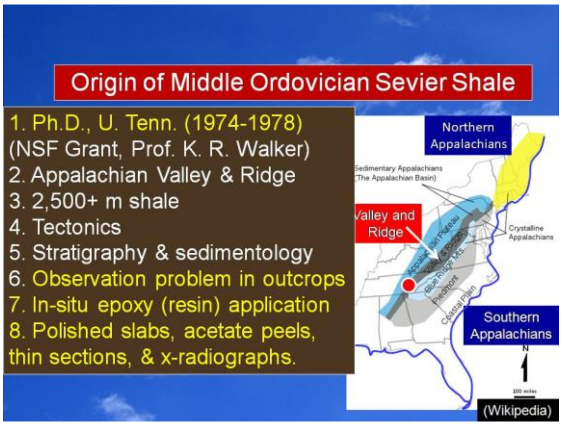

Fig. 191 Location map of Middle Ordovician Sevier Shale Basin, Southern Appalachians.

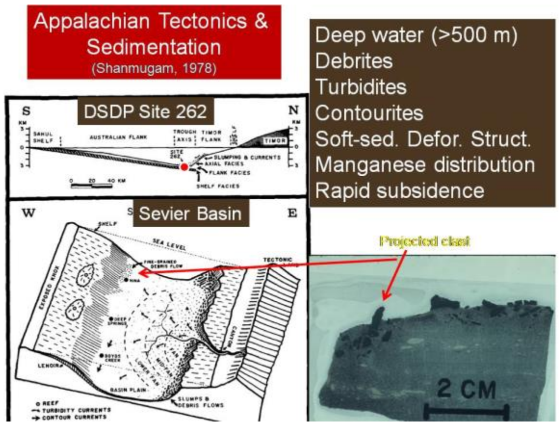

Fig. 192 Comparison of DSDP Site 262 near Timor with Sevier Basin. From Shanmugam (1978).

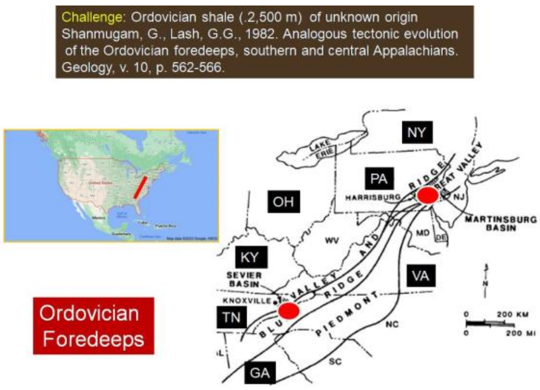

Fig. 193 Analogous tectonic evolution of the Ordovician foredeeps, southern and central Appalachians. Red dots show study areas. From Shanmugam and Lash (1982).

28. The tsunamite problem

Although tsunamis waves are huge (Fig. 1) and they are common (Fig. 2), studies of tsunamis and their deposits have been a challenging task in research (e.g., Bryant, 2001; Bourgeois, 2009, Shanmugam, 2006b, 2012b, among others). For example, the genetic term *tsunamite* is used for a potpourri of deposits formed from a wide range of processes (overwash surges, backwash flows, oscillatory flows, combined flows, soft-sediment deformation, slides, slumps, debris flows, and turbidity currents) related to tsunamis in lacustrine, coastal, shallow-marine, and deep-marine environments (Shanmugam, 2006b). Tsunamites exhibit enormous variability of features (e.g., normally graded sand, floating mudstone clasts, hummocky cross stratification, etc.). These sedimentary features may also be interpreted as deposits of turbidity currents (turbidites), debris flows (debrites), or storms (tempestites). However, sedimentary features play a passive role when these same deposits are reinterpreted as tsunamites on the basis of historical evidence for tsunamis and their triggering mechanisms (e.g., earthquakes, volcanic explosions, landslides, and meteorite impacts). This bipartite (sedimentological vs. historical) approach, which allows here classification of the same deposit as both turbidite and tsunamite, has blurred the distinction between shallow-marine and deep-marine facies. A solution to this problem is to classify deposits solely by a descriptive sedimentological approach. The notion that tsunami waves can directly deposit sediment in the deep sea is unrealistic because tsunami waves represent transfer of energy and they are sediment starved. During tsunamis and major storms, submarine canyons serve as the physical link between shallow-water and deep-water environments for sediment transport. Tsunami-related deposition involves four progressive steps (Fig. 3): (1) triggering stage (offshore), (2) tsunami stage (incoming waves), (3) transformation stage (near the coast), and (4) depositional stage (outgoing sediment flows). In this progression, deep-water deposition can commence only after the demise of incoming tsunami waves due to their transformation into outgoing sediment flows. Deposits of these sediment flows already have established names (e.g., debrite and turbidite). In addition, tsunami-emplaced exotic boulder of large dimensiona (Fig..4). (Frohlich et al. (2009), are difficult to recognize in the field (Fig. 5). Therefore, the term tsunamite for these deposits is obsolete.

There has been a lively debate since the 1980s on distinguishing between paleo-tsunami deposits and paleo-cyclone deposits using sedimentological criteria (Shanmugam, 2012b). Tsunami waves not only cause erosion and deposition during inundation of coastlines in subaerial environments, but also trigger backwash flows in submarine environments. These incoming waves and outgoing flows emplace sediment in a wide range of environments, which include coastal lake, beach, marsh, lagoon, bay, open shelf, slope and basin. Holocene deposits of tsunami-related processes from these environments exhibit a multitude of physical, biological and geochemical features. These features include basal erosional surfaces, anomalously coarse sand layers, imbricate boulders, chaotic bedding, rip-up mud clasts, normal grading, inverse grading, landward-fining trend, horizontal planar laminae, cross-stratification, hummocky cross-stratification, massive sand rich in marine fossils, sand with high K, Mg and Na elemental concentrations and sand injections. These sedimentological features imply extreme variability in processes that include erosion, bed load (traction), lower flow regime currents, upper-flow regime currents, oscillatory flows, combined flows, bidirectional currents, mass emplacement, freezing en masse, settling from suspension and sand injection. The notion that a 'tsunami' event represents a single (unique) depositional process is a myth. Although many sedimentary features are considered to be reliable criteria for recognizing potential paleo-tsunami deposits, similar features are also common in cyclone-induced deposits. At present, paleo-tsunami deposits cannot be distinguished from paleo-cyclone deposits using sedimentological features alone, without historical information. The future success of distinguishing paleo-tsunami deposits depends on the development of criteria based on systematic synthesis of copious modern examples worldwide and on the precise application of basic principles of process sedimentology.

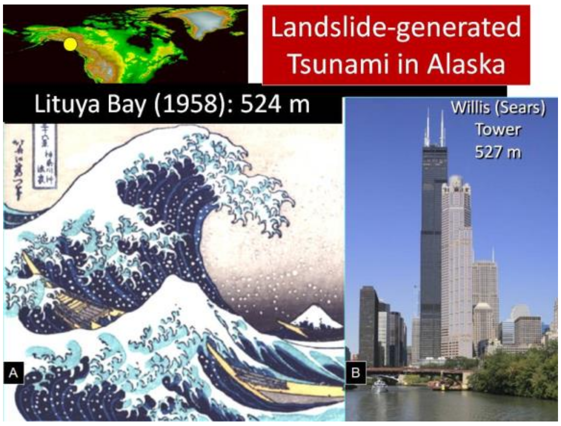

Fig. 194 A. Lituya Bay (1958) with a wave height of 524 m can easily topple the radio antenna at the top of the Willis (Sears) Tower at a height of 527 m (B).

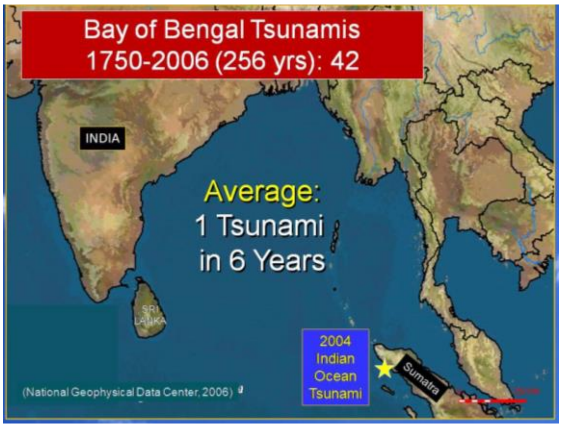

Fig. 195 Occurrence of tsunamis in the Bay of Bengal. (National Geophysical Data Center, 2006)

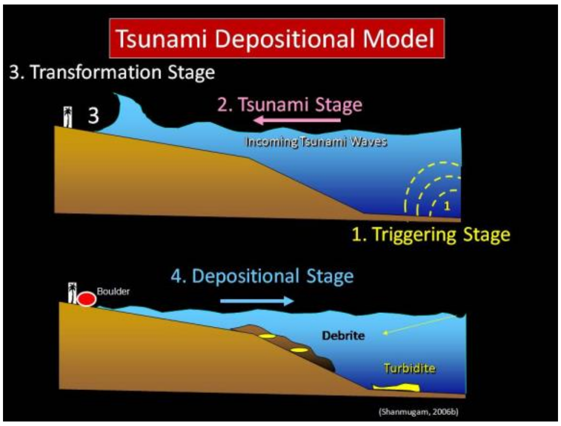

Fig. 196 Four stage depositional model for tsunamis. (Modified after Shanmugam, 2006b).

Fig. 197 Tsunami-emplaced exotic boulder. From Frohlich et al. (2009).

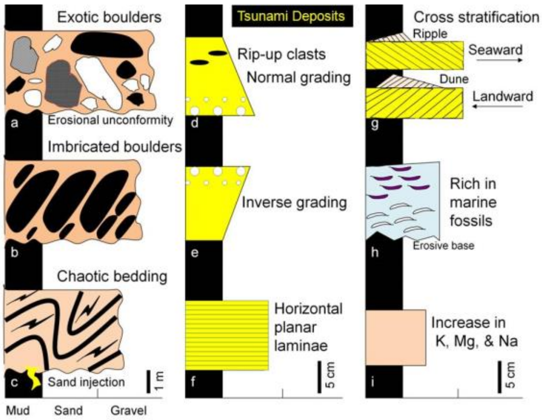

Fig. 198 Diverse features of Tsunami deposits. From Shanmugam (2012b).

29. Global case studies of soft–sediment deformation structures (SSDS)

Soft-sediment deformation structures (SSDS) have been the focus of attention for over 150 years (e.g., Allen, 1977, 1984; Alfaro et al., 2016; Collinson, 1994, Helwig, 1970; Lowe, 1975, 1976; Maltman, 1994a, b; Shanmugam, 2016a, 2017a, c, d; Van Loon, 2009, Van Loon et al., 2016, among many others). Existing unconstrained definitions allow one to classify a wide range of features under the umbrella phrase "SSDS". As a consequence, a plethora of at least 120 different types of SSDS (*e.g.*, convolute bedding, slump folds, load casts, dish-and-pillar structures, pockmarks, raindrop imprints, explosive sand–gravel craters, clastic injections, crushed and deformed stromatolites, *etc*.) have been recognized in strata ranging in age from Paleoproterozoic to the present time. The two factors that control the origin of SSDS are prelithification deformation and liquidization. A sedimentological compendium of 140 case studies of SSDS worldwide, which include 30 case studies of scientific drilling at sea (DSDP/ODP/IODP), published during a period between 1863 and 2017, has yielded at least 31 different origins. Earthquakes have remained the single most dominant cause of SSDS because of the prevailing "seismite" mindset. Selected advances on SSDS research are: (1) an experimental study that revealed a quantitative similarity between raindrop-impact cratering and asteroid-impact cratering; (2) IODP Expedition 308 in the Gulf of Mexico that documented extensive lateral extent (>12 km) of mass-transport deposits (MTD) with SSDS that are unrelated to earthquakes; (3) contributions on documentation of pockmarks, on recognition of new structures, and on large-scale sediment deformation on Mars.

Problems that hinder our understanding of SSDS still remain. They are: (1) vague definitions of the phrase "soft-sediment deformation"; (2) complex factors that govern the origin of SSDS; (3)

omission of vital empirical data in documenting vertical changes in facies using measured sedimentological logs; (4) difficulties in distinguishing depositionalprocesses from tectonic events; (5) a model-driven interpretation of SSDS (*i.e.*, earthquake being the singular cause); (6) routine application of the genetic term "seismites" to the "SSDS", thus undermining the basic tenet of process sedimentology (*i.e.*, separation of interpretation from observation); (7) the absence of objective criteria to differentiate 21 triggering mechanisms of liquefaction and related SSDS; (8) application of the process concept "high-density turbidity currents", a process that has never been documented in modern oceans; (9) application of the process concept "sediment creep" with a velocity connotation that cannot be inferred from the ancient record; (10) classification of pockmarks, which are hollow spaces (*i.e.*, without sediments) as SSDS, with their problematic origins by fluid expulsion,

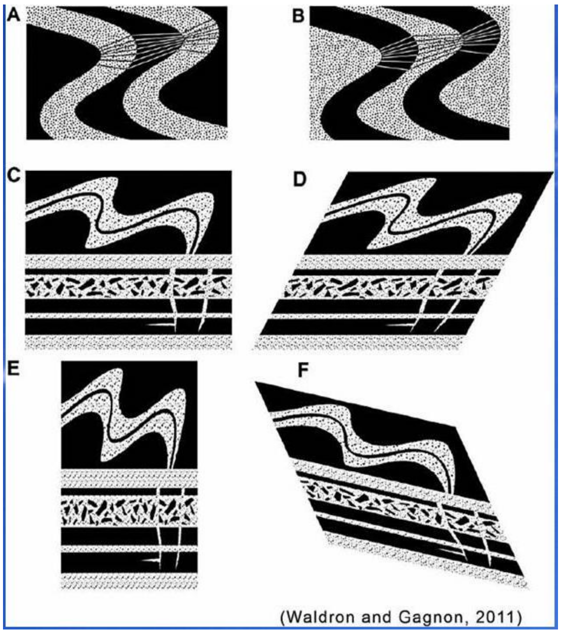

Fig. 199 Idealized diagrams of structures in 6 types of deformed sedimentary rocks (Sand: Stippled; Mud: Black). A—Type 1: Typical geometry of folds in clastic sedimentary strata deformed at low metamorphic grade, showing dip isogons (lines joining points of equal dip on successive surfaces). Sandstone layers typically show tighter curvature on inner arcs (class 1 geometry; Ramsay, 1967) while mud layers have tight curvature on outer arcs (class 3); B — Type 2: Reversal of normal geometrical relationships characteristic of folds formed while sand was liquefied; C — Type 3: Undeformed configuration with: angular mud clasts surrounded by sand; sand-filled dikes cross-cutting mud layers; and folded liquefied sand layers; D — Type 4: Type 3 with superimposed simple shear parallel to bedding; E — Type 5: Type 3 with superimposed pure shear parallel to bedding; F — Type 6: Type 3 with superimposed arbitrary strain. From Waldron and Gagnon (2011), with permission from Elsevier.

sediment degassing, fish activity, *etc*.; (11) application of the Earth's climate-change model; and most importantly, (12) an arbitrary distinction between depositional process and sediment deformation. Despite a profusion of literature on SSDS, our understanding of their origin remains muddled. A solution to the chronic SSDS problem is to utilize the robust core dataset from scientific drilling at sea (DSDP/ODP/IODP) with a constrained definition of SSDS.

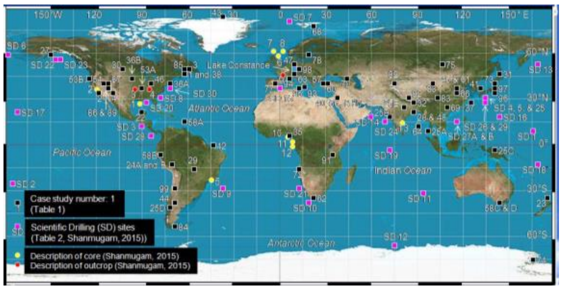

Fig. 200 Map showing locations of case studies of soft-sediment deformation structures (SSDS). From Shanmugam (2017a).

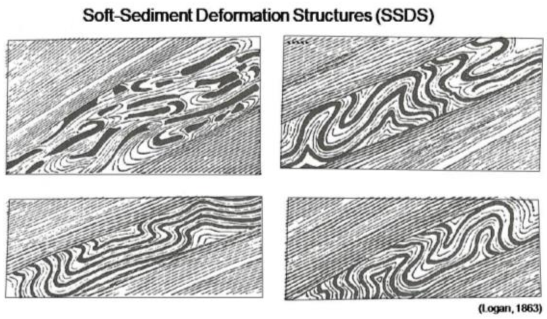

Fig. 201 Detailed sketches by Sir William Edmond Logan of localized deformed beds within otherwise undeformed Devonian limestones, Gaspe Peninsula, Quebec, Canada (Logan, 1863).

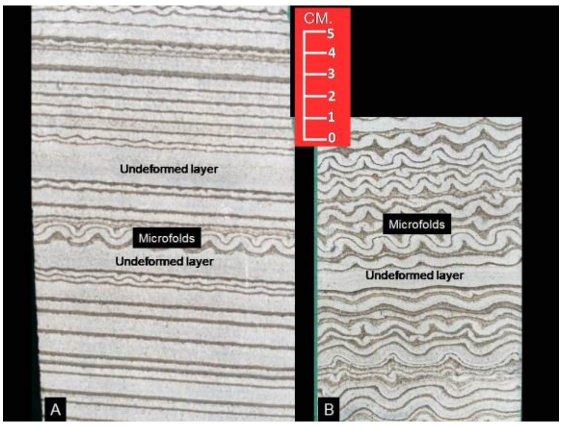

Fig. 202 Core photographs showing microfolds in anhydrite (white) layers with intervening undeformed anhydrite layers. See Kirkland and Anderson (1970).

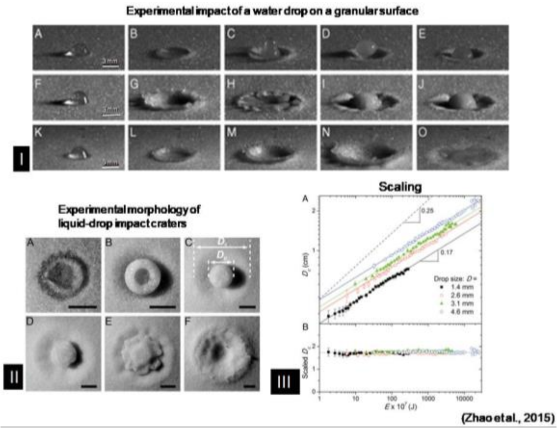

Fig. 203 Experimental results of granular impact cratering by liquid drops (Zhao et al., 2015).

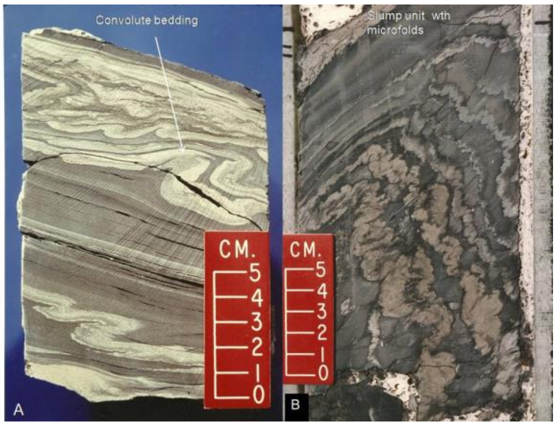

Fig. 204 Core photos of Convolute bedding (A) and Slump unit with microfolds (B).

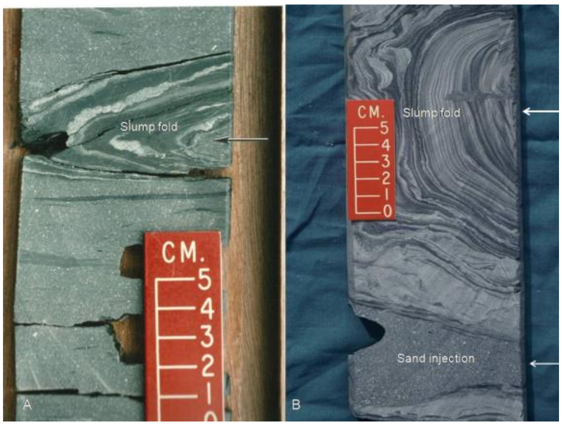

Fig. 205 (A) Core photograph showing slump-fold axis (arrow) of a heterolithic facies unit in sandstone, Cretaceous, West Africa. (B) Core photograph showing slump-folded heterolithic (sand and mud) facies and associated sand injection, Paleocene, Faeroe Basin, U.K. Continental Margin. Source: From Shanmugam (2012.

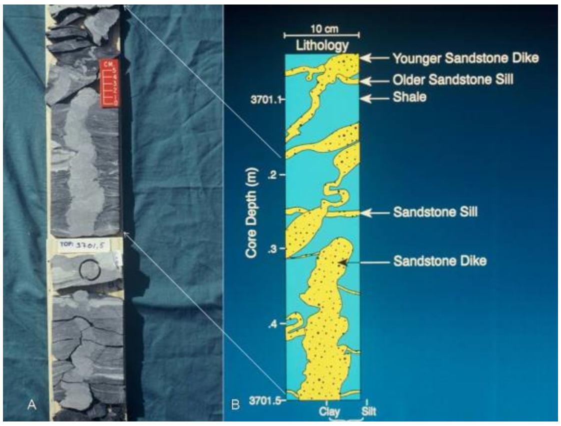

Fig. 206 Sand injections in mudstone. A. Core photo. B. Sketch.

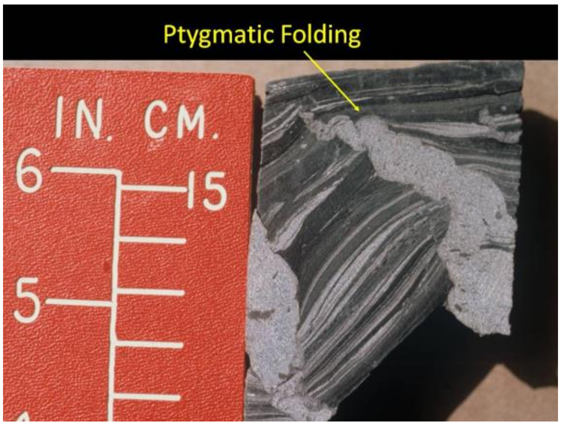

Fig. 207 Sand injection with ptygmatic folding (arrow).

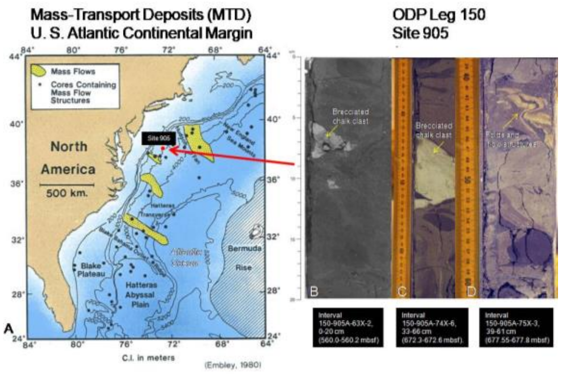

Fig. 208 A . Map showing the distribution of MTD on the U.S. Atlantic Continental Margin (Embley, 1980). B, C, and D. ODP cores showing breccias (Shipboard Scientific Party, 1994 and J. E. Damuth).

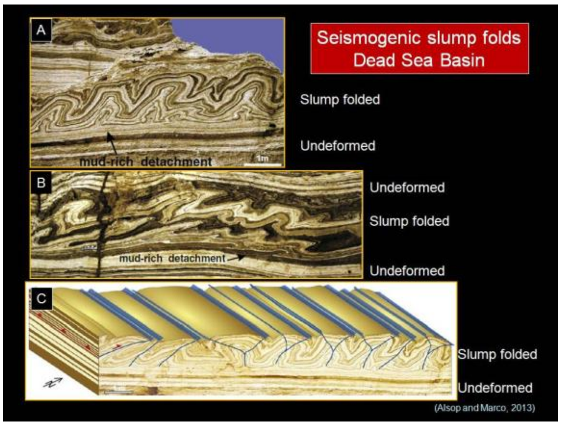

Fig. 209 (A and B) Photographs showing slump folded layers with undeformed layers above and below. (C) Sketch. Dead Sea Basin. These are genuine seismites. Compiled from Alsop and Marco (2013).

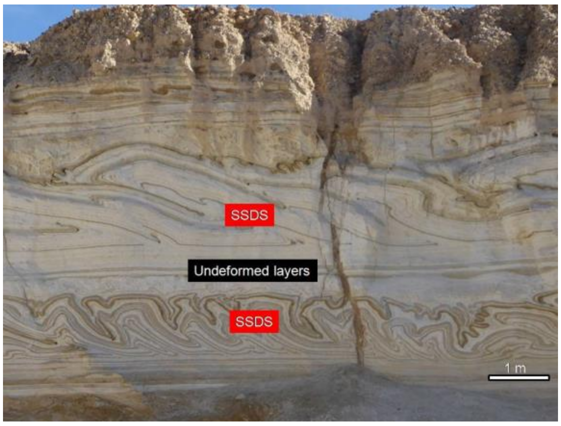

Fig. 210 Outcrop photograph showing two layers of seismicity─induced soft-sediment deformation structures (SSDS), in this case slump folds, with an intervening interval of undeformed layers. Perazim Wadi in the Quaternary Lisan Formation, a dry wash in the Ami'az Plain SW of Ein Boquet in Israel. Although this formation is not of deep-water origin, it illustrates the seismicity-induced sediment deformation in tectonically active settings. Source: Photo courtesy of Professor Emeritus R.D. Hatcher, Jr., Department of Earth and Planetary Sciences, The University of Tennessee, Knoxville.

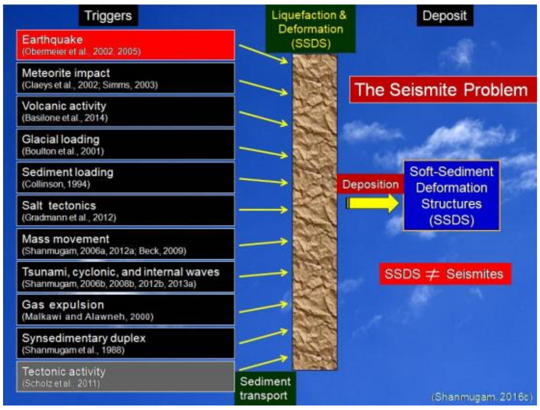

Fig. 211 The genetic term "Seismite" should be used with caution because there are multiple triggers of SSDS (Shanmugam (2016c).

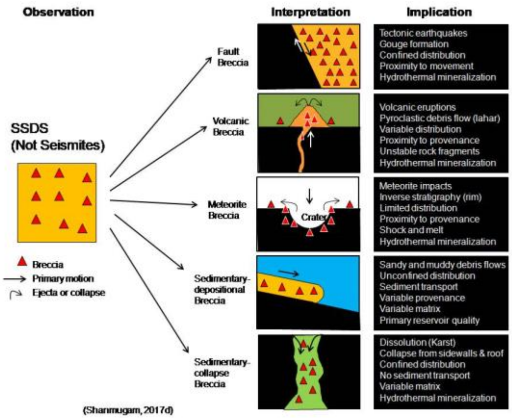

Fig. 212 The genetic term "Seismite" should be used with caution because there are multiple origins of breccias (Shanmugam, 2017d).

30. Porosity enhancement from chert dissolution beneath erosional unconformity**: Alaska, USA**

Shanmugam and Higgins (1988) studied "Porosity enhancement from chert dissolution beneath Neocomian unconformity: Ivishak Formation, North Slope, Alaska". Secondary porosity caused by chert dissolution is common in the hydrocarbon-producing fluvial facies of the Ivishak Formation (Triassic), Prudhoe Bay Field, North Slope, Alaska. Petrographic observations suggest that macroporosity caused by chert dissolution tends to increase toward the Neocomian unconformity. In the Prudhoe Bay field, a lateral increase in core porosity (from 15% at about 30 km from the unconformity to 30% near the unconformity) and in permeability (from 50 md at about 30 km from the unconformity to 800 md near the unconformity) is evident toward the unconformity. This increase occurs within the fluvial facies (zone 4) of nearly uniform grain size and framework composition (chert litharenite). Major chert dissolution probably took place during the Neocomian uplift when the Ivishak Formation was exposed to acidic meteoric waters in the near-surface environment.

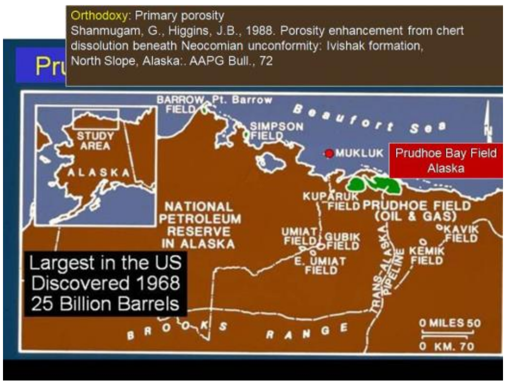

Fig. 213 Location map of Prudhoe Bay Field, Alaska.

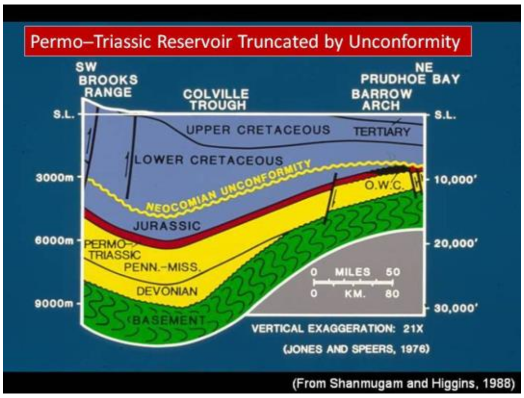

Fig. 214 Stratigraphic cross section showing the truncation of the Permo–Triassic Reservoir by fhe Unconformity near Prudhoe Bay. From Shanmugam and Higgins (1988). AAPG.

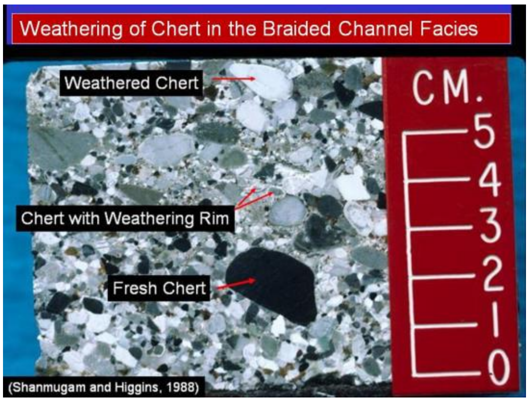

Fig. 215 Core photo showing Weathering of Chert in the Braided Channel Facies of the Ivishak Formation, Prudhoe Bay, Alaska.

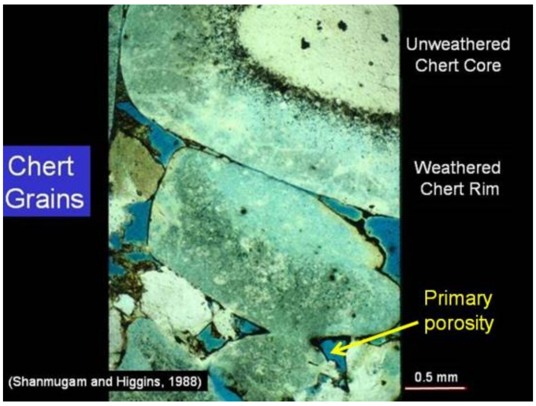

Fig. 216 Thin section photo showing weathered chert rim. Ivishak Formation, Prudhoe Bay, Alaska.

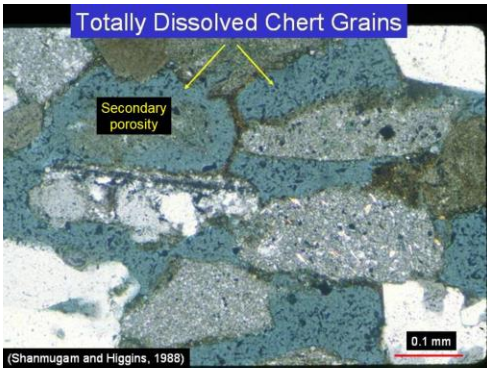

Fig. 217 Thin section photo showing totally dissolved chert grains indicated by clay rims.

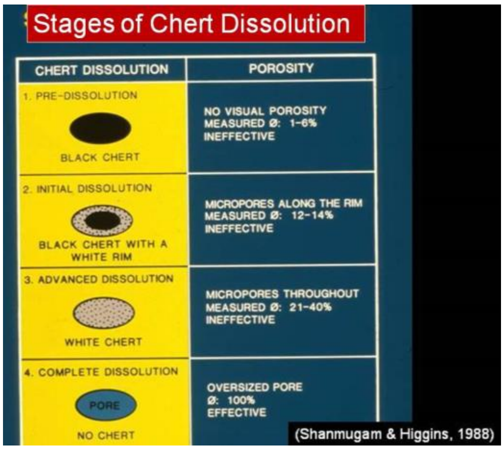

Fig. 218 Four Stages of Chert Dissolution in the Ivishak Formation, Prudhoe Bay, Alaska. From Shanmugam and Higgins (1988). AAPG.

Fig. 219 Karst Region of South China is considered as the modern analogue in terms of heavy rain during the Unconformity formation in the Prudhoe Bay area. From Sweeting (1978).

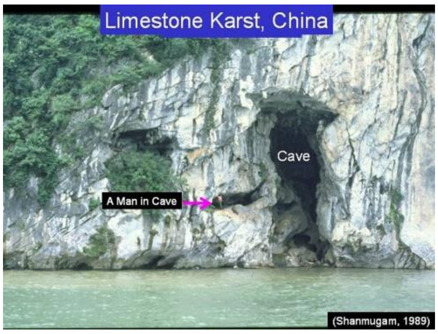

Fig. 220. A cave in the limestone karst near Guilin, South China. From Shanmugam (1989).

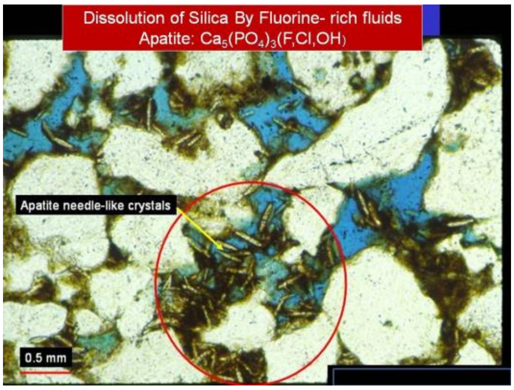

Fig. 221 Thin section showing Apatite crystals (within red circle), which resulted in dissolution of Silica by Fluorine- rich fluids caused by Apatite: $Ca_5(PO_4)_3(F,Cl,OH)$

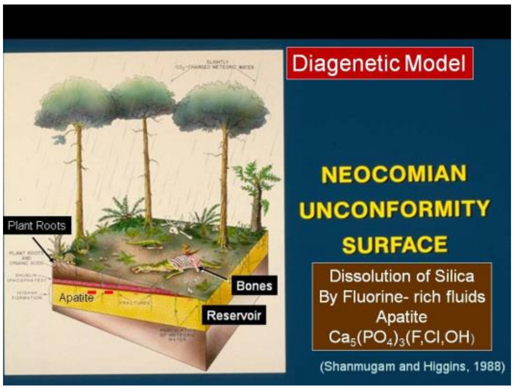

Fig. 222 A diagenetic model showing the Unconformity surface and generation of Fluorine-rich fluids caused by Apatite $Ca_5(PO_4)_3(F,Cl,OH)$.

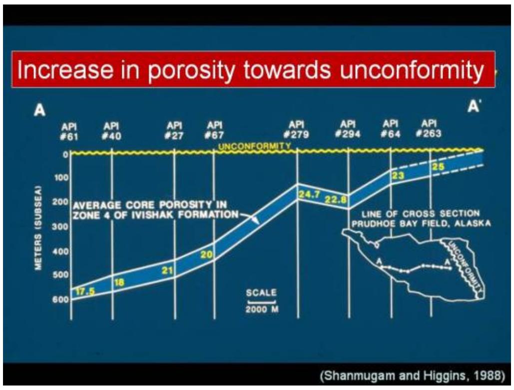

Fig. 223 Empirical data showing increase in porosity towards the unconformity. From Shanmugam and Higgins (1988). AAPG.

31. The Climate Change and CO_2

There are skeptics who vigorously question the validity of Anthropogenic Global Warming. They include:

1. Chandrasekharam, D. (2021).
2. Christy, John R., (2022).
3. Curry, J. (2023).
4. Dyson, Freeman (2007).
5. Epstein, A. (2022).
6. Happer, W. (2022 and 2023).
7. Koonin, S. E. (2021).
8. Lindzen, R. (2023a, 2023b).
9. Lomborg, B. (2007).
10. Moore, P. (2021).
11. Shanmugam, G. (2023b and 2024).

In this section, I briefly address some key issues surrounding Climate Change with Figs. 1 to 13. I also provide some recent updates on the possible culprits who blew up the Nord Stream Pipelines.

The Solar Supremacy of Energy

The Sun is the primary energy source for our planet's energy budget and contributes to processes throughout Earth (Fig. 224) (*UCAR/The COMET Program*) https://scied.ucar.edu/learning-zone/earth-system/energy-from-sun.

Although we classify energy into two groups (Table 4), namely (1) Fossil Fuels (i.e., Coal, Natural Gas, and Oil) and (2) Renewable Energy (E.g., Solar, Wind, and Hydro), both groups derive their energy from the Sun (Fig. 225). This solar supremacy is fundamental in the Climate Change debate.

Fossil Fuels

Coal is a type of fossil fuel, formed when dead plant matter decays into peat and is converted into coal by the heat and pressure of deep burial over millions of years.

Photosynthesis is a biological process used by many cellular organisms to convert sunlight energy into chemical energy. Most plants, algae and cyanobacteria perform photosynthesis.

Natural Gas is formed when layers of organic matter (primarily marine microorganisms) decompose under anaerobic conditions and are subjected to intense heat and pressure underground over millions of years. The energy that the decayed organisms originally obtained from the sun via photosynthesis is stored as chemical energy within the molecules of methane and other hydrocarbons.[7]

Oil (liquid hydrocarbon) is a fossil fuel derived from fossilized organic materials, such as zooplankton and algae. Vast amounts of these remains settled to sea or lake bottoms where they were covered in stagnant water under anoxic conditions. With increasing burial, intense heat and pressure built up caused the organic matter to change, first into a waxy material known as kerogen, and then into petroleum.

Renewable Energy

Solar energy refers to radiant light and heat derived directly from the Sun

Wind, the natural movement of air or other gases relative to a planet's surface, is caused by the uneven heating of the earth surface by the Sun.

This uneven heating causes Earth's surface and atm osphere to be warmer near the equator than

near the poles. In the atmosphere, warmer air rises as cooler air sinks. This movement of air p roduces wind, which circulates and redistributes he at in the atmosphere.

Hydro is also the result of the Sun. For example, the Sun evaporates ocean water. Water evaporated by the sun forms clouds and rain to give us flowing streams and rivers. We build Dam across rivers to generate hydropower (Fig. 2).

Biomass. Wood and wood residues is the largest biomass energy source today. Unlike Solar and Wind, burning either fossil fuels or biomass releases carbon dioxide (CO_2), a greenhouse gas. In other words, the distinction between fossil fuels and biomass in terms of saving the planet from Anthropogenic Global Warming by preferring biomass is ludicrous.

The Climate Change Problem

The geologic record shows that the Earth's climate has always been changing naturally during the past 600 million years in terms of CO_2 and temperature, without CO_2 emissions from Fossil

Fuels by humans. A plot of CO_2 vs. Temperature for the last 600 million years shows basically no correlation for most of this time (Berner, 2004; Scotese et al., 2021). There were both warming and cooling periods prior to the appearance of human beings on the Planet Earth. The Anthropogenic Global Warming (AGW) is attributed to the Industrial Age that commenced in 1760 in the Great Britain and later in the USA. The principal driver behind the Industrial Revolution has been Fossil Fuels (i.e., Oil, Natural Gas, and Coal). Since 1900, Fossil Fuels have been the single most important driver of the modern human civilization. If the Net–Zero CO_2 policy were to be implemented, large numbers of people would die and the modern human civilization would come to a sudden halt, and humans left alive would have to revert back to the lifestyles of the Neanderthals who lived 40,000 years ago without the benefits of Fossil Fuels. The failure of the Net–Zero policy is already evident by (1) the Germany's shift back to coal from unreliable wind to face the energy crisis caused by the Russia-Ukraine War on 24th February 2022, (2) the bankruptcy of Sri Lanka in 2022 caused by the ESG (Environmental, Social, and Governance) policy that banned chemical fertilizers, and (3) the major victory by the Dutch pro-farmers party (BBB) in the 2023 provincial elections in opposition to the Dutch government's climate policy to eliminate nitrogen emissions by reducing 30% of livestocks in the Netherlands. A climate-change model for 200 Years (1900-2100) is proposed based on four basic parameters, namely, CO_2, Temperature, Population, and GDP per capita. The model shows a steady increase in all four parameters from 1900 to 2100. In this model, calculations based on the Max Planck's Curve by Van Wijngaarden and Happer (2020), an increase in CO_2 and Temperature by 2100 would be trivial and that would not hinder either the population growth or the GDP growth. Therefore, Climate Change is not an existential threat. The proposed roadmap for the future is to continue to use the Fossil Fuels as usual. The ultimate driver of the Earth's climate is the omnipotent Sun, not humans. The CO_2 in the atmosphere helps not only to modulate the Earth's Temperature suitable for human survival, but also to enhance Global Greening. Therefore, we should shift our resources and attention away from Global Warming and aim towards eliminating Global Poverty (Shanmugam, 2023b, 2024).

The Nord Stream Pipeline Problem

We all wonder as to "Who blew up the Nord Stream Pipeline in 2022 in the Baltic Sea?" (Hersh, 2023). This sabotage had resulted in emitting 220,000 tones of methane in six days (see Shanmugam, 2023b). Well, the Russian President Vladimir Putin offered some meaningful insights into this problem during his interview with Tucker Carlson in Kremlin on February 6, 2024 (Putin, 2024).

The Groupthink Problem

In the Happer's (2023) YouTube video "CO2, the gas of life", the Q&A session with critical questions and his brilliant answers was truly educational. In addition to his main point on CO2, the three additional points that emerge from his lecture were:

(1) Peer-review practice is flawed.

(2) Groupthink destroys scientific progress.

(3) Not all Scientists are principled.

I have been battling these three demons in Science for nearly 40 years in peer-reviewed publications (Shanmugam, 2022f, 2022g, 2023d). I am not alone. In Richard Lindzen's (2023b) Podcast "Manufacturing consent in times of crisis", he provided an excellent historical account on peer reviews. The Groupthink problem must be eliminated in resolving the Climate Change problem.

"Climate: The Movie (The Cold Truth)" by Martin Durkin
(March 19, 2024)

The "Climate: The Movie (The Cold Truth)" was produced by Tom Nelson, a Member of CO_2 Coalition. The movie includes interviews with a number of prominent scientists that include:

1. CO_2 Coalition Co-founder and Chairman Dr. William Happer (Emeritus, Physics, Princeton).
2. CO_2 Board members Dr. Patrick Moore (co-founder of Greenpeace) and Dr. John Clauser (2022 Nobel Laureate in Physics).
3. CO_2 Coalition members: Dick Lindzen (MIT) , Roy Spencer (University of Alabama in Huntsville) and Tony Heller.
4. Prof. John Christy (University of Alabama in Huntsville).
5. Prof. Steve Koonin (New York University).
6. Prof. Willie Soon (Harvard and Smithsonian).

"Climate: The Movie" highlights a different perspective on the climate change debate and is supported by scientists who have signed the Clintel's World Climate Declaration. This group of researchers seeks to present an alternative narrative in the face of the dominant discourse.

The movie begins with an emotional cry from Greta Thurnberg "People are dying. Entire ecosystems are collapsing. We are in the beginning of a mass extinction, and all you can talk about is money and fairy tales of eternal economic growth. How dare you!" On the other more rational side, Prof. William Happer says that the Climate Change Fear is a hoax! The entire movie is designed to promote the Science using empirical data and common sense.

Rating: Five Stars out of Five!

Duration: 1:19:53: Just right.

Comments by Scientists and Images: Pragmatic and Brilliant. This movie is an antidote to Al Gore's movie (2006) "An Incovenient Truth".

Written and Directed by Martin Durkin: Excellent
Produced by Tom Nelson: Kudos!
Sound by Alastair McFlurry: Fantastic!!!

In short, this is a great movie. I strongly recommend to everyone to watch the movie with the entire family. This movie must be a required watching ITEM for all students all over the world.

ENJOY THE MOVIE:
https://www.climatethemovie.net/home

Related articles by the Reviewer:

Shanmugam, G. (2023). 200 Years of Fossil Fuels and Climate Change (1900-2100). The Journal of the Geological Society of India, v. 99, 1043-1062.

Shanmugam, G. (2024). Fossil fuels, climate change, and the vital role of CO_2 to people and plants on planet Earth. Bulletin of the Mineral Research and Exploration, v. 174, in press. https://dergi.mta.gov.tr/article/show/2800.html Retrieved October 17, 2023

Movie review by
G. Shanmugam, Ph.D.
CO_2 Coalition member

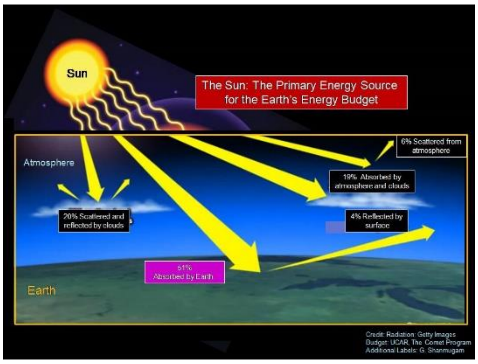

Fig. 224 The Sun is the Primary Energy Source for the Earth's Energy Budget. Credit: Top: Radiation: Getty Images. Bottom: Budget: UCAR, The Comet Program. Additional Labels: G. Shanmugam

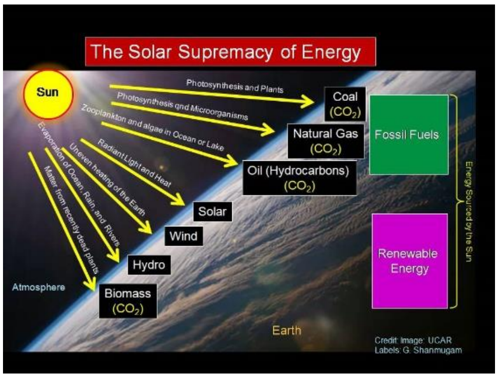

Fig. 225 The Sun is the Primary Energy Source for the Earth's Fossil Fuels and Renewable Energy. Like Fossil Fuels, burning of Biomass also emits CO_2.

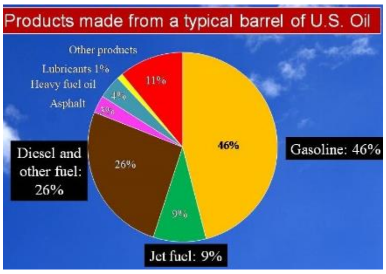

Fig. 226 Modern civilization cannot exist without oil. From Shanmugam (2023b). Credit U.S. Energy information Administration. Public Domain.

Table 4. Fossil fuels vs. Renewable energy. Modified after Shanmugam (2024).

Serial Number	Property	Fossil Fuels	Renewable Energy
1	Types	Oil Natural gas Coal	Solar Wind Hydro Biomass Geothermal*
2	Percentage of world's energy	80%	3%
3	Usage in critical areas, such as agriculture, production of fertilizers, heavy machinery, aviation, shipping, trucking and other ground transportation, sanitation, road construction, pipeline construction, military complexes, war machines, space industry, healthcare industry, among many others.	Yes	No
4	Petroleum products critical to modern living	>6,000 syringes, medical equipment, gloves, N–95 masks, Aspirin, antibacterial, cough syrups, lubricants, ointments	0 (Zero)
5	Energy density	Very high (Concentrated) composed of hydrocarbons	Low (Dilute)
6	Occurrence	Subsurface	Subaerial
7	Reliability	Very high. Continuous supply.	Low Sun and the wind are intermittent, uncontrollable, unreliable, sources of energy (Lawson, 2022; Schreiber, 2022)
8	Energy storage	Cheap and efficient	Expensive and inefficient
9	Emission of CO_2	Low (Happer, 2022)	Zero
10	Damage to environment	Ninety percent of the internal combustion engine (ICE) lead–acid batteries are recycled (Eberling, 2022). Minimum Emission of CO_2 (Lindzen, 2012; Happer, 2022)	Only five percent of the EV lithium-ion batteries are recycled (Eberling, 2022). Yes (e.g. killing of birds by wind turbines)
11	Group think	Low	Very high
12	Influence by International Organizations and Social Media	Accentuate the negative and ignore the positive attributes	Accentuate the positive and ignore the negative attributes
13	Research funding	Low	Very high. German funding for renewable energy research reaches 1.31 billion Euros (Meza, 2022)
14	Availability	Unlimited reserve with potential for new discoveries (CNOOC, 2002). Fracking of shale gas.	Unlimited
15	The ultimate effect of the Net–Zero policy (IEA, 2021; Lee et al. 2023)	Planet Earth with Neanderthal–like humans, and with real–world earthquakes, volcanic activities, meteorite impacts, tropical cyclones, and tsunamis	Not applicable

16		Ethical Methods of extraction of Fossil fuels do not employ renewable energy	Hypocritical Methods of extraction of renewable energy do utilize Fossil Fuels. 1. Wind turbines and Solar panels ─the means of collecting renewable energy─ are made with petrochemical products (Hockstad, 2016) 2. The green─energy elites, such as, Al Gore, Leonardo DiCaprio, and Bill Gates, fly to Davos in Switzerland to attend the World Economic Forum, where they promote renewable energy. However, their private jets consume enormous amounts of jet fuels emitting CO_2.
*Not the focus of this article			

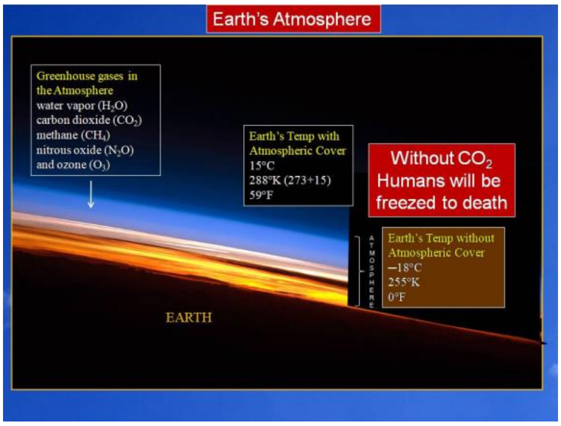

Fig. 227 Humans will perish without CO_2. From Shanmugam (2023b).

Fig. 228 Modern civilization cannot exist without Petroleum products. From Shanmugam (2023b).

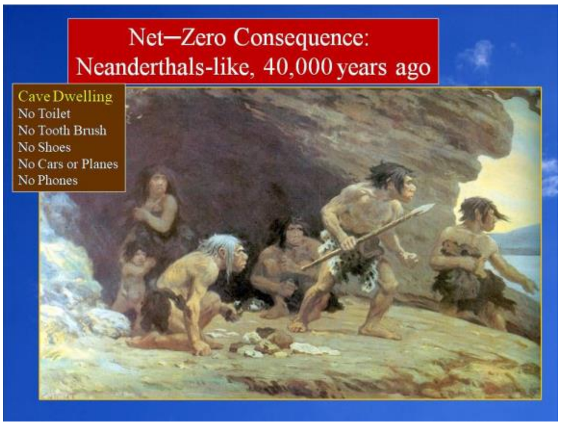

Fig. 229 Under Net─Zero Policy, Humans must learn to adopt cave dwelling of Neanderthals-like living, which existed 40,000 years ago. From Shanmugam (2024). Image: Wikipedia.

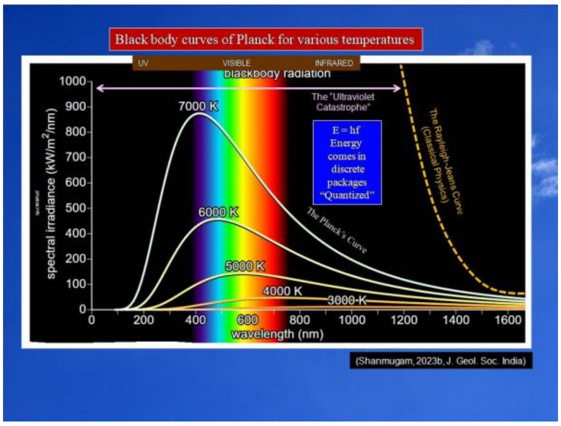

Fig. 230 Black body curves of Planck for various temperatures and comparison with classical theory of Rayleigh-Jeans. The Planck- Einstein relation (E=hf), a formula integral to quantum mechanics, says that a quantum of energy (E), commonly thought of as a photon, is equal to the Planck constant (h) times a frequency of oscillation of an atomic oscillator. Diagram source: Elert (1988- 2022). Additional labels by G. Shanmugam. Note the peaks of Planck curves shift to lower wavelengths (leftward, from infrared to UV) with increasing radiation. Scale: 1 Nanometer=0.001 Micrometer.

Fig. 234 Comments from Dr. Sultan Al Jaber, the President of COP28. COP28: The 2023 United Nations Climate Change Conference or Conference of the Parties (COP).

Fig. 235 A Forecast for Dubai in 2050 if COP55 were to be held in UAE without Fossil Fuels. Camels will substitute airlines for transportation.

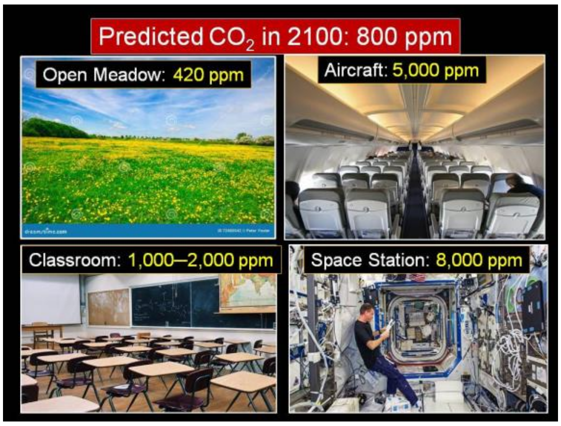

Fig. 233 Present CO_2 levels at various venues. Humans live comfortably at these CO_2 levels. For example: Classroom CO_2 levels vary from 1,000 to 2,000 ppm.

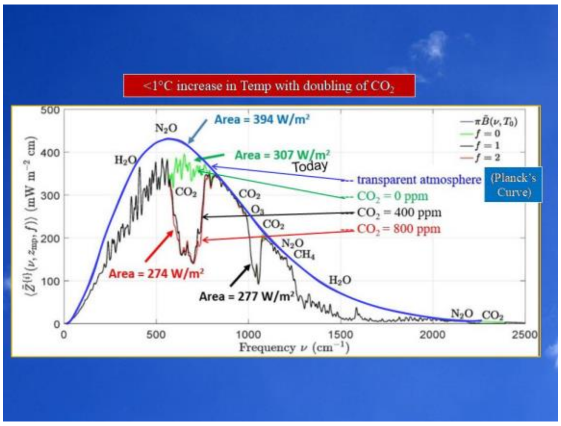

Fig. 231 Calculations: <1°C increase in Temp with doubling of CO_2 to 800 ppm. van Wijngaarden and Happer (2020).

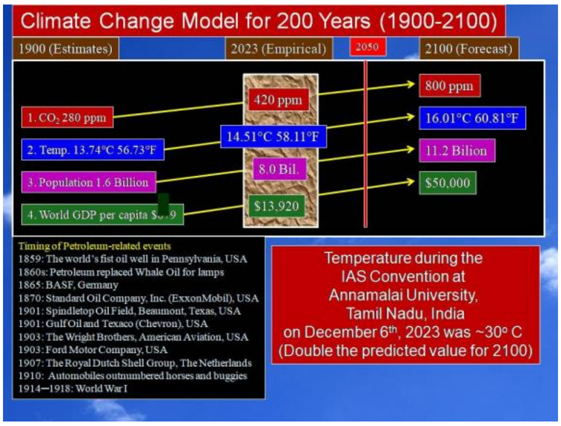

Fig. 232 Climate Change Model. Modified after Shanmugam (2023b).

Fig. 236 Conclusions on Climate Change. From Shanmugam (2024).

32. J. Robert Oppenheimer and the atomic bomb

'Oppenheimer' is a 2023 epic, biographical film about an American theoretical physicist Julius Robert Oppenheimer. He is considered the "father of the atomic bomb". The film is brilliantly written and directed by Christopher Nolan. The film, based on the 2005 biography "American Prometheus" by Kai Bird and Martin J. Sherwin, chronicles the complex and consequential career of J. Robert Oppenheimer. The story begins with Oppenheimer's postgraduate studies at the University of Cambridge (England) and at the University of Göttingen (Germany), details his direction of the Manhattan Project during World War II in developing nuclear weapons at the Los Alamos National Laboratory (LANL) in New Mexico (USA), and ends with his eventual fall from grace due to his 1954 security hearing based on the false premise that J. Robert Oppenheimer was a communist spy who was passing secret information on nuclear research to the Soviet Union.

Nolan's 'Oppenheimer' is the pinnacle of movie making. Nolan has delicately interwoven the intricate domains of quantum physics, human ingenuity, cruel politics, morality, legality, and ethics into a timely masterpiece and into an explosive emotional thriller. The four principal cast members (1) Cillian Murphy as J. Robert Oppenheimer, (2) Emily Blunt as Katherine "Kitty" Oppenheimer (wife), (3) Matt Damon as Gen. Leslie Groves, and (4) Robert Downey Jr. as Lewis Strauss perform their role flawlessly. Murphy, in particular, uncannily acts and resembles the real─life J. Robert Oppenheimer. In addition, the performances by Florence Pugh as Jean Tatlock and by Tom Conti as Albert Einstein are superb. The story is told in alternating black and white (Strauss' version of events) and color (Oppenheimer's version of events) scenes. The haunting musical score by Ludwig Göransson synchronizes perfectly with the movie plot. When the bomb explodes at the Trinity climax scene, the sound goes totally silent! Oppenheimer's story is the real─life vindication of the truth after 68 years (1954─2022). A must watch Nolan's thriller for this Nuclear Age!

Thus, the said movie has triggered me to make an attempt to comprehensively capture the chronology of events covering 153 years of history (1870─2023) associated with J. Robert Oppenheimer, some events not covered in the movie plot is included in this review article. The purpose is to permanently etch in history the scientific contributions made by J. Robert Oppenheimer and by his colleagues at the Manhattan Project, which not only ended the World War II, but also sprung open a new world of freedom for humanity.

Let there be no doubt that J. Robert Oppenheimer was a genuine patriotic American of our time and therefore, my only fervent hope is that our generation acknowledges, remembers, and admires their contributions and sacrifices, without which the fragile freedom that we enjoy today, even after 80 years later, would not have been possible. His legacy is one of historical greatness.

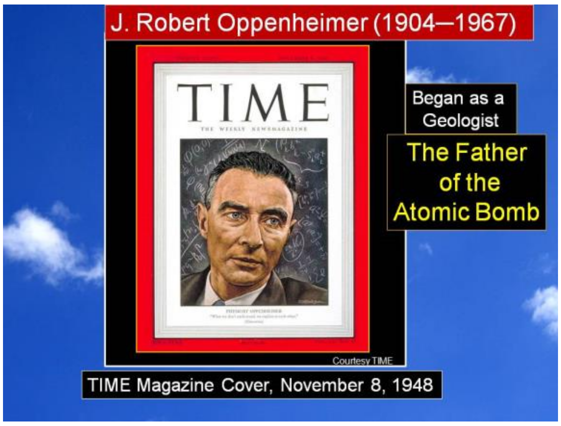

Fig. 237 TIME Magazine Cover of J. Robert Oppenheimer, November 8, 1948.

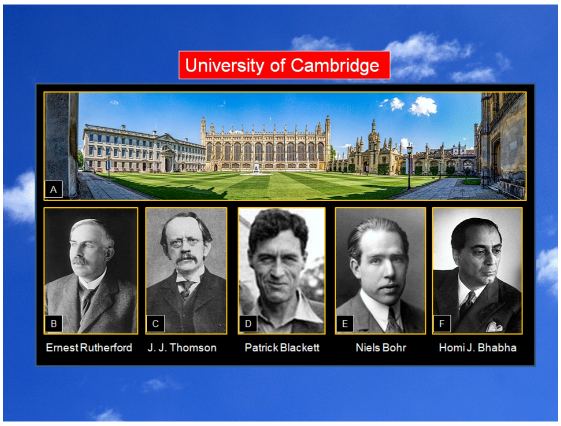

Fig. 238 Scientists at the University of Cambridge, UK

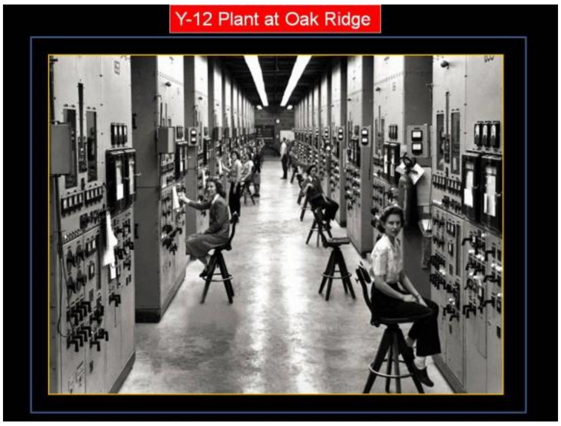

Fig. 239 Y-12 Plant at Oak Ridge, Tennessee.

Table 5. Timeline of key events covering 153 years of history (1870–2023) associated with J. Robert Oppenheimer (before, during, and after his lifetime). Modified after Shanmugam (2023d)

Serial Number	Date	Event	Comment
1	**1904** **April 22nd**	Julius Robert Oppenheimer was born to an affluent Jewish family in New York City, New York.	Known as J. Robert Oppenheimer
2	**1909**	At an early age of 5, J. Robert Oppenheimer was introduced to Mineralogy by his grandfather Benjamin.	
3	**1911 September**	Enrolled in the Ethical Cultural School in New York City.	
4	**1916**	At age 12, J. Robert Oppenheimer delivered an invited lecture at the prestigious New York Mineralogical Club.	
5	**1921**	Graduated as valedictorian of his high school class— The Ethical Culture School of New York.	
6	**1922**	Enrolled at Harvard University.	
7	**1925**	Received Bachelor's degree in chemistry from Harvard University. At Harvard, 1. He took six courses a semester. 2. He studied Greek, Latin, Eastern Philosophy, and Poetry. 3. He never read Newspapers or interested in Politics. 4. He never showed interest in dating. 5. He ate mostly chocolate and artichokes. His lunch consisted of butter toast with chocolate syrup.	
8	**1925**	Began graduate work in physics at Cavendish Laboratory in Cambridge, England under J. J. Thomson. He was unable to succeed as an experimental Physicist at Cambridge because he did not possess the basic qualities, namely, dexterity, attention to details, and patience.	
9	**1925**	At Cambridge, J. Robert Oppenheimer was diagnosed with Dementia praecox, the old name for Schizophrenia (Yorston, 2023) because of his failed attempt to kill his tutor, Patrick Blackett.	
10	**1926**	At Cambridge, J. Robert Oppenheimer was fascinated by the lectures on Quantum Mechanics given by Paul Dirac. In the spring of 1926, Max Born invited J. Robert Oppenheimer at Cambridge to come to Göttingen in Germany. J. Robert Oppenheimer took the advice and moved from Cavendish Laboratory to the University of Göttingen to finish his graduate studies under Max Born. This was a turning point in J. Robert Oppenheimer's life from one of failure and misery in experimental physics to one of success and glory in theoretical physics.	
11	**1927**	Received Ph.D. in Physics from the University of Göttingen in less than a year. After his Ph.D. Oral exam, James Franck, one of the internal examiners, a Nobel Prize winner, famously said "I am glad, that's over. He was at the point of questioning me."	
12	**1927**	Published a seminal paper 0n quantum chemistry and molecular physics, which is the the Born–Oppenheimer (BO) approximation. It is the best-known mathematical approximation in molecular dynamics. Specifically, it is the assumption that the wave functions of atomic nuclei and electrons in a molecule can be treated separately, based on the fact that the nuclei are much heavier than the electrons.	
13	**1927–1928**	National Research Fellow at Harvard and Caltech.	
14	**1929**	International Education Board Fellow at the University of Leyden, in the Netherlands, and the Technische Hochschule in Zürich, Switzerland (Losin, 1967).	
15	**1929**	He and his brother bought a ranch in the Sangre de Cristo Mountains in New Mexico. They called it Perro Caliente because J. Robert Oppenheimer shouted "Hot Dog" when he found out the cabin was available.	
16	**1929–1942**	Joined the faculty at the University of California, Berkeley, and Caltech. J. Robert Oppenheimer was described as aloof, arrogant, articulate, adventurous, and enigmatic. But he was always tempered with intellectual generosity to his students. Some of them went on to receive Nobel Prizes because of his mentoring. He often spent time learning Sanskrit and the Bhagavad Gita. This practice was by design and had	J. Robert Oppenheimer was a master of foreign languages, which include German, French, Dutch,

		deeper meanings. To J. Robert Oppenheimer, study of Physics was only an entry point to understanding the larger mystical nature of the Universe.	Greek, Latin, and Sanskrit.
17	**Late 1920s**	Diagnosed with a mild case of tuberculosis. He spent time in New Mexico for its dry air.	
18	**1931**	His mother Ella Oppenheimer died in California.	
19	**1933**	Melba Phillips, one of J. Robert Oppenheimer's first Ph.D. students, completed her degree at the University of California, Berkeley at a time when few women pursued careers in science. In 1935, J. Robert Oppenheimer and Phillips published their description of the Oppenheimer-Phillips effect, an early contribution to nuclear physics that explained the behavior of accelerated nuclei of radioactive hydrogen atoms. In 1952, Phillips was also known for refusing to cooperate with a U.S. Senate judiciary subcommittee's investigation on internal security during the McCarthy era that led to her dismissal from her professorship at Brooklyn College and from her research position at Columbia University Radiation Laboratory.	
20	**Mid 1930s**	He got involved in social causes and set aside 3% of his salary to help Jews who wish to flee from anti–Jew laws in Nazi Germany.	
21	**1936**	Oppenheimer was appointed as a Full Professor at UC, Berkeley.	
22	**1936–1943**	Relationship between J. Robert Oppenheimer and Jean Tatlock persisted even after his marriage to Kitty.	
23	**1939 August 2nd**	Albert Einstein wrote a letter to the U. S. President Franklin Roosevelt.	
24	**1939 August 9th**	Albert Einstein and Leo Szilard wrote a letter to President Franklin Delano Roosevelt (FDR) alerting him about the German's ongoing research on nuclear weapons. But Roosevelt did not respond to this letter immediately because the U.S. was not involved in the World War II in 1939.	
25	**1940 November**	J. Robert Oppenheimer married Katherine (Kitty) Puening Harrison. She was already pregnant with son Peter at the time of her marriage. Kitty got married to J. Robert Oppenheimer the same day she obtained divorce from her husband Harrison.	
26	**1941 May**	Son Peter was born.	
27	**1941 December 7th**	A surprise military strike by the Japanese Navy Air Service against the U.S. Naval Base at Pearl Harbor in Honolulu, Hawaii. Until then the U.S. was a neutral country in World War II. In response to the Pearl Harbor attack, President Roosevelt took action, and the U.S. entered the World War II. These events led to the origin of the Manhattan Project with J. Robert Oppenheimer in developing nuclear weapons.	**1941 December 7th**
28	**1942 January**	Organized a program on fast neutron theoretical physics at the University of California at Berkeley.	
29	**1942 May**	J. Robert Oppenheimer was hired onto the S–1 Committee as the "Coordinator of rapid rupture" (Veritasium, 2023).	
30	**1942 June**	Joined the Chicago Met Lab to lead an effort on fast neutron physics, and prepared an outline for the entire neutron physics program.	
31	**1942 July– September**	Assembled theoretical study group in Berkeley to examine the principles of bomb design. Emerged as the natural leader.	
32	**1942 August 13th**	The Manhattan Engineer District is formally established.	
33	**1942 October 15th**	General Leslie R. Groves appointed J. Robert J. Robert Oppenheimer to head "Project Y", planned to be the new central laboratory for weapon physics research and design, which would become known as the Los Alamos National Laboratory (LANL). General Groves' decision was based on Oppenheimer's (1) brilliant intellect, (2) uncanny ability to explain complex issues in simple terms, (3) motivation, (4) a sense of urgency, (5) charisma, and (6) administrative abilities.	Hans Bethe later commented that "Oppenheimer was the ideal leader for the project because he understood every detail of the project better than anyone else."
34	**1942 November 16th**	General Groves and J. Robert Oppenheimer visit the Los Alamos, a mesa in New Mexico and select it for "Site Y".	

35	**1943–1945**	J. Robert Oppenheimer served as the Scientific Director of the Los Alamos National Laboratory (LANL). Early recruitments included John Manley, Robert Wilson, John Williams, Joseph Kennedy, Hans Bethe, Robert Serber, Emil John Konopinski, Richard Feynman, among others.	
36	**1943 April**	A series of Conferences are held among 100 scientific staff at Los Alamos Laboratory for exchanging ideas. Robert Serber gave indoctrination lectures. This is a critical function introduced by J. Robert Oppenheimer.	
37	**1943 June**	K–25 Plant construction begins in Oak Ridge, TN.	
38	**1944 January 5th**	Jean Tatlock died.	The cause of death at 29 is in dispute.
39	**1944**	Daughter Katherine “Toni” Oppenheimer was born in Los Alamos.	
40	**1945 May 30th**	Secretary of War Henry Stimson rules out Kyoto, the ancient Capital of Japan, as the target for atomic attack.	
41	**1945 July 16th**	J. Robert Oppenheimer witnessed the successful Trinity test. The “Gadget” was the first ever plutonium device detonated in the world. Designing and building the Gadget was the pinnacle of Science and Engineering research.	
42	**1945 July 17th–August 2nd**	The Potsdam Conference in Germany where President Truman gave orders to bomb Japan.	
43	**1945 August 6th**	The United States detonated an atomic bomb over the Japanese city of Hiroshima killing 70,000–126,000 civilians. The bomb named “Little Boy”, an enriched uranium gun-type fission weapon, was used.	
44	**1945 August 9th**	The United States detonated an atomic bomb over the Japanese city of Nagasaki killing 60,000–80,000 civilians. The bomb named “Fat Man”, a plutonium implosion-type nuclear weapon, was used.	
45	**1945 August 14th**	Japanese News Agency announces surrender.	
46	**1945 October 16th**	J. Robert Oppenheimer resigned as the first director of Los Alamos Laboratory, accepting a post at Caltech.	
47	**1947**	J. Robert Oppenheimer became director of the Institute for Advanced Study in Princeton, New Jersey.	
48	**1947 August 25th**	The Manhattan Engineering District is abolished.	
49	**1948**	TIME Magazine published Oppenheimer photo on the cover of November 8th 1948 issue.	
50	**1953 December**	President Dwight D. Eisenhower ordered that a "blank wall be placed between Dr. Oppenheimer and any secret data" pending a security hearing.	
51	**1953**	During the Second Red Scare, the U.S. Department of Energy revoked J. Robert Oppenheimer’s security clearance and asked him to resign from his government position. He refused and demanded a hearing.	
52	**1954 June 29th**	After a behind the door security hearing in which Edward Teller testified against J. Robert Oppenheimer, J. Robert Oppenheimer's security clearance was revoked by the US Atomic Energy Commission, just 32 hours before it was set to expire.	
53	**1955 January 4th**	In a TV interview with CBS Edward R. Murrow (1955), J. Robert Oppenheimer described the IAS where he was the Director as a “decompression chamber” for intellectuals. His colleagues included Albert Einstein, Niels Bohr, Freeman Dyson, Richard Feynman, among others. This TV program, which exemplified J. Robert Oppenheimer’s charm, superior intellect, and wit, overturned American opinion on him temporarily damaged by the revocation of his security clearance.	
54	**1957–1966**	In 1957, J. Robert Oppenheimer bought a beach estate in the “Gibney Beach” and relocated there in St. John, the U.S. Virgin Islands. During the next decade, they spent considerable amount of time there away from the Public Eye. This area is locally called “Oppenheimer Beach” (Stein, 2023).	

55	**1957 September**	France appointed J. Robert Oppenheimer as an Officer of the National Order of the Legion of Honor.	
56	**1960**	Along with Albert Einstein, Bertrand Russell, and Joseph Rotblat he established the World Academy of Art and Science in 1960.	
57	**1960–1965**	He continued lecturing around the world on the Non-Proliferation of nuclear weapons.	
58	**1962 April 29th**	President John F. Kennedy invited him to a White House dinner for Nobel Prize winners. J. Robert Oppenheimer did attend that, Dinner.	
59	**1962 May 3rd**	J. Robert Oppenheimer was elected a Foreign Member of the Royal Society in Great Britain.	
60	**1963**	Prior to his assassination on November 22nd 1963, President John F. Kennedy boldly moved into rehabilitating J. Robert Oppenheimer by awarding him the Enrico Fermi Award.	
61	**1963 December 2nd**	J. Robert Oppenheimer received the Enrico Fermi Award on December 2nd from President Lyndon Johnson.	
62	**1966**	In 1965, J. Robert Oppenheimer was diagnosed with cancer of the throat. In those days, treatment options were limited. On his deathbed, J. Robert Oppenheimer regretted over his squandered opportunities to focus and complete research in the 1930s and to win a Nobel Prize. According to Kean (2023), Kitty requested Freeman Dyson to work with J. Robert Oppenheimer during his final days. Dyson declined and later said, “But I had to tell her that it was too late. I told her that I would like to sit quietly with Robert and hold his hand. His days as a scientist were over. It was too late to cure his anguish with equations.”	It is futile to speculate what he should or should not have done in his younger days. There were many challenges at LANL that pushed to the point of resigning. But he did not quit. He stayed and completed the task, which changed the world forever.
63	**1967 February 18th**	J. Robert Oppenheimer died in Princeton, New Jersey. He was undergoing chemotherapy for his lung cancer, fell into a coma, and died.	
64	**1967**	As a show of vindication, his funeral service was attended by more than 600 scientists and other academic personnel to illustrate their support for his patriotic life.	
65	**1967**	His ashes were deposited in the waters of St. John, the U.S. Virgin Islands.	
66	**2005**	Book “*American Prometheus*” by Kai Bird Martin J. Sherwin (2005) was published.	
67	**2022 December 16th**	The U.S. Department of Energy formally reversed the 1954 ruling that had stripped J. Robert Oppenheimer of his security clearance.	
68	**2023 July 21st**	Movie “Oppenheimer”, directed by Christopher Nolan, was released in the United States and the United Kingdom. This movie is based on the Book “*American Prometheus*”.	
69	2023	Oppenheimer’s reputation has been fully rehabilitated.	
70	End Results	Lewis Strauss was humiliated by the Senate’s rejection of his confirmation of Secretary of Commerce. Edward Teller was shunned by scientists. J. Robert Oppenheimer was fully rehabilitated.	The Un–American activities leveled against J. Robert Oppenheimer were proven wrong.
71	Lesson Learned	J. Robert Oppenheimer’s story left an enduring scientific, cultural, and political legacy for the humankind. His philosophy: “We know that as long as men are free to ask what they will, free to say what they think, free to think what they must, science will never regress, and freedom itself will never be wholly lost.” (Emperors and Conquerors, 2023).	J. Robert Oppenheimer was a true patriotic American.
72	**Summary**	J. Robert Oppenheimer is known for being: • Precocious • Fearless • Knowledgeable in Nuclear Physics	**A Genius of Our Time**

		Astrophysics Cosmology Quantum Chemistry Mathematics Engineering Mineralogy German French Dutch Greek Latin Sanskrit Bhagavad Gita Eastern Philosophy Poetry European furniture French postimpressionist and Fauvist artworks 19th Century Classics Sailing Horseback riding • Weird diet and drinking habits • Chain smoker • Clumsy social behavior • Had mistresses • Diagnosed with Schizophrenia • Donor for social causes • Despite 20 years of surveillance, J. Edgar Hoover and the FBI failed to produce any proof that J. Robert Oppenheimer was a member of the Communist Party. • Linked to 50 Nobel Laureates • Quick thinker • Fast learner • Brilliant Scientist • Inspiring Teacher • Pioneering Researcher • Excellent Administrator • Director of Los Alamos National Laboratory that developed atomic bombs, which ended the World War II. • Advocated Nonproliferation of nuclear weapons • Promoter of Arts and Sciences worldwide • His legacy is one of historical greatness.	

Table 6. Comparison of Characters J. Robert Oppenheimer vs. Lewis Strauss in the Movie “Oppenheimer”

Serial Number	**Property**	J. Robert Oppenheimer	Lewis Strauss
1	Character	Hero	Villain
2	Actor	Cillian Murphy	Robert Downey Jr.
3	Scenes (Character’s version)	Color	Black and White
4	Philosophy	Left leaning	Right leaning
5	Personality	Vindictive	Charitable
6	Academic qualification	World-renowned scientist The “Father of the Atomic Bomb”	Politician
7	Knowledge	A Genius	Average
8	U. S, Government position	Served as the Scientific Director of the Los Alamos National Laboratory (LANL). Responsible for developing the atomic boms, which ended the World War II.	Chair of the U. S. Atomic Energy Commission

9	Preference on Nuclear waepon	Atomic Bomb (Fission)	Hydrogen Bomb (Fusion)
10	Washington status	Outsider	Insider
11	Public humiliation	Security clearance revoked by the Atomic Energy Commission (AEC)	Cabinet position denied by the U.S. Senate
12	Vindication	Total vindication by the U.S. Govt in 2022.	No vindication
13	Legacy	Attained historical Greatness	Strauss was behind the AEC hearings that revoked Oppenheimer's security clearance.

Fig. 240 The World's First Atomic Bomb, Trinity Test, NM, USA: July 16, 1945

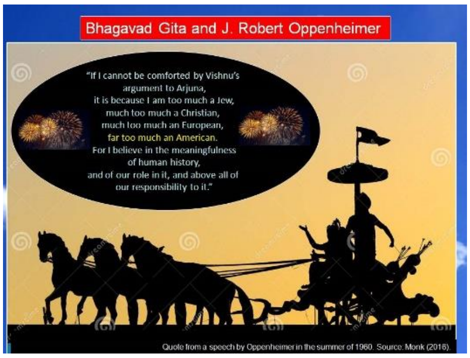

Fig. 241 In reflecting his philosophy and role in the development of atomic bomb, J. Robert Oppenheimer described his principles during a speech in the summer of 1960, proving he was a genuine patriotic American (Monk, 2026). Mahabharata image credit: Nitish Kumar and Dreamstime.com. The Bhagavad Gita and Mahabharata dates back to the second half of the first millennium BCE.

Fig. 242 Oppenheimer won seven Academy Awards including the Best Picture.

33. The peer─review problem

Shanmugam (2022g) examined the complex issue of the peer-review practice in journalism. The following are the main points. Albert Einstein, one of the greatest physicists of all time, had a deep disdain for peer review. The peer-review process, introduced over a thousand years ago in Syria and fully formalized by the Royal Society of London during 1665-1752, is an integral part of quality control in publishing articles and in awarding research grants. However, there are many lingering problems, which include: 1) anointed experts, 2) blind peer reviews, 3) delays, 4) orthodoxy, 5) bias, 6) groupthink, 7) Peer rejection of ideas (including Nobel-Prize winners), 8) inconsistency, 9) politics, 10) fake peer review and plagiarism, 11) "Sham peer review" in the U.S. medical community, 12) settling old scores, 13) online publications, 14) acknowledgements, 15) controversies in geological sciences, and 16) imbalance of peer reviewers in the biomedical research. Transparency, which is the underpinning trait of science journalism, is lost in the secrecy of blind peer review. Under the blind peer review, there are at least eight examples of scientific papers that were rejected before going on to win a Nobel Prize. Furthermore, there are 33 striking cases of peer rejection in science, including the notorious theory of "continental drift" by Alfred Wegener. My own examples of papers in process sedimentology and petroleum geology show that the same manuscript was rejected by one journal, but was accepted by another, suggesting that the blind peer review is obsolete. A solution is to adopt an Open Peer Review (OPR). Barring an open peer review, an alternative path is to publishing the entire peer-review comments and recommended decisions of all reviewers (anonymous and identified) at the end of a paper. This practice not only would force the anonymous reviewer to be objective and accountable but also would allow the entire peer-review process to be transparent.

34. Nature Photography

Photography is my hobby. I have published some of these photographs on the covers of International Journals (Figs. 243─253.).

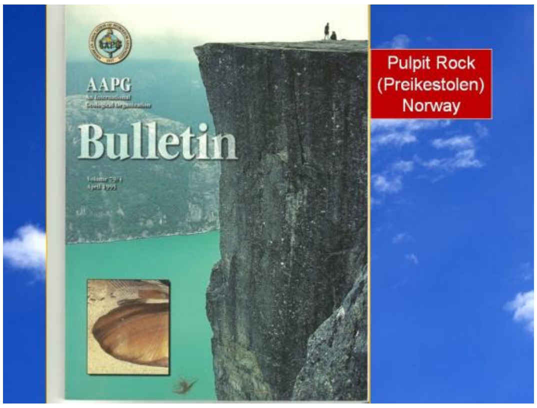

Fig. 243 AAPG Bulletin Cover Photo: Pulpit Rock (Preikestolen), Norway

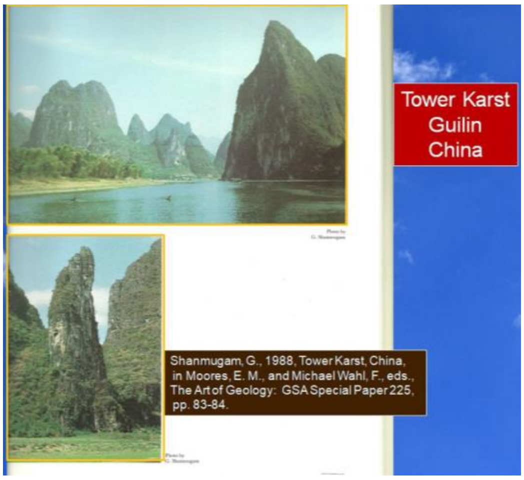

Fig. 246 GSA Special Paper Photo: Tower Karst, Guilin, China

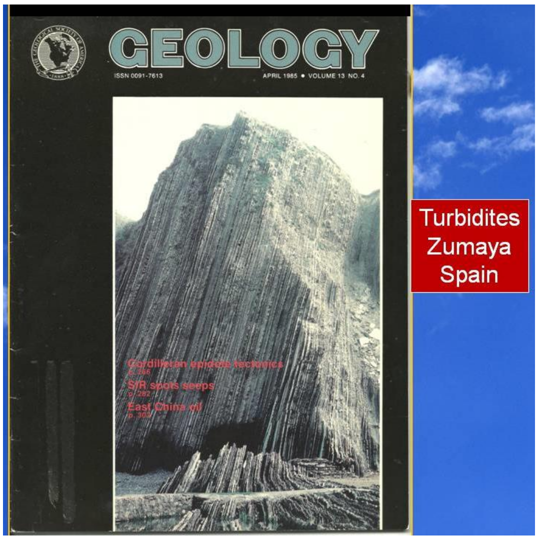

Fig. 244 GEOLOGY Cover Photo: Turbidites, Zumaya, Spain

Fig. 247 AAPG Bulletin Cover Photo: Cotopaxi Volcano, Ecuador

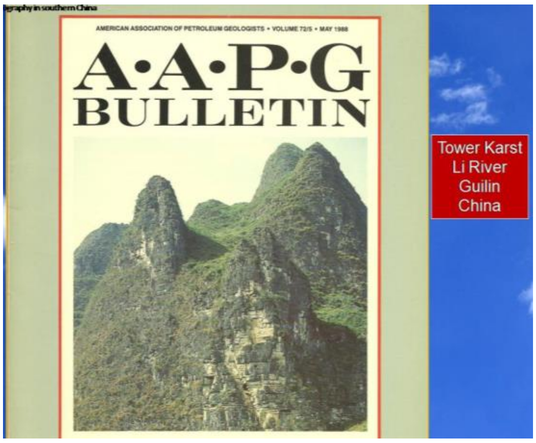

Fig. 245 AAPG Bulletin Cover Photo: Tower Karst, Li River, Guilin China

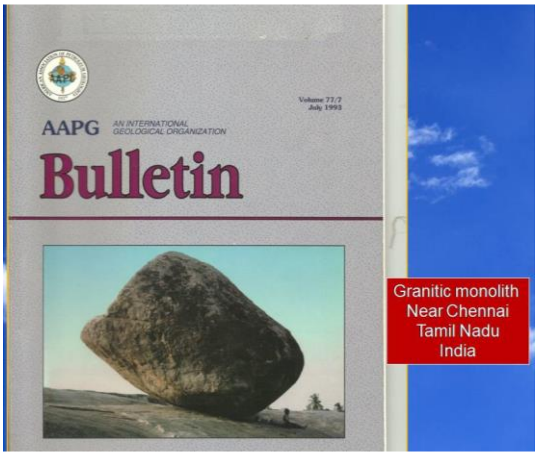

Fig. 248 AAPG Bulletin Cover Photo: Granitic monolith, Near Chennai, Tamil Nadu, India

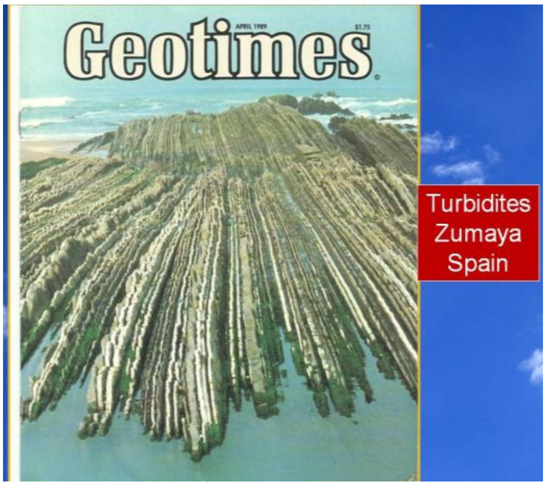

Fig. 249 Geotimes Cover Photo: Turbidites, Zumaya, Spain

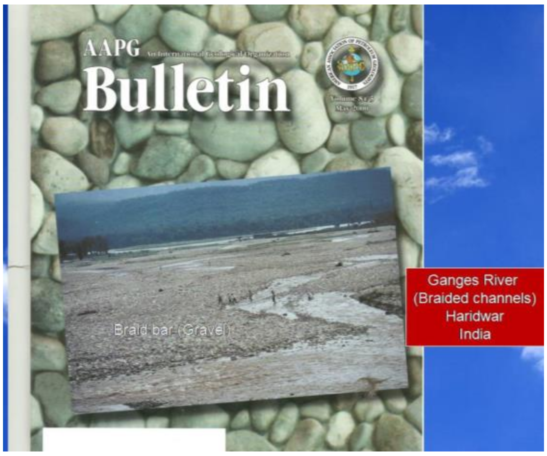

Fig. 250 AAPG Bulletin Cover Photo: Ganges River (Braided channels), Haridwar, India

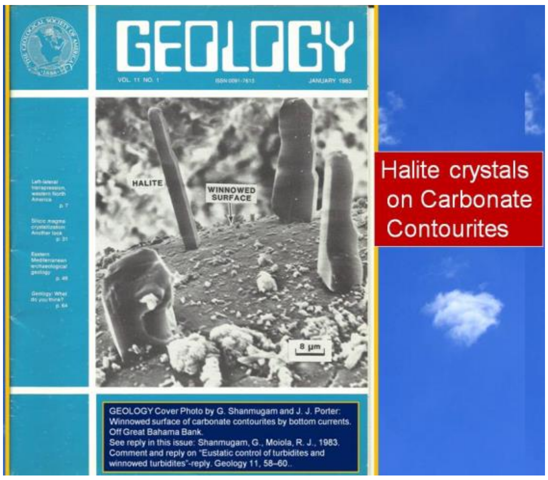

Fig. 251 GEOLOGY Cover Photo: SEM Photo of Halite crystals on Carbonate Contourites.

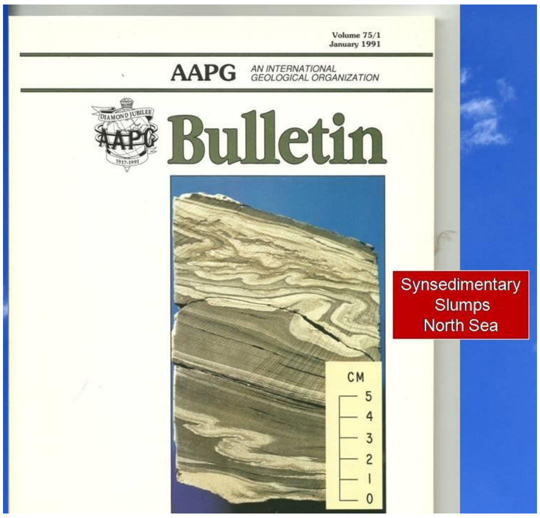

Fig. 252 AAPG Bulletin Cover Photo: Synsedimentary Slumps, North Sea.

Fig. 253 2018–2023: Indian Geological Journal Covers by G. Shanmugam

Publications of Journal Cover Photos

Shanmugam, G., 1981, Basin plain turbidites, Spain: Jour. Sed. Petrology, v. 51, p. 1400.

Shanmugam, G., 1982, Convolute division of a turbidite bed, Spain: Jour. Sed. Petrology, v. 52, p. 298.

Shanmugam, G., 1982, Channel-margin turbidite facies, Spain: Jour. Sed. Petrology, v. 52, p. 382.

Shanmugam, G., and Porter, J. J., 1983, Growth of halite crystals: Geology, cover photo, v. 11, No. 1.

Shanmugam, G., 1985, Basin plain turbidites, Spain: Geology, cover photo, v. 13, No. 4.

Shanmugam, G., 1988, Karst topography in southern China: AAPG Bull., cover photo, v. 72, No. 5.

Shanmugam, G., 1988, Basin plain turbidites, Spain: Earth-Science Reviews, cover photo, v. 25, Nos. 1, 2, 3, 4, 5, and 6.

Shanmugam, G., 1988, Zumaya Flysch, Spain, in Moores, E. M., and Michael Wahl, F., eds., The Art of Geology: GSA Special Paper 225, p. 23.

Shanmugam, G., 1988, Tower Karst, China, in Moores, E. M., and Michael Wahl, F., eds., The Art of Geology: GSA Special Paper 225, pp. 83-84.

Shanmugam, G., 1989, Zumaya Flysch, Spain: Geotimes, cover photo, v. 34, No. 4.

Shanmugam, G., and Stephens, C.F., 1991, Slumps, subsurface, North Sea: AAPG Bull., cover photo, v. 75, No. 1

Shanmugam, G., 1993, Granitic monolith, south India: AAPG Bull., cover photo, v. 77, No. 7

Shanmugam, G., 1995, Pulpit Rock, Norway: AAPG Bull., cover photo, v. 79, No. 4.

Shanmugam, G., 1998, Cotopaxi Volcano, Ecuador: AAPG Bull., cover photo, v. 82, No. 3.

Shanmugam, G., 2000, Ganges River, India: AAPG Bull., cover photo, v. 84, No. 5.

35. Publications and Recognition (Figs. 254─267)

I have published over 380 research works, including two volumes of Elsevier's Handbook of Petroleum Exploration and Production (Shanmugam, 2006a and 2012a) and their Chinese editions. His most recent Elsevier book "Mass Transport, Gravity Flows, and Bottom Currents" contains 540 case studies covering environments on Earth, Mars, and Jupiter, but with a majority on deep-water processes on Earth (Shanmugam, 2021a).

Awards, Recognition, and Nomination

- 1968: IIT Medal for the top-ranking student in Applied Geology, Civil Engineering Department, Indian Institute of Technology, Bombay (IITB), India.
- 1995: Best paper award from NAPE (Nigerian Association of Petroleum Explorationists) for his paper "Deepwater Exploration: Conceptual Models and their Uncertainties"
- 2003: His paper 'High-density turbidity currents: are they sandy debris flows?' published in the *Journal of Sedimentary Research* in 1996, has achieved the status of the single most cited paper in sedimentological research published in three world-renowned periodicals - *Journal of Sedimentary Research*, *Sedimentology*, and *Sedimentary Geology* - during the survey period of 1996-2003 (Source: International Association of Sedimentologists Newsletter, August 2003; Racki, 2003).
- He was interviewed by the SUN TV, Chennai, India (Televised on December 30th 2003) on his controversial research papers on turbidite sedimentation and their implications for petroleum reservoirs.
- 2018: I was the recipient of the University of Tennessee College of Arts & Sciences 2018 Professional Achievement Award. Award Date: September 21, 2018. Knoxville, Tennessee. https://artsci.utk.edu/dialogue/honor-college-alumni/
- 2018: I was also the recipient of FeTNA 2018 "Tamil American Pioneer Award" for his extraordinary professional achievements in academia. FeTNA: Federation of Tamil Sangams of North America. Award Date: June 30, 2018. Frisco, Texas. http://tap.fetna.org/category/2018/
- 2020: I was the recipient of Springer Journal of Palaeogeography Special Prize for Excellent papers published during 2012-2018 based on Science Citation Index (SCI).
- 2019-2021: I was nominated for the SEPM 2020 William F. Twenhofel Medal, which is the top award given every year for contributions in Sedimentary Geology.
- 2022: Founding Member of the International Society of Palaeogeography (ISP), Beijing, China
- 2023: CNKI/Thomson Reuters PCSI Stats: Top-1% most-highly cited publications for the period 2012-2022: "Submarine fans: A critical retrospective (1950-2015)", J. of Palaeogeogr. (2016)
- I am an Emeritus Member of SEPM (Society for Sedimentary Geology); member since 1970.
- Research.com selected 57 Leading Scientists from the University Texas at Arlington with 4 from Earth Sciences on September 1, 2023. They are:

1. A. Basu
2. G. Shanmugam

3. J. E. Damuth
4. 4. W. Balsam

- Research.com selected 57 Leading Scientists from the University Texas at Arlington with 4 from Earth Sciences on on May 8, 2024, here: https://research.com/university/earth-science/university-of-texas-at-arlington

They are (Fig. 267):

1. Q. Hu
2. A. Basu
3. G. Shanmugam
4. J. E. Damuth

- I became an invited Member of CO_2 Coalition in April 2023.

1997 AAPG Annual Convention Debate Panelist, Dallas, Texas

Topic: Processes of Deep-Water Clastic Sedimentation and Their Reservoir Implications: What Can We Predict?

Moderator: H. E. Clifton.

Panelists: A.H. Bouma, J.E. Damuth, D.R. Lowe, G. Parker, and G. Shanmugam

He has published 38 discussions and replies**.**

Organizer of International Deep-Water Sandstone Workshops: 15
Examples:

- the UK Department of Trade and Industry (DTI) in Scotland (1995 and 1997);
- Petrobras, Mobil, and Unocal in Brazil and in Dallas, Texas (1998 and 1999);
- Oil and Natural Gas Corporation (ONGC) in India (2002 and 2004);
- Reliance Industries Ltd. in India (2006–09);
- Research Institute of Petroleum Exploration and Development (RIPED), PetroChina in Beijing (2009–10);
- Yanchang Oilfield Exploration and Development, Research Institute of Yan'an Branch (China) (2014);
- China University of Petroleum, Qingdao, China (2014).

Organizer of clastic facies field course (3 weeks) for Saudi Aramco, Dhaharan, Saudi Arabia:

1990 (3-21 November), Saudi Aramco, Saudi Arabia. Field area includes Qassim and vicinity. Modern and anient deposits were investigated in the field. Seismic profiles, well logs, and cores from petroleum-producing fields were used in class exercises

International invited Lectures delivered (1980-2023): 92

2018-Present: Editorial Board

- Associate Editor-in-Chief of the *Journal of Palaeogeography* (Springer/Elsevier)
- Editorial Board Member of the *Petroleum Exploration and Development* (Elsevier).
- Editorial Board Member of the Journal of Indian Association of Sedimentologists.

Research

He conducted outcrop studies of deep-water deposits in the Southern Appalachians (Tennessee, United States), Ouachita Mountains (Arkansas and Oklahoma, United States), and Peira Cava area (French Maritime Alps, SE France). I described deep-water strata using conventional cores and outcrops (1:20 to 1:50 scale), which include 32 deepwater sandstone petroleum reservoirs worldwide, totaling over 10,000 m in cumulative thickness during 1974–2011.

He also conducted field studies of coal deposits in Victoria (Australia), coniferous rain forests in the North Island (New Zealand), limestone karst in Guilin (China), fluvial deposits in Gujarat (India), 2004 Indian Ocean Tsunami-related coastal deposits in Tamil Nadu (India), shallow-marine deposits in Qassim area (Saudi Arabia), and estuarine deposits in the Oriente Basin (Ecuador).

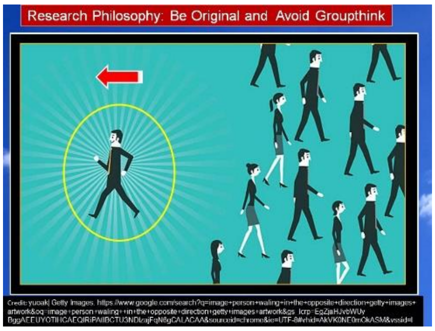

Fig. 254 Research Philosophy: Be Original and Avoid Groupthink

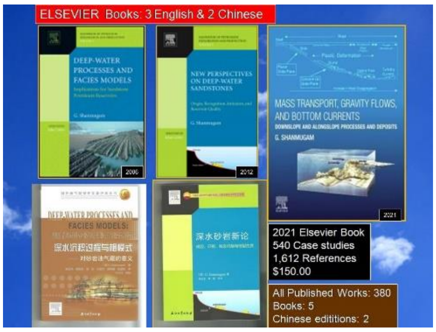

Fig. 255 All Published Works: 380, Books: 5, Chinese editions: 2

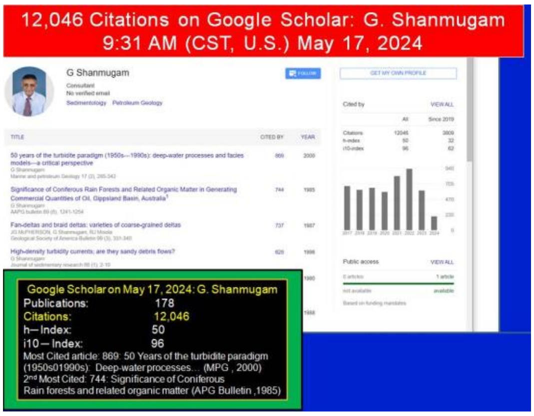

Fig. 256 G. Shanmugam as a Google Scholar Citations: 12,046 (May 17, 2024)

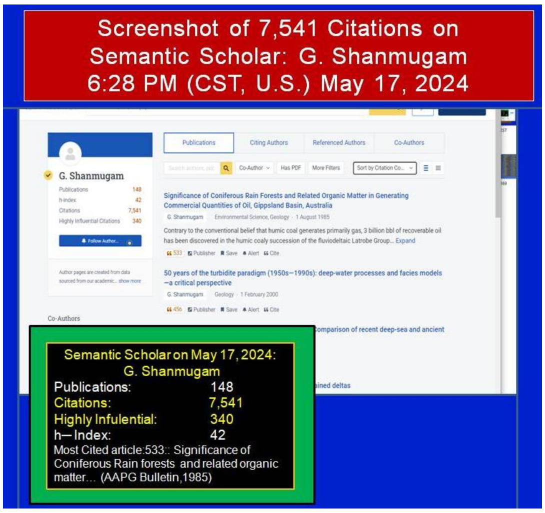

Fig. 257 G. Shanmugam as a Semantic Scholar Citations: 7,541 (May 17, 2024)

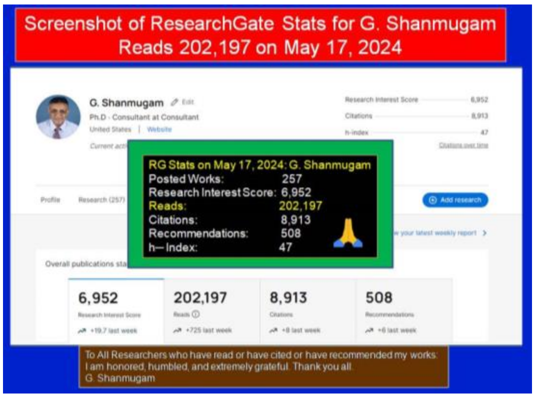

Fig. 258. Screenshot of Research Gate Stats for G. Shanmugam. Reads 202,197 on May 17, 2024

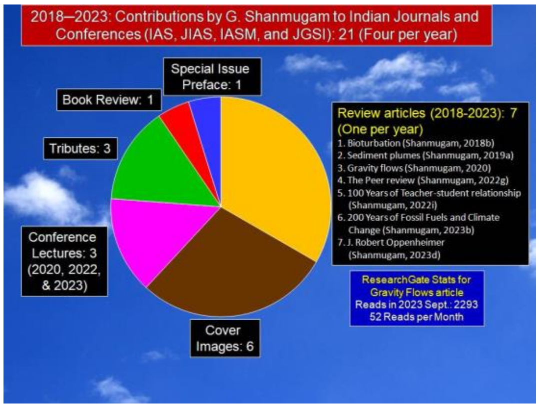

Fig. 259 2018–2023: Contributions by G. Shanmugam to Indian Journals and Conferences (IAS, JIAS, IASM, and JGSI): 21 (Four per year).

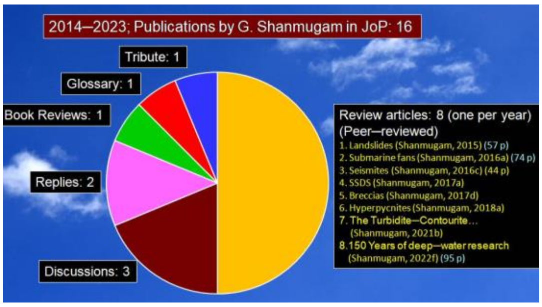

Fig. 260 2014–2023; Publications by G. Shanmugam in the Journal of Palaeogeography (JoP).

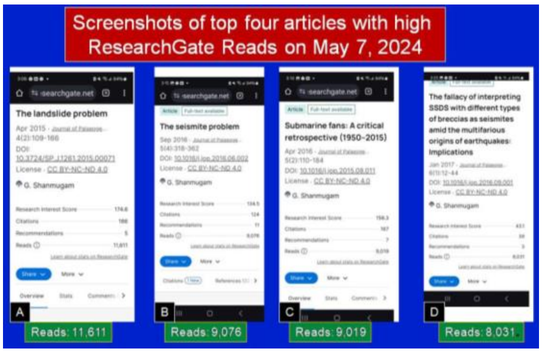

Fig. 261 Screenshots of top four articles with high Research Gate Reads on May 7, 2024

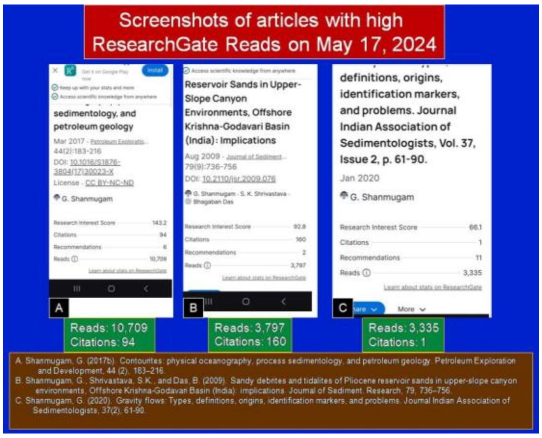

Fig. 262 Screenshots of articles with high Research Gate Reads on May 17, 2024

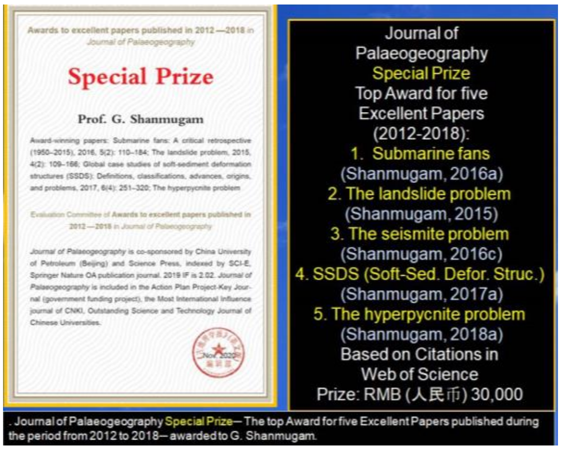

Fig. 263. Journal of Palaeogeography Special Prize─ The top Award for five Excellent Papers published during the period from 2012 to 2018─ awarded to G. Shanmugam.

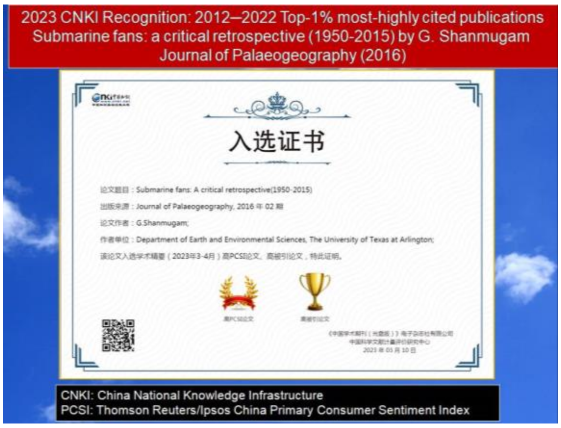

Fig. 264 2023 CNKI Recognition: 2012─2022 Top-1% most-highly cited publications Submarine fans: a critical retrospective (1950-2015) by G. Shanmugam, Journal of Palaeogeography (2016)

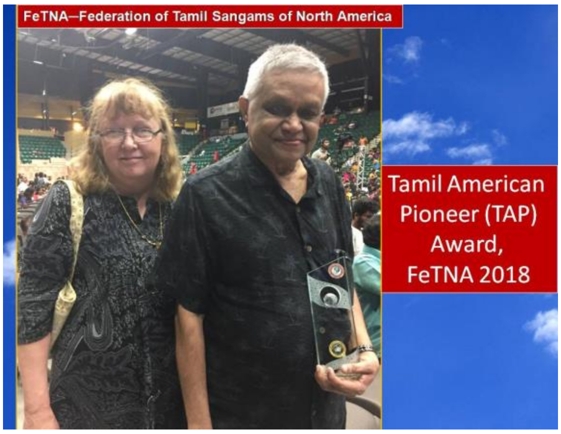

Fig. 265 Tamil American Pioneer (TAP) Award, FeTNA 2018. FeTNA: Federation of Tamil Sangams of North America.

Fig. 266 G. Shanmugam receiving award from the Dean, Dr. Theresa M. Lee, Brown Hall, UTK, September 21, 2018

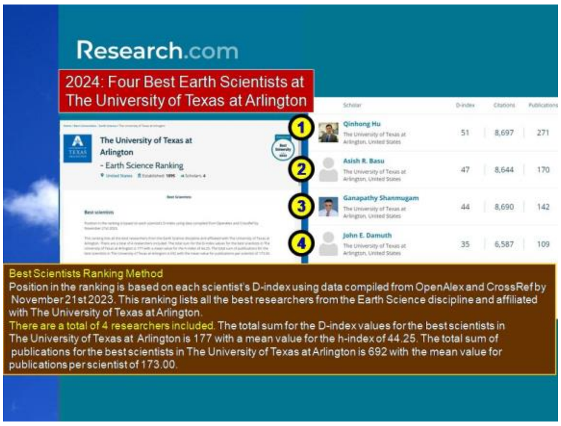

Fig. 267 2024: Four Best Earth Scientists at The University of Texas at Arlington

36. A Perspective

I find my scientific journey very inspiring (Fig. 268). My Scientific Journey can be described as "INDIA":

Insightful,
Neoteric,
Delightful,
Intellectual, and
Award winning.

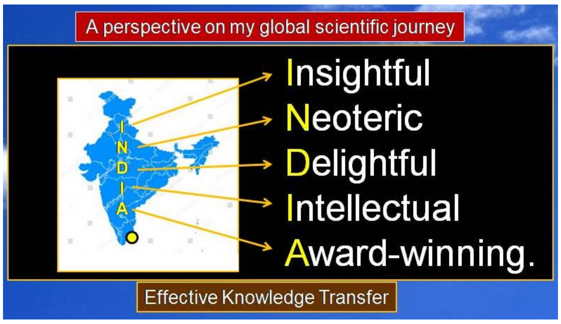

Fig. 268 A perspective on my global scientific journey

In understanding geological processes, we have come a long way. And yet, we still have a long way to go. In fact, there are many unresolved issues in recognizing various genetic depositional and deformational facies, which include:

1) Turbidites,
2) Sandy debrites,
3) Hyperpycnites,
4) Hybridites,
5) Baroclinites,
6) Tsunamites, and
7) Seismites.

Future researchers would serve well, if one attempts to adopt the following suggestions:

1) Avoid groupthink.
2) Avoid introducing new terminology for an existing concept.
3) Cite relevant articles, even if they were published a hundred years ago.
4) Apply common sense.
5) Be willing to openly criticize Government-funded propaganda.

Acknowledgements

My sincere thanks to the late Prof. T. N. Muthuswami Iyer who made my Scientific Journey possible. I thank Prof. G. M. Bhat for inviting me to submit this article (Fig. 269). Dr. S. Asokan provided a helpful review. I thank Prof. T. Ramkumar for inviting me to present a Special Lecture at the 39th IAS Convention in celebrating the 70th Anniversary of the Earth Science Department at Annamalai University. I also thank Prof. G. N. Nayak, the President of the Indian Association of Sedimentologists, for inviting me to present my lecture as the Convention Address. I am grateful to Prof. G. M. Bhat, current Editor-in-Chief of JGSI and former Managing Editor of JIAS for inviting me to serve on the Editorial Board of JIAS in 2018. I am grateful to all my teachers. Colleagues, editors, reviewers, and students who helped me during the past 62 years. In particular, I would like to recognize my colleagues in oil companies (Fig. 270), at Mobil (Fig. 271) and at Reliance (Fig. 272). Most important, I wish to thank my wife, Jean Shanmugam, who helped in all aspects of my professional and personal life since 1976 when we got married.

Finally, I take this opportunity to thank a select group of scientists of Indian origin (Fig. 273). I am thankful to Abhijit Basu, Indiana University, who provided constant support during the past 40 years. I am grateful to **the late Prof. Zeng–Zhao Feng who was instrumental in my scientific activities in China (Fig. 266), such as the International Society of Palaeogeography (ISP) and the Journal of of Palaeogeography (JoP).** William Happer, who was born in British India (Tamil Nadu), currently a Professor of Physics, Emeritus, at Princeton University, helped me with my recent research on Climate Change (Shanmugam, 2024).

Fig. 269 10 Distinguished Scientists of Indian Origin who helped G. Shanmugam with his research publications.

Fig. 270 Oil Companies in the USA, China, and India where G. Shanmugam examined Petroleum Reservoirs

Fig. 271. Colleagues at Mobil.

Fig. 272. Scientists at Reliance Industries Ltd. India.

Fig. 273 Speech by the late Prof. Zeng─Zhao Feng at Founding Conference of the International Society of Palaeogeography (ISP) on July 16, 2022.

Bibliography

Alfaro, P., Moretti, M., Owen, G., (2016). The environmental significance of soft-sediment deformation. Sedimentary Geology, 344, iiieiv.

Allen, J.R.L., (1977). The possible mechanics of convolute lamination in graded sand beds. Journal of the Geological Society, London, 134, 19─31.

Allen, J.R.L., (1984). Sedimentary Structures, Their Character and Physical Basis, Unabridged One-Volume. Elsevier, Amsterdam, I, p. 593, and II, p. 663.

Allen, J.R.L., (1985). Loose-boundary hydraulics and fluid mechanics: selected advances since 1961. In: Brenchley, P.J., Williams, P.J. (Eds.), Sedimentology: Recent Developments and Applied Aspects. Published for the Geological Society by Blackwell Scientific Publications, Oxford, pp. 7-28.

Alsop, G.I., Marco, S., 2013. Seismogenic slump folds formed by gravity-driven tectonics down a negligible subaqueous slope. Tectonophysics 605, 48-69.

Apel, J.R., (1987). Principles of Ocean Physics, International Geophysics 38. Academic Press, London, 63 p.

Apel, J.R., (2000). Solitons near Gibraltar: views from the European remote sensing satellites. Report GOA 2000_1, Global Ocean Associates, Silver Spring, MD.

Apel, J.R., (2002). Oceanic internal waves and solitons. In: Jackson, C.R., Apel, J.R. (Eds.), An Atlas of Oceanic Internal Solitary-Like Waves and Their Properties (May 2002), by Global Ocean Associates, prepared for Office of Naval Research _ Code 322PO, pp. 1_40 ,http://www.internalwaveatlas.com/Atlas_PDF/IWAtlas_Pg001_Introduction.PDF. (accessed 14.05.12.).

Bagnold, R.A., (1956). The flow of cohesionless grains in fluids. Phil. Trans. R. Soc. Lond. Ser. A. Math. Phys. Sci. 249, 235─297.

Bagnold, R.A., (1962). Auto-suspension of transported sediment. Proc. R. Soc. Lond. Ser. A 265, 315-319.

Banerjee, I., 1989, Tidal sand sheet origin of the transgressive basal Colorado Sandstone (Albian): a subsurface study of the Cessford field, southern Alberta: Bulletin of Canadian Petroleum Geology, v. 37, p. 1–17.

Basilone, L., Lena, G., Gasparo-Morticelli, M., (2014). Synsedimentary-tectonic, soft-sediment deformation and volcanism in the rifted Tethyan margin from the Upper TriassicMiddle Jurassic deep-water carbonates in Central Sicily. Sedimentary Geology, 308, 63─79.

Bastia, R., Nayak, P., and Singh, P., (2006), Shelf Delta to Deepwater Basin: A Depositional Model for Krishna–Godavari Basin: American Association of Petroleum Geologists, International Conference, Perth, Australia, November 5–8, 2006.

,http://www.searchanddiscovery.net/documents/2007/07011bastia/index.htm. Accessed April 18, 2009

Beck, C., (2009). Lake sediments as Late Quaternary palaeoseismic archives: examples in north-western Alps and clues for earthquake-origin assessment of sedimentary disturbances. Earth-Science Reviews, 96, 327─344.

Berner, R.A. (2004). The Phanerozoic carbon cycle: CO2 and O2: Oxford University Press, 158p. ISBN-13: 978-0195173338.

Booth, J.S., O'Leary, D.W., Popenoe, P., Danforth, W.W., (1993). U.S. Atlantic continental slope landslides: their distribution, general attributes, and implications. In: Schwab, W.C., Lee, H.J., Twichell, D.C. (Eds.), SubmarineLandslides: Selected Studies in the U.S. Exclusive Economic Zone, 2002. U.S. Geological Survey Bulletin, pp. 14-22.

Boulton, G.S., Dobbie, K.E., Zatsepin, S., (2001). Sediment deformation beneath glaciers and its coupling to the subglacial hydraulic system. Quaternary International, 86, 3─28.

Bouma, A.H., (1962). Sedimentology of Some Flysch Deposits: A Graphic Approach to Facies Interpretation. Elsevier, Amsterdam, p. 168.

Bouma, A.H., Normark, W.R., Barnes, N.E. (Eds.), (1985a). Submarine Fans and Related Turbidite Systems. Springer-Verlag, New York.Bouma, A.H., Coleman, J.M., DSDP Leg 96 Shipboard Scientists, (l985b). Mississippi Fan: Leg 96 program and principal results. In: Bouma, A.H., Normark, W.R., Barnes, N.E. (Eds.), Submarine Fans and Related Turbidite Systems, Springer-Verlag, New York, pp. 247–252.

Bouma, A.H., DeVries, M.B., Stone, C.G., (1997}. Reinterpretation of depositional processes in a classic flysch sequence (Pennsylvanian Jackfork Group), Ouachita Mountains, Arkansas and Oklahoma, Discussion. AAPG Bull. 81, 470─472.

Bourgeois J (2009) Chapter 3. Geologic effects and records of tsunamis. In: Robinson AR, Bernard EN (eds)Tsunamis. The sea, vol 15. Harvard University Press, Cambridge, pp 53–91

Briggs, G., Cline, L.M., (1967). Paleocurrents and source areas of Late Paleozoic sediments of the Ouachita Mountains, Southeastern Oklahoma. Journal of Sedimentary Petrology, 37, 985─1000.

Brush Jr., L.M., (1965). Experimental work on primary sedimentary structures. In: Middleton, G.V. (Ed.), Primary Sedimentary Structures and Their Hydrodynamic Interpretation, 12. SEPM Special Publication, pp. 17-24.

Bryant E (2001) Tsunami: the underrated hazard. Cambridge University Press, Cambridge, UK. 320 p.

Carlson, P.R., Karl, H.A., (1988). Development of large submarine canyons in the Bering Sea indicated by morphologic, seismic, and sedimentologic characteristics. GSA Bulletin 100, 1594─1615.

Carlson, P.R., Karl, H.A., Edwards, B.D., et al., (1991). Mass sediment failure and transport features revealed by acoustic techniques, Beringian margin, Bering Sea, AK. Marine Geotechniques 10, 33─51.

Chandrasekharam, D. (2021). The NZE tamasha and the CoP 26.https:// timesofindia.indiatimes.com/blogs/dornadula-c/the-nze-tamasha-and-thecop- 26/ Retrieved May 10, 2023

Christy, John R., (2022). Data shows there's no climate catastrophe looming –climatologist Dr J Christy debunks the narrative. BizNewsTv. https:// www.youtube.com/watch?v=qJv1IPNZQao Retrieved May 2, 2023.

Coleman Jr., J.L., (1997). Reinterpretation of depositional processes in a classic flysch sequence(Pennsylvanian Jackfork Group), Ouachita Mountains, Arkansas and Oklahoma, Discussion. AAPG Bull. 81, 466─469.

Collinson, J.D., (1994). Sedimentary deformational structures. In: Maltman, A. (Ed.), The Geological Deformation of Sediments. Chapman & Hall, London, pp. 95─125.

Curray, J. R., Moore, D. G., (1974). Sedimentary and tectonic processes in the Bengal Deep-sea Fan and Geosyncline. In: Burk, C.A., Drake, C.L. (eds), Continental Margins. New York: Springer-Verlag, 617–627.

Curray, J. R., Emmel, F.J ., Moore, D. G., (2002). The Bengal Fan: morphology, geometry, stratigraphy, history and processes. Marine and Petroleum Geology, 19 (10): 1191–1223.

Curry, J. (2023). Jordan Peterson - The Predictions Are Wrong !! Judith Curry.

https://www.youtube.com/watch?v=Jl_6vtiTOPo Retrieved February 9, 2023

D'Agostino, A.E., Jordan, D.W., (1997). Reinterpretation of depositional processes in a classic flysch sequence (Pennsylvanian Jackfork Group), Ouachita Mountains, Arkansas and Oklahoma: discussion. Am. Assoc. Petrol. Geol. Bull. 473─475.

Dalrymple, R.W., Knight, R.J., Zaitlin, B.A., Middleton, G.V., (1990). Dynamics and facies model of a macrotidalsand-bar complex, Cobequid Bay_Salmon River estuary, (Bay of Fundy). Sedimentology 37, 577─612.

Dalrymple, R.W., Zaitlin, B.A., Boyd, R., (1992). Estuarine facies models: conceptual basis and stratigraphic implications. J. Sediment. Petrol. 62, 1130─1146.

Damuth, J.E., Flood, R.D., Kowsmann, R.O., Gorini, M.A., Belderson, R.H., Gorini, M.A., (1988). Anatomy and growth-pattern of Amazon deep-sea fan revealed by long-range side-scan sonar (GLORIA) and high resolution seismic studies. AAPG Bull. 72, 885-911.

Dasgupta, P., (2003}. Sediment-gravity flow_the conceptual problems. Earth-Sci. Rev. 62, 265-281.

de Castro, S., Hernandez-Molina, F.J., Rodriguez-Tovar, F.J., Llave, E., Ng, Z.L., Nishida, N., Mena, A., et al., (2020). Contourites and bottom current reworked sands: Bed facies model and implications. Marine Geology 428, 106-267.

De Leo, F. C., Ross, S. W. (2019). Large submarine canyons of the United Ocean Energy Management. OCS Study BOEM 2019-066. Bureau of Ocean Energy Management. CSA Ocean Sciences Inc. 51 p.

Dill, R.F., Marshall, N.F., Reimnitz, E., (1975). In: Situ Submersible Observations of Sediment Transport and Erosive Features in Rio Balsas Submarine Canyon, Mexico (Abs), vol. 7. Geological Society of America, pp. 1052─1053.

Dott Jr., R.H., (1963). Dynamics of subaqueous gravity depositional processes. AAPG Bull. 47, 104-128.

Duncan, J.M., Wright, S.G., (2005). Soil Strength and Slope Stability:. John Wiley & Sons, Inc, Hoboken, NJ, p. 297

Dyson, Freeman (2007). Freeman Dyson on Global Warming 1of 2 Bogus Climate Models. https://www.youtube.com/watch?v=JTSxubKfTBU Retrieved June 19, 2023

Dzulynski, S., Ksiazkiewicz, M., Kuenen, Ph H., (1959). Turbidites in flysch of the Polish Carpathian Mountains. GSA Bulletin, 70, 1089─1118.

Eberling, M. (2022). The environmental downside of electric vehicles. https://www.themainewire.com/2022/04/the-environmental-downside-of-electric-vehicles/ Retrieved 31, 202.

Elert, G. (1988-2022). Blackbody Radiation. In The Physics Hypertextbook. https://physics.info/planck/ Retrieved March 2, 2023.

Elverhøi, A., Norem, H., Anderson, E.S., Dowdeswell, J.A., Fossen, I., Haflidason, H., et al., 1997. On the origin and flow behavior of submarine slides on deep-sea fans along the Norwegian-Barents Sea continental margin. Geo-Mar. Lett. 17, 119-125.

Embley, R.W., (1980). The role of mass transport in the distribution and character of deep-ocean sediments with special reference to the North Atlantic. Mar. Geol. 38, 23-50.

Enos, P., (1977). Flow regimes in debris flow. Sedimentology 24, 133─142.

Epstein, A. (2022). Fossil Future: Why Global Human Flourishing Requires More Oil, Coal, and Natural Gas—Not Less. Portfolio/Penguin,480 p.

Ewing, M., Ettrium, S.L., Ewing, J.L., Le Pichon, X., (1971). Sediment transport and distribution in the Argentine basin: Part 3, nepheloid layer and process of sedimentation. In: Ahrens, L.A., Press, F., Runcorn, S.K., Urey, H.C. (Eds.), Physics and Chemistry of the Earth. Pergamon Press, London, pp. 55─77.

Fallgatter, C., Kneller, B., Paim, P.S.G., Milana, J.P., et al., (2017). Transformation, partitioning and flowedeposit interactions during the run-out of megaflows. Sedimentology, 64, 359─387.

Feng, Z.Z., (2017a). A successful symposium of "multi-origin of soft-sediment deformation structures and seismites". J. Palaeogeogr. 6 (1), 1─6.

Feng, Z.Z., (2017b). Preface of the Chinese version of the seismite problem. J. Palaeogeogr. 6 (1), 7─11.

Feng, Z.Z., (2017c). Preface: a brief review on 7 papers from the special issue of "The environmental significance of soft-sediment deformation" of the Sedimentary Geology 344 (2016). J. Palaeogeogr. 6 (4), 243─250.

Feng, Z.-Z., (2019). Words of the Editor-in-Chief—some ideas about the comments and discussions of hyperpycnal flows and hyperpycnites. J. Palaeogeogr. 8 (3), 301─305.

Flood, R.D., Hollister, C.D., (1974). Current-controlled topography on the continental margin off the eastern United States, in Burke, C.A. In: Drake, C.L. (Ed.), The Geology of Continental Margins. Springer-Verlag, New York, pp. 197─205.

Flood, R.D., Manley, P., Kowsmann, R.O., Appi, C.J., Pirmez, C., (1991). Seismic facies and Late Quaternary growth of Amazon submarine fan. In: Weimer, P., Link, M.H. (Eds.), Seismic Facies and Sedimentary Processes of Submarine Fans and Turbidite Systems, Springer-Verlag, New York, pp. 415–433.

Flood, R.D., Piper, D.J.W., Klaus, A., Burns, S.J., Busch, W.H.,Cisowski, S.M., Cramp, A., Damuth, J.E., Goni, M.A., Haberle, S.G., Hall, F.R., Hinrichs, K.-U., Hiscott, R.N.,

Kowsmann, R.O., Kronen Jr., J.D., Long, D., Lopez, M., McDaniel, D.K., Manley, P.L., Maslin, M.A., Mikkelsen, N., Nanayama, F., Normak, W.R., Pirmez, C., dos Santos, J.R.,

Schneider, R.R., Showers, W.J., Soh, W., Thibal, J., (1995). Proceedings of the Ocean Drilling Program. Ocean Drilling Program, College Station, Texas, p. 1233. Initial Reports 155

Fonnesu, Marco, Patacci, Marco, Haughton, Peter D.W., Felletti, Fabrizio, McCaffrey, William D., (2016). Hybrid event beds generated by local substrate delamination on a confined-basin floor. Journal of Sedimentary Research, 86(8), 929─943. https://doi.org/10.2110/jsr.2016.58.

Forel, F.A., (1885). Les ravins sous-lacustres des fleuves glaciaires. Comptes Rendus de. l'Acade'mie des. Science Paris, 101(16), 725─728.

Foreman, M. G. G., Callendar, W., MacFadyen, A., Hickey, B. M., Thomson, R. E., and di Lorenzo, E., (2008). Modeling the generation of the Juan de Fuca Eddy. Journal of Geophysical Research: Oceans, 113, C3, CiteID C03006

Fossen, H., (2010). Deformation bands formed during soft-sediment deformation: observations from SE Utah. Mar. Petrol. Geol. 27, 215─222.

Fossati, M., Piedra-Cueva, I., (2013). A 3D hydrodynamic numerical model of the Rı´o de la Plata and Montevideos coastal zone. Appl. Math. Model. 37, 1310─1332.

Frohlich C, Hornbach MJ, Taylor FW, Shen C-C, Moala A, Morton AE, Kruger J (2009) Huge erratic boulders in Tonga deposited by a prehistoric tsunami. Geology 37:131–134

Gao, S., D. Wang, Y. Yang, L. Zhou, Y. Zhao, W. Gao, Z. Han, Q. Yu, and G. Li. (2015). Holocene sedimentary systems on a broad continental shelf with abundant river input: Process–product relationships. In River-dominated shelf sediments of east Asian seas, ed. P.D. Clift, J. Harff, J. Wu, and Y. Qui, vol. 429, 223–259. London: Geological Society, Special Publications

Ge, Z., Nemec, W., Vellinga, A.J., Gawthorpe, R.L., 2022. How is a turbidite actually deposited? Science Advances, 8(3), eabl9124. https://doi.org/10.1126/sciadv. abl9124. Epub 2022 Jan 19. PMID: 35044818; PMCID: PMC8769550.

Gill, A.E., (1982). Atmosphere-Ocean Dynamics. International Geophysics Series, vol. 30. Academic Press, An Imprint of Elsevier, San Diego, CA, 662 p.

Gordon, A.L., (2013). Bottom water formation. In: Steele, J.H., Turekian, K.K., Thorpe, S.A. (Eds.), Encyclopedia of Ocean Sciences, second ed. Academic, San Diego, CA, pp. 415_421. ,https://doi.org/10.1016/B978-0-12-409548-9.04019-7..

Gradmann, S., Beaumont, C., Ings, S.J., (2012). Coupled fluid flow and sediment deformation in margin-scale salt-tectonic systems: 1. Development and application of simple, single-lithology models. Tectonics, 31, C4010.

Greene, H.G., Murai, L.Y., Watts, P., Maher, N.A., Fisher, M.A., Paull, C.E., et al., (2006). Submarine landslides in the Santa Barbara Channel as potential tsunami sources. Nat. Hazards Earth Syst. Sci. 6, 63─88.

Gupta, S.K., (2006), Basin architecture and petroleum system of Krishna Godavari Basin, east coast of India: The Leading Edge, v. 25, p. 830–837.

Hampton, M.A., (1972). The role of subaqueous debris flows in generating turbidity currents. Journal of Sedimentary Petrology, 42, 775─793.

Happer, W. (2022). 138. Climate Physics w/Professor William Happer. October 29, 2022. https://www.google.com/search?q=harper+climate+physics+youtube&oq= harper+climate+physics+youtube&aqs=chrome..69i57j33i160l2.19747j0j7&sourceid=chrome&ie=UTF-8#fpstate=ive&vld=cid:e59ba35f,vid:5Uf_AbyG6ho Retrieved Novermber 23, 2022.

Happer, W. (2023). YouTube. CO2, the gas of life. Old Guard Summit Meeting. Springfield, New Jersey. https://www.youtube.com/watch?v=tXJ7UZjFDHU Accessed February 5, 2024.

Harris, P.T., Whiteway, T., (2011). Global distribution of large submarine canyons: geomorphic differences between active and passive continental margins. Mar. Geol. 285, 69─86.

Haughton, P., Davis, C., McCaffrey, W., Barker, S., (2009). Hybrid sediment gravity flow deposits-classification, origin and significance. Marine and Petroleum Geology, 26, 1900─1918.

He, Y.-B., Luo, J.-X., Li, X.-D., Gao, Z.-Z., Wen, Z., (2011). Evidence of internal-wave and internal-tide deposits in the Xujiajuan Formation of the Xiangshan Group, Ningxia, China. Geo-Mar. Lett. 31, 509─523.

Heezen, B.C., Hollister, C.D., Ruddiman, W.F., (1966). Shaping of the continental rise by deep geostrophic contour currents. Science 152, 502─508.

Heller, P., Dickinson, W.R.,)1985). Submarine ramp facies model for delta-fed, sand-rich turbidite systems. AAPG Bulletin, 69, 960–976.

Helwig, J., (1970). Slump folds and early structures, northeastern Newfoundland Appalachians. Journal of Geology, 78, 172─187.

Hernández-Molina, F.J., Maldonado, A., Stow, D.A.V., (2008). Abyssal plain contourites. In: Rebesco, M., Camerlenghi, A. (Eds.), Contourites. Elsevier, Amsterdam, pp. 345-378. Developments in Sedimentology 60, Chapter 18.

Hernández-Molina, F.J., Serra, N., Stow, D.A.V., Ercilla, G., Llave, E., Van Rooij, D., (2011). Along-slope oceanographic processes and sedimentary products around Iberia. Geo-Mar. Lett. 31, 315-341.

Hernández-Molina, F.J., Stow, D.A.V., Alvarez-Zarikian, C., (2013). IODP Expedition 339 in the Gulf of Cadiz and off West Iberia: decoding the environmental significance of the Mediterranean outflow water and its global influence. Sci. Drill. 16, 1-11.

Hersh, Seymour, (2023). How America Took Out The Nord Stream Pipeline https://seymourhersh.substack.com/p/how-america-took-out-the-nordstream Retrieved February 8, 2023

Hiscott, R.N., Pickering, K.T., Bouma, A.H., Hand, B.M., Kneller, B.C., Postma, G., et al., (1997). Basin-floor fans in the North Sea, Sequence stratigraphic models vs. sedimentary facies, Discussion. AAPG Bull. 81, 662─665.

Hockstad, M. (2016). Petrochemicals: The Building Blocks for Wind and Solar Energy. AFPM (American Fuel & Petrochemica Manufacturers)https://www.afpm.org/ newsroom/blog/petrochemicals-building-blocks-wind-and-solar-energyRetrieved November 26, 2022.

Hollister, C.D., (1967). Sediment Distribution and Deep Circulation in the Western North Atlantic (Unpublished Ph.D. dissertation). Columbia University, New York, p. 467.

Hollister, C.D., Heezen, B.C., (1972). Geological effects of ocean bottom currents: Western North Atlantic. In: Gordon, A.L. (Ed.), Studies in Physical Oceanography, vol. 2. Gordon and Breach, New York, pp. 37-66.

Hollister, C.D., Johnson, D.A., Lonsdale, P.F., (1974). Current-controlled abyssal sedimentation: Samoan Passage, equatorial west Pacific. J. Geol. 82, 275-300

Hsü, K.J., (1989). Physical Principles of Sedimentology. Springer-Verlag, New York, p. 233.

Inman, D.L., Nordstrom, C.E., Flick, R.E., (1976). Currents in submarine canyons: an air-sea-land interaction. Annu. Rev. Fluid Mech. 8, 275─310.

Jackson, C.R. (Ed.), (2004). An Atlas of Oceanic Internal Solitary-like Waves and Their Properties, second ed. Global Ocean Associates (prepared for the Office of Naval Research) http://www.internalwaveatlas.com/Atlas2_index.html.

Johnson, A.M., (1970). Physical Processes in Geology. Freeman, Cooper and Co., San Francisco, CA, p. 577.

Karcz, I., and Shanmugam, G. (1974). Decrease in Scour Rate of Fresh Deposited Muds. Proc. American Society of Civil Engineers (ASCE). J. Hydraulics Division, 100 (HY11), 1735–1738.

Kirkland, D.W., Anderson, R.Y., (1970). Microfolding in the Castile and Todilto evaporites, Texas and New Mexico. GSA Bulletin, 81, 3259─3282.

Klein, G.D., (1966). Dispersal and petrology of sandstones of Stanley-Jackfork boundary, Ouachita foldbelt, Arkansas and Oklahoma. AAPG Bull. 50, 308-326.

Klein, G.D., (1970). Depositional and dispersal dynamics of intertidal sand bars. J. Sediment. Petrol. 40, 1095-1127.

Klein, G.D., (1971). A sedimentary model for determining paleotidal range. Geol. Soc. Am. Bull. 82, 2585-2592.

Klein, G.D., (1975). Resedimented pelagic carbonate and volcaniclastic sediments and sedimentary structures in Leg 30 DSDP cores from the western equatorial Pacific. Geology 3, 39-42.

Koonin, S. E. (2021). Unsettled: What Climate Science Tells Us, What It Doesn't, and Why It Matters. BenBella Books. 316 p.

Kuenen, Ph H., (1957). Sole markings of graded greywacke beds. The Journal of Geology, 65, 231─258.

Kuenen, Ph H., (1966). Experimental turbidite lamination in a circular flume. The Journal of Geology, 74, 523─545.

Kuhn, T.S., (1970). The structure of scientific revolutions. University of Chicago Press, Chicago, p. 172.

Kuhn, T.S., (1996). The structure of scientific revolutions. 3rd Edition. The University of Chicago Press, Chicago, p. 212

Lawson, A. (2022). Nord Stream 1: Gazprom announces indefinite shutdown of pipeline. The Guardian. https://www. theguardian.com/business/2022/sep/02/nord-stream- 1-gazprom-announces-indefinite-shutdown-of-pipelineRetrieved November 27, 2022.

Lee, H.J., Kayen, R.E., Edwards, B.D., Field, M.E., Gardner, J.V., Schwab, W.C., Twichell, D.C., (1996). Ground-truth studies of west coast and Gulf of Mexico submarine fans. In: Gardner, J.V., Field, M.E., Twichell, D.C. (Eds.), Geology of the United States'Sea Floor, the View from GLORIA. Cambridge University Press, New York, pp. 221─222.

Lindzen, R. (2023a). Richard Lindzen's Climate Reality Check: Bridging the Gap Between Data and Climate Policy. 15th International Conference on

Climate Change. February 23-25, 2023, Orlando, Florida (USA). The Hearland Institute. https://www.youtube.com/watch?v=h5D6hSYxlcM Retrieved June 15, 2023

Lindzen, R. (2023b). YouTube TV. Manufacturing consent in times of crisis. The DemystifySci Podcast. DS 183. https://www.youtube.com/watch?v=DjYaQRXRRnE Accessed February 5, 2024.

Logan, W.E., 1863. Report on the Geology of Canada. John Lovell, Montreal, Canada, p. 464.

Lonsdale, P., Nornaark, W.R., Newman, W.A., (1972). Sedimentation and erosion on Horizon Guyot. Geol. Soc. Am. Bull. 83, 289-316.

Lomborg, B. (2007). Cool It: The Skeptical Environmentalist's Guide to Global Warming. Knopf Publishing Group. 272 p.

Lovell, J.P.B., Stow, D.A.V., (1981). Identification of ancient sandy contourites. Geology 9, 347─349.

Lowe, D.R., (1975). Water escape structures in coarse grained sediments. Sedimentology, 22, 157─204.

Lowe, D.R., (1976a). Subaqueous liquefied and fluidized sediment flows and their deposits. Sedimentology, 23, 285─308.

Lowe, D.R., (1976b). Grain flow and grain flow deposits. Journal of Sedimentary Petrology, 46, 188─199.

Lowe, D.R., (1979). Sediment gravity flows: their classification, and some problems of application to natural flows and deposits. In: Doyle, L.J., Pilkey, O.H. (Eds.), Geology of Continental Slopes, 27. SEPM Special Publication, pp. 75─82.

Lowe, D.R., (1982). Sediment gravity flows: II. Depositional models with special reference to the deposits of high density turbidity currents. Journal of Sedimentary Petrology, 52, 279─297.

Lowe, D.R., (1997). Reinterpretation of depositional processes in a classic flysch sequence (Pennsylvanian Jackfork Group), Ouachita Mountains, Arkansas and Oklahoma, Discussion. AAPG Bull. 81, 460─465.

Macdonald, D.I.M., Moncrieff, A.C.M., Butterworth, P.J., (1993). Giant slide deposits from a Mesozoic fore-arc basin, Alexander Island, Antarctica. Geology 21, 1047─1050

Malkawi, A.I.H., Alawneh, A.S., (2000). Paleoearthquake features as indicators of potential earthquake activities in the Karameh Dam Site. Natural Hazards, 22, 1─16.

Maltman, A., (1994a). Deformation structures preserved in the rocks. In: Maltman, A. (Ed.), The Geological Deformation of Sediments. Chapman & Hall, London, pp. 261─307.

Maltman, A., (1994b). Introduction and overview. In: Maltman, A. (Ed.), The Geological Deformation of Sediments. Chapman & Hall, London, pp. 1─35.

Marr, J.G., Harff, P.A., Shanmugam, G., and Parker, G. (2001). Experiments on subaqueous sandy gravity flows: the role of clay and water content in flow dynamics and depositional structures. GSA Bulletin, 113, 1377–1386.

Marsaglia, K. M., B. Rodriguez, D. S. Weeraratne, H. G. Greene, N. Shintaku, and M. D. Kohler. (2019). "Tracing the Arguello Submarine Canyon System from Shelf Origins to an Abyssal Sink". Journal of Sedimentary Research 17 (1): 87–101

McPherson, J.G., and Shanmugam, G., Moiola, R.J. (1987). Fan-deltas and braid deltas: varieties of coarse-grained deltas. Geol. Soc. America Bulletin, 99, 331–340.

Menzies, J., van der Meer, J.J.M., Ravier, E., (2016). A kinematic unifying theory of microstructures in subglacial tills. Sediment. Geol. 344, 57─70.

Meza, E. (2022). German funding for energy research reaches 1.31 billion Euros. https://www.cleanenergywire.org/news/ german-funding-energy-research-reaches-131-billion-euros Retrieved November 26, 2022.

Middleton, G.V. (Ed.), (1965). Primary Sedimentary Structures and Their Hydrodynamic Interpretation, 12. SEPM Special Publication, p. 265.

Middleton, G.V., (1966). Experiments on density and turbidity currents: I. Motion of the head. Canadian Journal of Earth Sciences, 3, 523─546.

Middleton, G.V., (1967). Experiments on density and turbidity currents: III. Deposition of sediment. Canadian Journal of Earth Sciences, 4, 475─505.

Middleton, G.V., (1973). Johannes Walther's Law of the correlation of fades. GSA Bulletin, 84, 979e988.

Middleton, G.V., (1993). Sediment deposition from turbidity currents. Annual Review of Earth and Planetary Sciences, 21, 89─114.

Middleton, G.V., Hampton, M.A., (1973). Sediment gravity flows: mechanics of flow and deposition. In: Middleton, G.V., Bouma, A.H. (Eds.), Turbidites and Deep-Water Sedimentation. SEPM Pacific Section Short Course, Anaheim, CA, pp. 1─38.

Middleton, G.V., Wilcock, P.R., (1994). Mechanics in the Earth and Environmental Sciences. Cambridge University Press, Cambridge, p. 459.

Monk, R. (2014). Robert Oppenheimer: A Life Inside the Center. Anchor. 880 p. ISBN-13 : *978-0385722049*

Monk, R. (2016).Robert Oppenheimer: A Life Inside the Center with Ray Monk | Institute for Advanced Study. https://www.youtube.com/watch?v=1uGqrD8-hj0 Retrieved August 9, 2023

Moore, P. (2021). Greenpeace's Ex-President - Is Climate Change Fake? - Patrick Moore | Modern Wisdom Podcast 373. https://www.youtube.com/watch?v=E5K5i5Wv7jQ Retrieved June 18, 2023

Morales de Luna, T., Ferna´ndez Nieto, E.D., Castro Dı´az, M.J., (2017). Derivation of a multilayer approach to model suspended sediment transport: application to hyperpycnal and hypopycnal plumes. Commun. Comput. Phys. 22 (5), 1439─1485.

Mulder, T., Syvitski, J.P.M., Migeon, S., Fauge`res, J.-C., Savoye, B., (2003). Marine hyperpycnal flows: initiation, behavior and related deposits. A review. Mar. Petrol. Geol. 20, 861─882.

Murray, J., Renard, A.F., (1891). Report on Deep-Sea Deposits Based on Specimens Collected during He Voyage of H.M.S. Challenger in the Years 1872-1876. Government Printer, Challenger Reports, London.

Mutti, E., (1977). Distinctive thin-bedded turbidite facies and related depositional environments in the Eocene Hecho Group (southcentral Pyrenees, Spain). Sedimentology, 24, 107–131.

Mutti, E., (1985}. Turbidite systems and their relations to depositional sequences. In: Zuffa, G.G. (Ed.), Provenance of Arenites, D. Reidel Publishing Company, Dordrecht, pp. 65–93.

Mutti, E., (1992). Turbidite Sandstones. Agip Special Publicatio. Milan, p. 275.

Mutti, E. (2023). Turbidite systems : an outcrop-based analysis. E book. – Rio de Janeiro : PETROBRAS, 2023. 466 p. ISBN: 978-65-88763-05-6

Mutti, E., Ricci Lucchi, F., (1972). Turbidites of the northern Apennines: introduction to facies analysis (English translation by Nilsen, T.H., 1978). International Geology Review, 20, 125–166.

Natland, M.L., (1967). New classification of water-laid clastic sediments. AAPG Bulletin, 51, 476.

Nelson, C.H., Maldonado, A., Coumes, F., Got, H., Monaco, A., (1985). Ebro Fan, Mediterranean. In: Bouma, A.H., Normark, W.R., Barnes, N.E. (Eds.), Submarine Fans and Related Turbidite Systems, Springer-Verlag, New York, pp. 121–127.

Nelson, C.H., Twichell, D.C., Schwab, W.C., Lee, H.J., Kenyon, N.H., (1992). Upper Pleistocene turbidite sand beds and chaotic silt beds in the channelized, distal, outer-fan lobes of the Mississippi fan. Geology, 20, 693─696.

Nilsen, T.H., Abbott, P.L., 1979. Introduction. In:Nilsen, T.H., Arthur, M.A. (Eds.), Upper Cretaceous Deep-Sea Fan Deposits, San Diego, vol. 11. Geological Society of America Annual Meeting, San Diego, CA, pp. 137─166 (Fieldtrip).

Normark, W.R., (1970). Growth patterns of deep sea fans. AAPG Bulletin, 54, 2170–2195.

Normark, W.R., Carlson, P.R., (2003). Giant submarine canyons: is size any clue to their importance in the rock record? In: Chan, M.A., Archer, A.W. (Eds.), Extreme Depositional Environments: Mega End Members in Geologic Time:. Geological Society of America, Boulder, CO, pp. 175─190. Special Paper 370.

Normark, W.R., Damuth, J.E., The Leg 155 sedimentology group, (1997). Sedimentary facies and associated depositional elements of the Amazon Fan. In: Flood, R.D., Piper, D.J.W., Klaus, A., Peterson, J.C. (Eds.), Proceedings of the Ocean Drilling Program Scientific Results, pp. 611─651.

Normark, W. R., David J.W. Piper, Brian W. Romans, Jacob A. Covault, Peter Dartnell, Ray W. Sliter, (2009). "Submarine canyon and fan systems of the California Continental Borderland", Earth Science in the Urban Ocean: The Southern California Continental Borderland, In: Homa J. Lee, William R. Normark (Eds). Earth Science in the Urban Ocean: The Southern California Continental Borderland. The Geological Society of America Special Paper 454 DOI: https://doi.org/10.1130/2009.2454(2.7)

Obermeier, S.F., Pond, E.C., Olson, S.M., Green, R.A., (2002). Paleoliquefaction studies in continental settings. In: Ettensohn, F.R., Rast, N., Brett, C.E. (Eds.), Ancient Seismites. GSA Special Papers, 359, pp. 13─27.

Obermeier, S.F., Olson, S.M., Green, R.A., (2005). Field occurrences of liquefaction-induced features: a primer for engineering geologic analysis of paleoseismic shaking. Engineering Geology, 76(3e4), 209─234.

Parthasarathy, A., and Shanmugam, G. (1969). Sedimentologic characteristics and their significance - studies on Bagh Sandstones in and around Tankhala, Gujarat State: Proc. 56th Session of Indian Science Congress Association, Part 3, Section V, p. 209

Paull, C.K., Mitts, P., Ussler III, W., Keaten, R., Greene, H.G., (2005). Trail of sand in upper Monterey Canyon: offshore California. Geol. Soc. Am. Bull. 117, 1134─1145.

Pequegnat, W.E., (1972*. A deep bottom-current on the Mississippi Cone. In: Capurro, L.R.A., Reid, J.L. (Eds.), Contribution on the Physical Oceanography of the Gulf of Mexico. Texas A&M University Oceanographic Studies, 2. Gulf Publishing, Houston, TX, pp. 65─87.

Pickering, K.T., Hiscott, R.N., (2015). Deep Marine Systems: Processes, Deposits, Environments, Tectonics and Sedimentation. American Geophysical Union. Wiley, p. 696.

Pierson, T.C., Costa, J.E., (1987). Arheologic classification of subaerial sediment-water flows. In: Costa, J.E., Wieczorek, G.F. (Eds.), Debris Flows/Avalanches: Process, Recognition, and Mitigation, VII. Geological Society of America Reviews in Engineering Geology, pp. 1─12.

Piper, D.J.W., (1978). Turbidite muds and silts in deep-sea fans and abyssal plains. In: Stanley, D.J., Kelling, G. (Eds.), Sedimentation in Submarine Fans, Canyons, and Trenches. Hutchinson and Ross, Stroudsburg, PA, p. 163─176.

Piper, D.J.W., Brisco, C.D., (1975). Deep-water continental-margin sedimentation, DSDP Leg 28, Antarctica. .In: Hayes, D.E., et al., (Eds.), Initial Reports of the Deep Sea Drilling Project. U.S. Government Printing Office, Washington, DC, pp. 727-755.

Piper, D.J.W., Shor, A.N., Hughes Clarke, J.E., (1988). The 1929 'Grand Banks' earthquake, slump, and turbidity current. In: Clifton, H.E. (Ed.), Sedimentologic Consequences of Convulsive Geologic Events, 229. Geological Society of America Special Paper, pp. 77─92.

Piper, D.J.W., Pirmez, C., Manley, P.L., Long, D., Flood, R.D., Normark, W.R., et al., (1997). Mass-transport deposits of the Amazon Fan. In: Flood, R.D., Piper, D.J.W., Klaus, A., Peterson, L.C. (Eds.), Proceedings of the Ocean Drilling Program, Scientific Results 155, pp. 109-143.

Pirmez, C., Hiscott, R.N., Kronen Jr., J.D., (1997). Sandy turbidite successions at the base of channel-levee systems of the Amazon Fan revealed by FMS logs and cores: unraveling the facies architecture of large submarine fans. In: Flood, R.D., Piper, D.J.W., Klaus, A., Peterson, J.C. (Eds.), Proceedings of the Ocean Drilling Program Scientific Results, 155, pp. 7–33.

Pomar, L., Morsilli, M., Hallock, P., Ba´denas, B., (2012). Internal waves, an under-explored source of turbulence events in the sedimentary record. Earth-Sci. Rev. 111, 56─81.

Pope, E.L., Cartigny, M.J.B., Clare, M.A., Talling, P.J., Lintern, D.G., Vellinga, A., Hage, S., Ac¸ikalin, S., Bailey, L., Chapplow, N., Chen, Y., Eggenhuisen, J.T., Hendry, A., Heerema, C.J., Heijnen, M.S., Hubbard, S.M., Hunt, J.E., McGhee, C., Parsons, D.R., Simmons, S.M., Stacey, C.D., Vendettuoli, D., (2022). First source-to-sink monitoring shows dense head controls sediment flux and runout in turbidity currents, 2022 May 20 Science Advances, 8(20), eabj3220. https://doi.org/10.1126/sciadv.abj3220. Epub 2022 May18. PMID: 35584216; PMCID: PMC9116613.

Postma, G., Nemec, W., Kleinspehn, K.L., (1988). Large floating clasts in turbidites: A mechanism for their emplacement. Sedimentary Geology, 58, 47─61.

Purkey, S.G., Smethie, W.M., Gebbie, G., Gordon, A.L., Sonnerup, R.E., Warner, M.J., et al., (2018). A synoptic view of the ventilation and circulation of Antarctic bottom water from chlorofluorocarbons. Annu. Rev. Mar. Sci. 10, 503─527.

Putin, v. (2024). YouTube Video. Presudent Putin's with Tucker Carlson in Kremlin on February 6, 2024. https://www.youtube.com/watch?v=5joqUZTT4m0 Retrieved February 10, 2024.

Racki, G., (2003). Hot" articles in modern sedimentary research: Updated list. IAS Newsletter, 187, 3─5.

Ramsay, J.G., (1967). Folding and Fracturing of Rocks. McGraw Hill, San Francisco, p. 568.

Rebesco, M., Camerlenghi, A. (Eds.), (2008). Contourites, Developments in Sedimentology 60. Elsevier, Amsterdam, 663 p.

Rodriguez-Tovar, F. J., (2022). Ichnological analysis: A tool to characterize deep-marine processes and sediments. Earth-Science Reviews, 228, 104014.

Rodrigues, S., Hern_andez-Molina, F.J., Fonnesu, M., et al., (2022). A new classification system for mixed (turbiditecontourite) depositional systems: Examples, conceptual models and diagnostic criteria for modern and ancient records. Earth-Science Reviews. https://doi.org/10.1016/j.earscirev.2022.104030.

Sanders, J.E., (1963). Concepts of fluid mechanics provided by primary sedimentary structures. J. Sediment. Petrol. 33, 173-179.

Sanders, J.E., (1965). Primary sedimentary structures formed by turbidity currents and related resedimentation mechanisms. In: Middleton, G.V. (Ed.), Primary Sedimentary Structures and Their Hydrodynamic Interpretation, 12. SEPM Special Publication, pp. 192-219.

Sanders, J.E., Friedman, G.M., (1997). History of petroleum exploration in turbidites and related deepwater deposits. Northeastern Geol. Environ. Sci. 19 (1/2), 67-102.

Scholz, H., Frieling, D., Aehnelt, M., (2011). Synsedimentary deformational structures caused by tectonics and seismic events─examples from the Cambrian of Sweden, Permian and Cenozoic of Germany. In: Sharkov, E.V. (Ed.), New Frontiers in Tectonic ResearchdGeneral Problems, Sedimentary Basins and Island Arcs. InTech, Rijeka, Croatia, pp. 183─218.

Schwab, W.C., Lee, H.J., Twichell, D.C., Locat, J., Hans Nelson, C., McArthur, W.C., Kenyon, N.H., (1996). Sediment mass-flow processes on a depositional lobe, outer Mississippi Fan. Journal of Sedimentary Research, 66, 916–927.

Schleussner, C. (2022). “The Paris Agreement – the 1.5 °C Temperature Goal”. Climate Analytics.https://climateanalytics.org/ briefings/15c/Retrieved March 4, 2023.

Schreiber, R. (2022). Deutsche Bank Says Germans May Need to Switch from Gas-to-Wood for Heating this Winter, is Wood-to-Gas for Cars Next?https://www. thetruthaboutcars.com/2022/07/deutsche-bank-says-germans-may-need-to-switch-from-gas-to-wood-for-heating-this-winter-is-wood-to-gas-for-cars-next/ November 26, 2022.

Scotese, C.R., Song, H., Mills, B.J.W., van der Meer, D.G. (2021). Phanerozoic paleotemperatures: The earth’s changing climate during the last 540 million years. Earth-Science Reviews, v.215, April 2021, 103503

Shanmugam, G. (1968). Geology of Tankhala Area, Gujarat State: Bombay, India: Civil Engineering Department, Indian Institute of Technology: Unpublished M.Sc. Dissertation in Applied Geology, IIT, Bombay, India, p. 84.

Shanmugam, G. (1970), ACE Language computer program for moment statistics in size-shape studies of sedimentary particles: Geol. Bull. of Civil Engineering Dept., Indian Institute of Technology, Bombay, 1, 13-17.

Shanmugam, G. (1972). Petrographic Study of Simpson Group (Ordovician) Sandstones, Southern Oklahoma. Ohio University: Unpublished M.S. Thesis in Geology, Athens, Ohio, p. 85.

Shanmugam, G. (1978). The Stratigraphy, Sedimentology, and Tectonics of the Middle Ordovician Sevier Shale Basin in East Tennessee (Unpublished Ph.D. dissertation). The University of Tennessee, Knoxville, TN, p. 222.

Shanmugam, G. (1980). "Petroleum Development Geology" by Parke A. Dickey: AAPG Bull. v. 64, pp. 2040- 2041.

Shanmugam, G. (1985a), Significance of coniferous rain forests and related Organic matter in generating commercial quantities of oil, Gippsland basin, Australia: AAPG Bulletin, 69, 1241-1254.

Shanmugam, G. (1985b). Ophiolite source rocks for Taconic-age flysch: Trace- element evidence: Discussion: Geol. Soc. America Bulletin, 96, 1221-1222.

Shanmugam, G. (1985c). Types of porosity in sandstones and their significance in interpreting provenance. In: Zuffa, G.G. (Ed.), Provenance of Arenites. D. Reidel Publishing Company, pp. 115–137.

Shanmugam, G. (1988). Origin, recognition and importance of erosional unconformities in sedimentary basins. In: Kleinspehn, K.L., Paola, C. (Eds.), New Perspectives in Basin Analysis. Springer-Verlag, New York, pp. 83-108.

Shanmugam, G., (1989), Porosity development in sandstones beneath erosional unconformities, in Flis, J.E., Price, R.C., and Sarg, J.F., eds., Search for the subtle trap hydrocarbon exploration in mature basins: West Texas Geological Society Publication 89-85, p. 269-281.

Shanmugam, G. (1990a). Deep-marine facies models and the interrelationship of depositional components in time and space. In: Brown, G.C., Gorsline, D.S., Schweller, W.J. (Eds.), Deep-Marine Sedimentation: Depositional Models and Case Histories in Hydrocarbon Exploration & Development, vol. 66. SEPM Pacific Section Short Course, San Francisco, CA, pp. 199–246.

Shanmugam, G. (1990b). Porosity prediction in sandstones using erosional unconformities. In: Meshri, I.D., Ortoleva, P.J. (Eds.), Prediction of Reservoir Quality Through Chemical Modelling. AAPG Memoir, pp. 1–23

Shanmugam, G. (1992). Submarine canyons. 7th Edition of Encyclopedia of Science and Technology, McGraw-Hill Book Company, New York, pp. 548–552.

Shanmugam, G. (1996). High-density turbidity currents: are they sandy debris flows? J. Sediment. Research, 66, 2–10.

Shanmugam, G. (1997). The Bouma Sequence and the turbidite mind set. Earth-Science Reviews, 42, 201–229.

Shanmugam, G., (1998). Dimensions and geometries of the components of deep-water systems. Mobil Technology Company Special Publication, Dallas, Texas, p. 110.

Shanmugam, G. (2000). 50 years of the turbidite paradigm (1950s–1990s): deep-water processes and facies models—a critical perspective. Marine and Petroleum Geology, 17, 285–342.

Shanmugam, G. (2001). Book Review: "Fine-Grained Turbidite Systems" edited by A.H. Bouma and C.G. Stone: Episodes, v. 24, no. 4, p. 284 (2001).

Shanmugam, G. (2002a). Ten turbidite myths. Earth-Science Reviews, 58, 311–341.

Shanmugam, G. (2002b). Book Review: "Fine-grained turbidite systems" edited by A.H. Bouma and C.G. Stone:*American Association of Petroleum Geologists Bulletin*, vol. 86, No. 6, pp.1133-1134 (June, 2002).

Shanmugam, G. (2003). Deep-marine tidal bottom currents and their reworked sands in modern and ancient submarine canyons. Marine and Petroleum Geology, 20, 471–491.

Shanmugam, G. (2006a). Deep-Water Processes and Facies Models: Implications for Sandstone Petroleum Reservoirs. Elsevier, Amsterdam, p. 476.

Shanmugam, G. (2006b). The tsunamite problem. J. Sedimentary Research, 76, 718–730.

Shanmugam, G. (2007). The obsolescence of deep-water sequence stratigraphy in petroleum geology. Indian Journal of Petroleum Geology, 16(1), 1–45.

Shanmugam, G. (2008a). The constructive functions of tropical cyclones and tsunamis on deepwater sand deposition during sea level highstand: implications for petroleum exploration. AAPG Bulletin, 92, 443–471.

Shanmugam, G. (2008b). Chapter 5 Deep-water bottom currents and their deposits. In: Rebesco, M., Camerlenghi, A. (Eds.), Contourites, Developments in Sedimentology, Vol. 60. Elsevier, Amsterdam, pp. 59–81.

Shanmugam, G. (2008c). Leaves in turbidite sand: the main source of oil and gas in the deep-water Kutei Basin, Indonesia: discussion. AAPG Bull. 92, 127–137.

Shanmugam, G. (2008d). Slides, slumps, debris flows, and turbidity currents. In: Steele, J.H., Turekian, K.K., Thorpe, S.A. (Eds.), Encyclopedia of Ocean Sciences, second ed. Elsevier, ISBN: 978-0-12-374473-9, pp. 447–467.

Shanmugam, G. (2008e). Book Review: "Economic and Palaeoceanographic Significance of Contourite Deposits". Edited by A. R. Viana and M. Rebesco. Geological Society (London) Special Publication 276, 2007. Book review in Journal of Sedimentary Research: URL: http://spot.colorado.edu/~jsedr/BookReviews/bookreviews.htm

Shanmugam, G. (2009a). Comment on "Late Holocene Rupture of the Northern San Andreas Fault and Possible Stress Linkage to the Cascadia Subduction Zone" by C. Goldfinger, K. Grijalva, R. Bürgmann, A. E. Morey, J. E. Johnson, C. Hans Nelson, J. Gutie´rrez-Pastor, A. Ericsson, E. Karabanov, J. D. Chaytor, J. Patton, and E. Grácia. Bull. Seismol. Soc. America, 99-4, 2594-2598.

Shanmugam, G. (2009b). Book Review: "The Cambridge Handbook of Earth Science Data", by Paul Henderson & Gideon M. Henderson, 2009. Cambridge University Press, The Edinburgh Building, Cambridge CB2 8RU, UK (published in the United States of America by Cambridge University Press, New York). Paperback, 277 pages. Price GBP 17.99; USD 30.00. ISBN 978-0-521-69317-2.

Shanmugam, G. (2011). Book Review: "Deep-Sea Sediments" by Hüeneke, H., Mulder, T. (Eds.), 2011. Elsevier, Amsterdam, Developments in Sedimentology 63". Geologos.

Shanmugam, G. (2012a). New Perspectives on Deep-Water Sandstones: Origin, Recognition, Initiation, and Reservoir Quality, 9. Elsevier, Handbook of Petroleum Exploration and Production, Amsterdam, p. 524.

Shanmugam, G. (2012b). Process-sedimentological challenges in distinguishing paleo-tsunami deposits. In: Kumar, A., Nister, I. (Eds.), Paleo-tsunamis. Natural Hazards, 63, pp. 5–30.

Shanmugam, G. (2013). Modern internal waves and internal tides along oceanic pycnoclines: challenges and implications for ancient deep-marine baroclinic sands. AAPG Bulletin, 97, 767–811.

Shanmugam, G. (2014). Review of research in internal-wave and internal-tide deposits of China, discussion. Journal of Palaeogeography, 3 (4), 332–350.

Shanmugam, G. (2015). The landslide problem. Journal of Palaeogeography, 4(2), 109–166.

Shanmugam, G. (2016a). Submarine fans: a critical retrospective (1950–2015). Journal of Palaeogeography, 5(2), 110–184.

Shanmugam, G. (2016b). The contourite problem. In: Mazumder, R. (Ed.), Sediment Provenance. Elsevier, pp. 183–254. Chapter 9.

Shanmugam, G. (2016c). The seismite problem. Journal of Palaeogeography, 5(4), 318–362.

Shanmugam, G. (2017a). Global case studies of soft-sediment deformation structures (SSDS): definitions, classifications, advances, origins, and problems. Journal of Palaeogeography, 6(4), 251–320.

Shanmugam, G. (2017b). Contourites: physical oceanography, process sedimentology, and petroleum geology. Petroleum Exploration and Development, 44 (2), 183–216.

Shanmugam, G. (2017c). The response of stromatolites to seismic shocks: tomboliths from the Palaeoproterozoic Chaibasa Formation, E India: discussion and liquefaction basics. Journal of Palaeogeography, 6 (3), 224–234.

Shanmugam, G. (2017d). The fallacy of interpreting SSDS with different types of breccias as seismites amid the multifarious origins of earthquakes: implications. Journal of Palaeogeography, 6(1), 12–44.

Shanmugam, G. (2018a). The hyperpycnite problem. Journal of Palaeogeography, 7(3), 197–238.

Shanmugam, G. (2018b). Bioturbation and trace fossils in deep-water contourites, turbidites, and hyperpycnites: a cautionary note. In: Special Issue dedicated to George Devries Klein by the Journal of the Indian Association of Sedimentologists (JIAS). Journal Indian Association of Sedimentologists, 35 (2), 13–32.

Shanmugam, G. (2018c). A global satellite survey of density plumes at river mouths and at other environments: plume configurations, external controls, and implications for deep-water sedimentation. Petrol. Explor. Development, 45(4), 640–661.

Shanmugam, G. (2018d). Preface to the Special Issue dedicated to George Devries Klein by the Journal of the Indian Association of Sedimentologists (JIAS). Journal Indian Association of Sedimentologists, 35(2), 1-5.

Shanmugam, G. (2018e). An extended tribute to Professor George Devries Klein (1933-2018): A sedimentologic pioneer and a petroleum geologist. *Journal of The Indian Association of Sedimentologists*, *35*(1), 107–118

Shanmugam, G., (2018f). Comment on "Iconological analysis of contourites: Past, present and future" by Francisco J. Rodriguez-Tovar and F. Javier Hernández-Molina [Earth- Science Reviews, 182 (2018), 28–41]. Earth-Science Reviews 184 (2018) 46–49

Shanmugam, G. (2019a). Global significance of wind forcing on deflecting sediment plumes at river mouths: implications for hyperpycnal flows, sediment transport, and provenance. Journal Indian Association of Sedimentologists, 36(2), 1–37.

Shanmugam, G. (2019b). Reply to discussions by Zavala (2019) and by Van Loon, Hüeneke, and Mulder (2019) on Shanmugam, G. (2018, Journal of Palaeogeography, 7 (3): 197–238): the hyperpycnite problem. Journal of Palaeogeography, 8 (4): 408–421.

Shanmugam, G. (2019c). Slides, Slumps, Debris Flows, Turbidity Currents, Hyperpycnal Flows, and Bottom Currents. In: J. Kirk Cochran, Henry J. Bokuniewicz and Patricia L. Yager (Editors-in-Chief), Encyclopedia of Ocean Sciences (Third Edition) Volume 4, pp. 228-257.

Shanmugam, G. (2020). Gravity flows: Types, definitions, origins, identification markers, and problems. Journal Indian Association of Sedimentologists, 37(2), 61-90.

Shanmugam, G. (2021a). Mass transport, gravity flows, and bottom currents: Downslope and alongslope processes and deposits. Elsevier, Amsterdam, **ISBN:** 9780128225769, p. 608.

Shanmugam, G. (2021b). "The turbidite-contourite-tidalite-baroclinite-hybridite problem: orthodoxy vs. empirical evidence behind the "Bouma Sequence". Jour. Palaeogeography, v. 10, No. 1. Online https://doi.org/10.1186/s42501-021-00085-

Shanmugam, G. (2021c). Deep-water processes and deposits. In Encyclopedia of geology, ed. David Alderton and Scott A. Elias, 2nd ed., Elsevier, Amsterdam, pp. 965–1009.

Shanmugam, G. (2022a). Book Review of "River Planet: Rivers from Deep Time to the Modern Crisis by Martin Gibling". Jour. Palaeogeography, v. 11, No. 1, 145=150.

Shanmugam, G. (2022b). Comment on "Ichnological analysis: A tool to characterize deep-marine processes and sediments" by Francisco J. Rodriguez-Tovar [Earth-Science Reviews, 228 (2022), 104014]. Earth-Science Reviews. Article in press.

Shanmugam, G. (2022c). Comment on "A new classification system for mixed (turbidite-contourite) depositional systems: Examples, conceptual models and diagnostic criteria for modern and ancient records" by S. Rodrigues, F.J. Hernández-Molina, M. Fonnesu, E. Miramontes, M. Rebesco, D. C. Campbell [*Earth-Science Reviews* (2022), https://doi.org/10.1016/j.earscirev.2022.104030]" Earth-Science Reviews. Article in press.

Shanmugam, G. (2022d). Sedimentary Basins: Processes, deposits, palaeogeography, and challenges. Keynote Lecture, 37th Convention of the Indian Association of Sedimentologists, University of Jammu, India, April 27, Wednesday, 10:00 AM (Jammu, India Time), 2022, Virtual Platform. In: IAS Abstract volume. P. 6-26.

Shanmugam, G. (2022e). 150 Years (1872-2022) of research on deep-water processes, deposits, settings, triggers, and deformation: A difficult domain of progress, dichotomy, diversion, omission, and groupthink. Keynote Lecture. 5th International Conference on Palaeogeography. May 14, Saturday, 9:50-10:20 AM (Beijing Time), 2022, Wuhan, China.

Shanmugam, G. (2022f). 150 Years (1872-2022) of research on deep-water processes, deposits, settings, triggers, and deformation: A difficult domain of progress, dichotomy, diversion, omission, and groupthink. Jour. Palaeogeography, v. 11, No. 4, 469-564.

Shanmugam, G. (2022g). The peer-review problem: a sedimentological perspective. *Journal of the Indian Association of Sedimentologists*, 39, 3-24.

Shanmugam, G. (2022h). "Fossil Future: Why Global Human Flourishing Requires More Oil, Coal, and Natural Gas--Not Less" by Alex Epstein. Book Review: Journal of the Indian Association of Sedimentologists, v. 39 (2), pp. 58─68.

Shanmugam, G. (2022i). 100 years of the Divine Teacher - Student relationship among the three Generations of Indian Geoscientists (1920s – 2020s): A remarkable Story of Knowledge transfer from T. N. Muthuswami Iyer "TNM" through A. Parthasarathy to G. Shanmugam and beyond. IAS Magazine, 1, 1, 2-40.

Shanmugam, G. (2022j). Update: A tribute to Sarbani Patranabis-Deb (13th November, 1966─31st October, 2022): A superb sedimentologist. Journal of the Indian Association of Sedimentologists, 39, 2 (A shorter version). IAS Magazine, 1, 2─8.

Shanmugam, G. (2023a). Climate Change: Fossil Fuels, Renewable Energy, Cyclones, Hypocrisy, Governance, CO_2 Coalition, Model, Lessons Learned, and Roadmap. OHIO University Geological Sciences Alumni Symposium, Virtual Lecture, 10:10 -10:40 AM, EST, Saturday, April 15, 2023, OHIO University, Athens, Ohio, USA.

Shanmugam, G. (2023b). 200 Years of Fossil Fuels and Climate Change (1900-2100). The Journal of the Geological Society of India, v. 99, 1043-1062.

Shanmugam, G. (2023c). A tribute to Prof. Zeng─Zhao Feng (6th July, 1926─5th January, 2023): Reminiscing about an iconic sedimentologist in China. Journal of Palaeogeography (JoP), Editorial, 12, 8-24.

Shanmugam, G. (2023d). The Life and Travails of J. Robert Oppenheimer, the Nuclear Scientist. IAS Magazine, 2, No 1, 3─52.

Shanmugam, G. (2023e). My Scientific Journey from Annamalai University to America and Beyond (1962-2023): Process Sedimentology, Appalachian Tectonics, Physical Oceanography, Fossil Fuels, Climate Change, and J. Robert Oppenheimer. Convention Address. In 39th Convention of the Indian Association of Sedimentologists and International Conference on "Voyage of Sedimentology from the Mountains to the Oceans: An Innovative Trajectory". IAS @ AU─2023. 6─8th, December, 2023. Department of Earth Sciences, Annamalai University, Annamalai Nagar 608 002, Tamil Nadu, India. Abstracts Volume. P. 1─ 29.

Shanmugam, G. (2024a). Fossil fuels, climate change, and the vital role of CO_2 to people and plants on planet Earth. Bulletin of the Mineral Research and Exploration**,** v. 170, in press. https://dergi.mta.gov.tr/article/show/2800.html Retrieved October 17, 2023

Shanmugam, G. (2024b). A remarkable decade of learning and sharing knowledge through the Journal of Palaeogeography (JoP) (2014─2024): Reminiscences from an Associate Editor-in-Chief. Journal of Palaeogeography (JoP), Editorial, 13, in press.

Shanmugam, G., and Benedict, G.L. (1978). Fine-grained carbonate debris flow, Ordovician basin margin, Southern Appalachians. J. Sediment. Petrology, 48, 1233–1240.

Shanmugam, G., and Benedict III, G.L. (1983). Manganese distribution in the carbonate fraction of shallow and deep marine lithofacies, Middle Ordovician, eastern Tennessee. Sediment. Geology, 35, 159–175.

Shanmugam, G., and Walker, K.R. (1978). Tectonic significance of distal turbidites in the Middle Ordovician Blockhouse and lower Sevier formations in east Tennessee. Am. Journal of Science, 278, 551-578.

Shanmugam, G., and Lash, G. G. (1982). Analogous tectonic evolution of the Ordovician foredeeps, southern and central Appalachians. Geology, 10, 562-566.

Shanmugam, G., and Moiola, R.J. (1979). Book Review: "Principles of Sedimentology" by G. M. Friedman and J. B. Sanders: Jour. Sedimentary Petrology, v. 49, p. 679-680.

Shanmugam, G., and Moiola, R.J. (1982). Eustatic control of turbidites and winnowed turbidites. Geology, 10, 231-235.

Shanmugam, G., and Moiola, R. J. (1984). Eustatic control of calciclastic turbidites. Marine Geology, 56, 273–278.

Shanmugam, G., and Moiola, R.J. (1988). Submarine fans: characteristics, models, classification, and reservoir potential. Earth-Science Reviews, 24, 383–428.

Shanmugam, G., and Moiola, R.J. (1995). Reinterpretation of depositional processes in a classic flysch sequence (Pennsylvanian Jackfork Group), Ouachita Mountains, Arkansas and Oklahoma. AAPG Bulletin, 79, 672–695.

Shanmugam, G., Moiola, R.J., (1997). Reinterpretation of depositional processes in a classic flysch sequence (Pennsylvanian Jackfork Group), Ouachita Mountains, Arkansas and Oklahoma: reply. AAPG Bull. 81, 476─491.

Shanmugam, G., and McPherson, J.G. (1987). Sedimentation in the Chile Trench: depositional morphologies, lithofacies, and stratigraphy: discussion and reply. GSA Bulletin, 99(4), 598.

Shanmugam, G., Alhilali, K.A., 1988. Parameters influencing Porosity in sandstones: a model for sandstone porosity prediction: discussion. AAPG Bulletin, 72, 852–853.

Shanmugam, G., and Higgins, J.B. (1988). Porosity enhancement from chert dissolution beneath Neocomian unconformity: Ivishak Formation, North Slope, Alaska. AAPG Bulletin, 72, 523–535.

Shanmugam, G., Damuth, J.E., Moiola, R.J., (1985). Is the turbidite facies association scheme valid for interpreting ancient submarine fan environments? Geology, 13, 234–237.

Shanmugam, G., Moiola, R. J., and Sales, J. K. (1988). Duplex-like structures in submarine fan channels, Ouachita mountains, Arkansas. Geology, 16, 229-232.

Shanmugam, G., Spalding, T.D., and Rofheart, D.H. (1993). Process sedimentology and reservoir quality of deep- marine bottom-current reworked sands (sandy contourites): an example from the Gulf of Mexico. AAPG Bulletin, 77, 1241–1259.

Shanmugam, G., Lehtonen, L.R., Straume, T., Syversten, S.E., Hodgkinson, R.J., and Skibeli, M., (1994). .Slump and debris flow dominated upper slope facies in the Cretaceous of the Norwegian and Northern North Seas (61–67ºN): implications for sand distribution. AAPG Bulletin, 78, 910–937.

Shanmugam, G., Bloch, R.B., Mitchell, S.M., Beamish, G.W.J., Hodgkinson, R.J., Damuth, J.E., Straume, T., Syvertsen, S.E., and Shields, K.E., (1995). Basin-floor fans in the North Sea: sequence stratigraphic models vs. sedimentary facies. AAPG Bulletin, 79, 477–512.

Shanmugam, G., Bloch, R.B., Damuth, Hodgkinson, R.J., (1997). Basin-floor fans in the North Sea: sequence stratigraphic models vs. sedimentary facies: reply. AAPG Bull. 81, 666─672.

Shanmugam, G., Poffenberger, M., and Toro Alava, J. (2000). Tide-dominated estuarine facies in the Hollin and Napo (`T'and `U') formations (Cretaceous), Sacha field, Oriente Basin, Ecuador. AAPG Bulletin, 84, 652–682.

Shanmugam, G., Shrivastava, S.K., and Das, B. (2009). Sandy debrites and tidalites of Pliocene reservoir sands in upper-slope canyon environments, Offshore Krishna-Godavari Basin (India): implications. Journal of Sediment. Research, 79, 736–756.

Shepard, F.P., (1973). Submarine Geology. third ed. Harper & Row Publishers, New York, p. 517.

Shepard, F.P., Dill, R.F., (1966). Submarine Canyons and Other Sea Valleys. Rand McNally & Co., Chicago, IL, p. 381.

Shepard, F.P., Marshall, N.F., McLoughlin, P.A., Sullivan, G.G., (1979). Currents in submarine canyons and other sea valleys. AAPG Stud. Geol. 8, 173.

Shipboard Scientific Party, (1994). Site 905. In: Mountain, G.S., Miller, K.G., Blum, P., et al. (Eds.), Proceedings of Ocean Drilling Program, Initial Reports, 134. College Station, Texas, pp. 255e308. http://dx.doi.org/10.2973/odp.proc.ir.150.109.1994 Shipboard Scientific Party, (1995). Site 931. In: Flood, R.D., Piper, D.J.W., Klaus, A., et al. (Eds.), Proceedings of the ODP Initial Reports 155. Ocean Drilling Program, College Station, Texas, pp. 123─174.

Shirley, K., (2003), India gas find has major impact: American Association of PetroleumGeologists, Explorer. ,http://www.aapg.org/explorer/2003/01jan/india.cfm. Accessed April 18, 2009.

Slatt, R.M., Weimer, P., Stone, C.G., (1997). Reinterpretation of depositional processes in a classic flysch sequence (Pennsylvanian Jackfork Group), Ouachita Mountains, Arkansas and Oklahoma, discussion. AAPG Bull. 81, 449─459.

Southard, J.B., Stanley, D.J., (1976). Shelf-break processes and sedimentation. In: Stanley, D.J., Swift, J.P. (Eds.), Marine Sediment Transport and Environmental Management. John Wiley & Sons, New York, pp. 351─377.

St. Laurent, L., Alford, M.H., Paluszkiewicz, T., (2012). An introduction to the special issue on internal waves. Oceanography 25 (2), 15_19. Available from: https://doi.org/10.5670/oceanog.2012.37.

Stanley, D.J., Kelling, G. (Eds.), 1978. Sedimentation in Submarine Canyons, Fans, and Trenches. Dowden, Hutchinson and Ross, Inc., Stroudsburg, PA.

Stanley, D.J., Moore, G.T. (Eds.), (1983). The Selfbreak: Critical Interface on Continental Margins, No. 33. SEPM Special Publication, p. 467.

Stow, D.A.V., (1985). Deep-sea clastics: where are we and where are we going? In: Brenchly, P.J., Williams, P.J. (Eds.), Sedimentology: Recent Developments and Applied Aspects, published for the Geological Society by Blackwell Scientific Publications, Oxford, pp. 67–94.

Stow, D.A.V., Lovell, J.P.B., (1979). Contourites: their recognition in modern and ancient sediments. Earth-Sci. Rev. 14, 251-291.

Stow, D.A.V., Shanmugam, G., (1980). Sequence of structures in fine-grained turbidites: comparison of recent deepsea and ancient flysch sediments. Sediment. Geol. 25, 23-42.

Stow, D.A.V., Piper, D.J.W. (Eds.), (1984). Fine-Grained Sediments: Deep-Water Processes and Facies, No. 15. Geological Society Special Publication, p. 659.

Stow, D.A.V., Fauge`res, J.-C., (2008). Contourite facies and the facies model. In: Rebesco, M., Camerlenghi, A. (Eds.), Contourites. Elsevier, Amsterdam, pp. 223-256.

Stow, D.A.V., Smillie, Z., (2020). Distinguishing between deep-water sediment facies: Turbidites, contourites and hemipelagites. Geosciences, 10, 68. https://doi.org/10.3390/geosciences10020068.

Stow, D.A.V., Hunter, S., Wilkinson, D., Herna´ndez-Molina, F.J., (2008). Chapter 9 The nature of contourite deposition. In: Rebesco, M., Camerlenghi, A. (Eds.), Contourites, 60. Elsevier, Amsterdam, pp. 143─156. Developments in Sedimentology.

Subrahmanyam, C., and Chand, S., (2006), Evolution of the passive continental marginsof India—a geophysical appraisal: Gondwana Research, v. 10, p. 167–178.

Surlyk, F., {1987). Slope and deep shelf gully sandstones, Upper Jurassic, East Greenland. AAPG Bulletin, 71, 464–475.

Sweeing, M. M. 1978. The karst of Kweilin, Southern China: Geographical Journal, 144, 199-204.

Talling, P.J., (2013). Hybrid submarine flows comprising turbidity current and cohesive debris flow: Deposits, theoretical and experimental analyses, and generalized models. Geosphere, 9(3), 460─488.

Terwindt, J.H.J., (1981}. Origin and sequences of sedimentary structures in inshore mesotidal deposits of the North Sea. In: Nio, S.-D., Shuttenhelm, R.T.E., Van Weering, Tj.C.E. (Eds.), Holocene Marine Sedimentation in the North Sea Basin, No. 5. International Association of Sedimentologists Special Publication, pp. 4─26.

Thomson, R.E., (1981). Oceanography of the British columbiacoast. Canadian Special Publication Fisheires Aquatic Sciences, 56, 291.

Twichell, D.C., Roberts, D.G., (1982). Morphology, distribution, and development of submarine canyons in the United States Atlantic continental slope between Hudson and Baltimore Canyons. Geology 10, 408─412.

Twichell, D.C., Schwab, W.C., Nelson, C.H., Kenyon, N.H., Lee, H.J., (1992). Characteristics of a sandy depositional lobe on the outer Mississippi Fan from Sea MARC 1A sidescan sonar images. Geology, 20, 689–692.

Twichell, D.C., Schwab, W.C., Kenyon, N.H., (1995). Geometry of sandy deposits at the distal edge of the Mississippi Fan, Gulf of Mexico. In: Pickering, K.T., Hiscott, R.N., Kenyon, N.H., Ricci Lucchi, F., Smith, R.D.A. (Eds.), Atlas of Deep Water Environments, Architectural Style in Turbidite Systems. Chapman & Hall, London, pp. 282─286.

Vail, P.R., Audemard, F., Bowman, S.A., Eisner, P.N., Perez- Cruz, C., (1991). The stratigraphic signatures of tectoni Eustace and sedimentology - an overview. In: Einsele, G., Ricken, W., Seilacher, A. (Eds.), Cycles and Events in Stratigraphy. Springer-Verlag, Berlin, pp. 618─659.

Van der Lingen, G. J. (2018). Post-modernism andclimate change. Special Issue dedicated to George Devries Klein in celebrating his life and achievements. Jour. Indian Association of Sedimentologists, V. 35, No. 2, pp 6-12.

Van Loon, A.J., (2009). Soft-sediment deformation structures in siliciclastic sediments: an overview. Geologos, 15, 3─55.

Van Loon, A.J., Mazumder, R., De, S., (2016). The response of stromatolites to seismic shocks: tomboliths from the Palaeoproterozoic Chaibasa Formation, E India. Journal of Palaeogeography, 5(4), 381─390.

Van Loon, A. J. (Tom), Hu¨ eneke, H., Mulder, T., (2019). The hyperpycnite problem: comment. J. Palaeogeogr. 8 (3), 314─320.

van Wijngaarden, W. A. and Happer, W. (2020). Dependence of Earth's Thermal Radiation on Five Most Abundant Greenhouse Gases (June 8,2020), https://arxiv.org/pdf/2006.03098 Retrieved April 30, 2023

Visser, M.J., (1980). Neap-spring cycles reflected in Holocene subtidal large-scale bedform deposits: a preliminary note. Geology 8, 543─546.

Waldron, J.W.F., Gagnon, J.F., (2011). Recognizing softsediment structures in deformed rocks of orogens. Journal of Structural Geology, 33, 271─279.

Walker, R.G., (1973). Mopping up the turbidite mess. In: Ginsburg, R.N. (Ed.), Evolving Concepts in Sedimentology, The Johns Hopkins University Press, Baltimore, pp. 1–37.

Walker, R.G., (1978). Deep-water sandstone facies and ancient submarine fans: models for exploration for stratigraphic traps. AAPG Bulletin, 62, 932–966.

Walker, R.G., (1992). Facies, facies models, and modern stratigraphic concepts. In: Walker, R.G., James, N.P. (Eds.), Facies Models: Response to Sea Level Change, GEOtext 1. Geological Association of Canada, pp. 1─14.

Wang, H., N. Bi, Y. Wang, Y. Saito, and Z. Yang. (2010). Tide-modulated hyperpycnal flows off the Huanghe (Yellow River) Mouth, China. Earth Surface Processes and Landforms 35 (11): 1315–1329.

Wikipedia (2023a). Oppenheimer (film) https://en.wikipedia.org/wiki/Oppenheimer_(film) Retrieved August 9, 2023

Wikipedia (2023b). J. Robert Oppenheimer. https://en.wikipedia.org/wiki/J._Robert_Oppenheimer Retrieved August 21, 2023

Wikipedia (2023c). Harvard University. https://en.wikipedia.org/wiki/Harvard_University Retrieved August 21, 2023

Wikipedia (2023d). Percy Bridgman. https://en.wikipedia.org/wiki/Percy_Williams_Bridgman Retrieved August 21, 2023

Wikipedia (2023e). University of Cambridge. https://en.wikipedia.org/wiki/University_of_Cambridge Retrieved August 21, 2023

Wikipedia (2023f). Ernest Rutherford . https://en.wikipedia.org/wiki/Ernest_Rutherford

Retrieved August 21, 2023

Wikipedia (2023g). J. J. Thomson. https://en.wikipedia.org/wiki/J._J._Thomson
Retrieved August 21, 2023

Wikipedia (2023h). Patrick Blackett. https://en.wikipedia.org/wiki/Patrick_Blackett

Retrieved August 21, 2023

Wikipedia (2023i). Niels Bohr. https://en.wikipedia.org/wiki/Niels_Bohr Retrieved August 21, 2023

Wikipedia (2023j). Old building of the University in Göttingen, Lower Saxony, Germany. https://en.wikipedia.org/wiki/University_of_G%C3%B6ttingen Retrieved August 21, 2023

Wikipedia (2023k). Max Born . https://en.wikipedia.org/wiki/Max_Born

Retrieved August 21, 2023

Wikipedia (2023l). Werner Heisenberg. https://en.wikipedia.org/wiki/Werner_Heisenberg Retrieved August 21, 2023

Wikipedia (2023m). Enrico Fermi. https://en.wikipedia.org/wiki/Enrico_Fermi Retrieved August 21, 2023

Wikipedia (2023n). Wolfgang Pauli. https://en.wikipedia.org/wiki/Wolfgang_Pauli Retrieved August 21, 2023

Wikipedia (2023o). Ernest Lawrence. https://en.wikipedia.org/wiki/Ernest_Lawrence

Retrieved August 21, 2023

Wikipedia (2023p). University of California, Berkeley. https://en.wikipedia.org/wiki/University_of_California,_Berkeley Retrieved August 21, 2023

Wikipedia (2023q). Institute for Advanced Study. https://www.ias.edu/ Retrieved August 21, 2023

Wikipedia (2023r). Freeman Dyson. https://en.wikipedia.org/wiki/Freeman_Dyson Retrieved August 21, 2023

Wikipedia (2023s). Little Boy. https://en.wikipedia.org/wiki/Little_Boy Retrieved August 21, 2023

Wikipedia (2023t). Fat Man. https://en.wikipedia.org/wiki/Fat_Man Retrieved August 21, 2023

Wikipedia (2023u). Richard Feynman. https://en.wikipedia.org/wiki/Richard_Feynman Retrieved August 21, 2023

Wikipedia (2023v). Oppenheimer Crater. https://en.wikipedia.org/wiki/Oppenheimer_(crater) Retrieved August 21, 2023

Wikipedia (2023w). Day of Infamy Speech https://en.wikipedia.org/wiki/Day_of_Infamy_speech Retrieved September 1, 2023

Wikipedia (2023x). Potsdam Conference. https://en.wikipedia.org/wiki/Potsdam_Conference Retrieved August 21, 2023

Wikipedia (2023y). Columbia University. https://en.wikipedia.org/wiki/Columbia_University Retrieved August 21, 2023

Wikipedia (2023z). Harold Urey. https://en.wikipedia.org/wiki/Harold_Urey Retrieved August 21, 2023

Wikipedia (2023z1). Isidor Isaac Rabi. https://en.wikipedia.org/wiki/Isidor_Isaac_Rabi Retrieved August 21, 2023

Wikipedia (2023z2). Nuclear Chain Reaction. https://en.wikipedia.org/wiki/Nuclear_chain_reaction Retrieved August 21, 2023

Wikipedia (2023z3). Attack on Pearl Harbor. https://en.wikipedia.org/wiki/Attack_on_Pearl_Harbor Retrieved August 21, 2023

Wikipedia (2023z4). Melba Phillips. https://en.wikipedia.org/wiki/Melba_Phillips#Career Retrieved August 21, 2023

Wikipedia (2023z5). Willis Lamb. https://en.wikipedia.org/wiki/Willis_Lamb Retrieved August 21, 2023

Wikipedia (2023z6). Henry DeWolf Smyth . https://en.wikipedia.org/wiki/Henry_DeWolf_Smyth Retrieved August 21, 2023

Wikipedia (2023z7). George C. Marshall . https://en.wikipedia.org/wiki/George_C._Marshall Retrieved August 21, 2023

Wikipedia (2023z8). Bhagavad Gita https://en.wikipedia.org/wiki/Bhagavad_Gita Retrieved August 21, 2023.

Wikipedia (2023z9). Born–Oppenheimer approximation https://en.wikipedia.org/wiki/Born%E2%80%93Oppenheimer_approximation#:~:text=Robert%20Oppenheimer%2C%20the%20latter%20of,other%20properties%20for%20large%20molecules. **Retrieved August 21, 2023.**

Wikipedia (2023z10). Homi J. Bhabha https://en.wikipedia.org/wiki/Homi_J._Bhabh**Retrieved August 25, 2023.**

Wüst, G., (1933). Schichtung und Zirkulation des Atlantischen Ozeans. Das Bodenwasser und die Gliederung der Atlantischen Tiefsee. Wiss. Erg. Dt. Atl. Exp. "Mete" (1925e1927) 6(1), 106. In: Olson, B.E. (Ed.), Bottom Water and the Distribution of the Deep Water of the Atlantic, Slessers, M. (Translator). US Naval Oceanographic Office, Washington, DC, p. 145.

Zavala, C., (2019). The new knowledge is written on sedimentary rocks _ a comment on Shanmugam's paper "The hyperpycnite problem". J. Palaeogeogr. 8 (3), 306─313.

Zenk, W., 2008. Abyssal and contour currents. In: Rebesco, M., Camerlenghi, A. (Eds.), Contourites. Elsevier, Amsterdam, pp. 37-57.

Zhao, R., Zhang, Q., Tjugito, H., Cheng, X., 2015. Granular impact cratering by liquid drops: Understanding raindrop imprints through an analogy to asteroid strikes. Proceedings of the National Academy of Sciences, 112(2), 342─347.